ผลของตัวทำละลายอินทรีย์ที่มีต่อรูปร่างของผลึกและการดูดกลืนรังสีอัลตราไวโอเลต ของซิงค์ออกไซด์ที่สังเคราะห์โดยวิธีโซลโวเทอร์มอล

นางสาว ปารวี โทนโต๊ะ

วิทยานิพนธ์นี้เป็นส่วนหนึ่งของการศึกษาตามหลักสูตรปริญญาวิศวกรรมศาสตรมหาบัณฑิต
สาขาวิชาวิศวกรรมเคมี ภาควิชาวิศวกรรมเคมี
คณะวิศวกรรมศาสตร์ จุฬาลงกรณ์มหาวิทยาลัย
ปีการศึกษา 2547
ISBN 974-17-7061-8

EFFECT OF ORGANIC SOLVENTS ON CRYSTAL SHAPE AND ULTRAVIOLET ABSORPTION OF ZINC OXIDE SYNTHESIZED VIA SOLVOTHERMAL METHOD

Miss Parawee Tonto

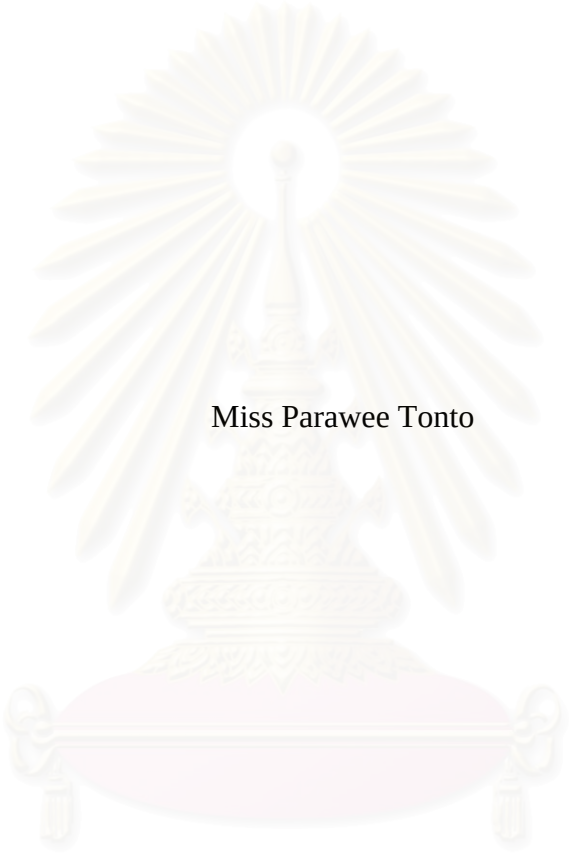

A Thesis Submitted in Partial Fulfillment of the Requirements
for the Degree of Master of Engineering in Chemical Engineering
Department of Chemical Engineering
Faculty of Engineering
Chulalongkorn University
Academic Year 2004

ISBN 974-17-7061-8

Thesis Title	EFFECT OF ORGANIC SOLVENTS ON CRYSTAL SHAPE AND ULTRAVIOLET ABSORPTION OF ZINC OXIDE SYNTHESIZED VIA SOLVOTHERMAL METHOD
By	Miss Parawee Tonto
Field of Study	Chemical Engineering
Thesis Advisor	Suphot Phatanasri, D.Eng.
Thesis Co-advisor	Okorn Mekasuwandumrong, D.Eng.

Accepted by the Faculty of Engineering, Chulalongkorn University in Partial Fulfillment of the Requirements for the Master's Degree

.....……Dean of the Faculty of Engineering
(Professor Direk Lavansiri, Ph.D.)

Thesis Committee

.....Chairman
(Montree Wongsri, D.Sc.)

.....Thesis Advisor
(Suphot Phatanasri, D.Eng.)

.....Thesis Co-advisor
(Okorn Mekasuwandumrong, D.Eng.)

.....Member
(Waraporn Tanakulrungsank, D.Eng.)

.....Member
(Akawat Sirisuk, Ph.D.)

ปารวี โทนโต๊ะ: ผลของตัวทำละลายอินทรีย์ที่มีต่อรูปร่างของผลึกและการดูดกลืนรังสีอัลตราไวโอเลตของซิงค์ออกไซด์ที่สังเคราะห์โดยวิธีโซลโวเทอร์มอล (EFFECT OF ORGANIC SOLVENTS ON CRYSTAL SHAPE AND ULTRAVIOLET ABSORPTION OF ZINC OXIDE SYNTHESIZED VIA SOLVOTHERMAL METHOD) อ. ที่ปรึกษา: ดร. สุพจน์ พัฒนะศรี, อาจารย์ที่ปรึกษาร่วม: ดร.โอกร เมฆาสุวรรณดำรง, 134 หน้า ISBN 974-17-7061-8

ผลึกขนาดนาโนเมตรของซิงค์ออกไซด์สังเคราะห์ได้จากปฏิกิริยาทางความร้อนของซิงค์อะเซเตต 10-25 กรัม ในตัวทำละลายอินทรีย์ต่างๆ ที่อุณหภูมิ 200 และ 300 องศาเซลเซียส รูปร่างของซิงค์ออกไซด์ที่สังเคราะห์ได้เป็นแท่งขนาดนาโนเมตร ที่ปลายของแท่งขนาดนาโนเมตรพบว่าเป็นโครงสร้างเฮกซะโกนอล เมื่อปริมาณซิงค์อะซิเตตและอุณหภูมิในการเกิดปฏิกิริยาเพิ่มค่าเฉลี่ยความยาวและเส้นผ่านศูนย์กลางของซิงค์ออกไซด์เพิ่มขึ้นด้วย อย่างไรก็ตามอัตราการโตระหว่างระนาบของซิงค์ ออกไซด์คงที่ ซึ่งสนับสนุนได้ว่าปริมาณของซิงค์อะซิเตตและอุณหภูมิของการเกิดปฏิกิริยาไม่มีผลต่ออัตราการโตระหว่างระนาบของผลึกซิงค์ออกไซด์ ซิงค์ออกไซด์ที่สังเคราะห์ได้ในไกลคอล (1,3 โพรเพนไดออล, 1,4 บิวเทนไดออล, 1,5 เพนเทนไดออล และ 1,6 เฮกเซนไดออล) อัตราการโตของผลึกเพิ่มขึ้นเมื่อจุดเดือดของไกลคอลเพิ่มขึ้น ในขณะเดียวกันในแอลกอฮอล์ (1-บิวทานอล, 1-เฮกซานอล, 1-ออกทานอล และ 1-เดกคานอล) และ ในตัวทำละลายเบนซิน, โทลูอีน และ ไซลีน อัตราการโตเพิ่มขึ้นเมื่อจุดเดือดของตัวทำละลายอินทรีย์เหล่านี้เพิ่มขึ้นด้วย อัตราการโตที่คงที่ขึ้นอยู่กับตัวทำละลายอินทรีย์ที่ใช้ ผลกระทบของสภาวะการเกิดปฏิกิริยาและการเกิดผลึกถูกแสดงได้โดยการใช้เทคนิค XRD, SEM, TEM, IR และ EDS โครงสร้างของการเกิดปฏิกิริยาที่พบคือปฏิกิริยาเอสเทอริฟิเคชั่นของสารตั้งต้นซิงค์อะซิเตตด้วยแอลกอฮอล์

ภาควิชา.....วิศวกรรมเคมี..... ลายมือชื่อนิสิต.....

สาขาวิชา.....วิศวกรรมเคมี..... ลายมือชื่ออาจารย์ที่ปรึกษา.....

ปีการศึกษา.....2547..... ลายมือชื่ออาจารย์ที่ปรึกษาร่วม.....

##4670379021 : MAJOR CHEMICAL ENGINEERING
KEY WORD: ZnO/solvothermal/nanorods/solvent
PARAWEE TONTO: EFFECT OF ORGANIC SOLVENTS ON CRYSTAL SHAPE AND ULTRAVIOLET ABSORPTION OF ZINC OXIDE SYNTHESIZED VIA SOLVOTHERMAL METHOD. THESIS ADVISOR: SUPHOT PHATANASRI, D.Eng. THESIS CO-ADVISOR: OKORN MEKASUWANDUMRONG, D.Eng. 134 pp. ISBN 974-17-7061-8

ZnO nanoparticles were successfully synthesized by solvothermal reaction of zinc acetate 10-25 g in various organic solvents at 200-300°C for 2h. The as-synthesized ZnO shape represented an aggregation of nanorods. Moreover, hexagonal structure was observed at the end of rod. It was found that when the amount of zinc acetate and the temperature of reaction increased, the average length and diameter were increased. However, the growing ratio between ZnO planes was constant. It suggests that the amount of zinc acetate and the temperature of reaction did not affect the growing rate ratio between planes of ZnO crystal. The aspect ratio of ZnO as-synthesized in glycol (1,3 propanediol, 1,4 butanediol, 1,5 pentanediol and 1,6 hexanediol) increased when the boiling point of glycol increased. The ZnO synthesized in alcoholic solvents (1-butanol, 1-hexanol, 1-octanol and 1-decanol) exhibited the aspect ratio similarly to those synthesized in inert solvents (benzene, toluene and xylene) and the aspect ratios of both were increased proportionally to boiling point of different solvents. The aspect ratio of using an individual solvent was constant without changing synthesis condition. The effect of reaction conditions and crystallization mechanism were proposed by interpretation of SEM, TEM, IR and EDS results. It could propose that a mechanism of solvothermal reaction might be an esterification of starting zinc acetate precursor and alcohol on surface of zinc acetate seeds.

Department…Chemical Engineering…… Student's signature……
Field of Study Chemical Engineering….. Advisor's signature……...
Academic year……2004……...Co-advisor's signature……...

ACKNOWLEDGEMENTS

The author would like to express her greatest gratitude to her advisor, Dr. Suphot Phatanasri for his invaluable guidance throughout this study. Special thanks to Dr. Okorn Mekasuwandumrong, her co-advisor, for her kind supervision of this research. In addition, I would also grateful to Dr. Montree Wongsri, as the chairman, Dr. Waraporn Tanakulrungsank and Dr. Akawat Sirisuk, a member of thesis committee.

The author would like to acknowledge to Thailand Research Fund (TRF), Graduate School of Chulalongkorn University and TJTTP-TBIC for their financial support throughout the master course.

Best regards are expressed to, Professor Dr. Piyasan Praserthdam, Miss. Patta Soisuwan and many best friends in Centre of Excellence on Catalysis and catalytic Reaction Engineering, Department of Chemical Engineering who have provided encouragement and cooperation throughout this study.

Finally, she also would like to dedicate this thesis to her parents who have always been the source of her support and encouragement.

CONTENTS

Page

LIST OF TABLES

LIST OF FIGURES

Page

Page

Page

Page

Page

Page

CHAPTER I

INTRODUCTION

Solid nanostructured materials have been attracting due to their potential use as active components or interconnects in fabricating nanoscale electronic, optical, optical electronic, electrochemical, and electromechanical devices. The precise control of morphology of semi-conducting oxide materials at nanometric scale is of importance for a fine-tuning of their physical properties such as electrical properties or magnetic, optical and mechanical characteristics. Different shapes of ZnO powder are such prismatic, ellipsoidal, nanowire, nanorods (Gou et al, 2002), nanotube (King et al, 2004) and whiskers (Hu et al, 2001). All of the shapes can be prepared via different synthesis methods or under different conditions.

Zinc oxide is recognized as one of the most promising oxide semiconductor materials because of its good optical, electrical and piezoelectrical properties. It has received a considerable amount of attention over last few years because of many applications. It has found in various fields and has a good potential to be applied for high temperature electronics including short wavelength display diodes and lasers. Especially, ZnO nanostructured materials are expected to possess properties having applications in shock resistance, sound insulation, varistors, gas-sensors, catalysts, light emitting diodes (LEDs), photodetectors, solar cells and ultraviolet nanolasers. ZnO in polymer matrix are good reputation composite, which can absorb and shield electromagnetic waves and eliminate static charge deposition in some electro devices.

In a last decade, ZnO particles have been prepared by various methods such as solvothermal synthesis (Inoue et al, 1992), hydrothermal synthesis (Sue et al, 2004), thermal decomposition (Yang et al, 2004), spray pyrolysis (Zhoa et al, 1998), sol-gel synthesis (Kamalasanan et al, 1996), wet chemical techniques (Wu et al, 20004), chemical vapor deposition (CVD) (Kim et al, 2003) and precipitation method (Rodriguez et al, 2001). In such method, required characteristics are obtained by controlling the crystal type, crystal size, particle shape and particle size distribution.

Cheng et al (2004) reported a few achieved preparations resulting in 1-D ZnO nanostructure such as wet chemical technique. However, the wet chemical method mostly failed to produce small diameter ZnO nanorods and rods shape nanoparticles. The spray pyrolysis process exhibited great application prospects for pure uniform ultrafine particles and by this method, morphology and composition of product particles can be controlled (Zhoa et al, 1998). Besides wet chemical and spay pyrolysis techniques, sol-gel method represented more advantage of them because it requires much lower temperature to obtain the products.

Solvothermal synthesis is one of the interesting methods. It is improved from the hydrothermal synthesis by using organics solvent instead of water at elevated temperature (200-300°C) under autogeneous pressure of organics during the preparation process. This technique is based on thermal decomposition of organometallic compound in organic solvent and the technique has been successfully applied for the synthesis of various types of nanosized metal oxide with large surface area, high crystallinity and high thermal stability (Inoue et al, 1995; Iwamoto et al, 2001; Mekasuwandumrong et al, 2004). Moreover, it has successfully prepared small diameter single crystalline and high crystallization ZnO nanorods in one step.

Thermal decomposition of zinc inorganic salt is one of the versatile ways to obtain ZnO nanomaterials, in which zinc acetate ($Zn(CH_3COO)_2$) is often chosen as a precursor because of its high solubility and low decomposition temperature .

Different levels growth controls for ZnO nanorods (including positional, orientational, diameter and density control) have been achieved, however, controlling shape of nanostructure can be obtained difficultly. Zhang et al (2004) suggested that shape and size of nanomaterials influenced sensitively on electrical and optical properties.

In this study, the solvothermal method was employed to synthesize ZnO nanorods which a novel seed growth process in 1 step of highly oriented ZnO nanorods by using low temperature reaction and short time reaction.

In this thesis, the obtained ZnO have been use to investigate:

1. The effect of temperature, concentration and organic solvent on the properties of ZnO nanoparticles
2. The crystallization mechanism of ZnO by thermal reaction of zinc acetate in alcohol.

The present thesis is arranged as follows:

Chapter II presents literature reviews of the preparation method in previous works related to this research.

Chapter III composes of the basic theory about ZnO, i.e. the general properties and various preparation methods to obtain the ZnO nanoparticles.

Chapter IV describes preparation method of ZnO by solvothermal method and characterization.

Chapter V exhibits the experimental results.

In the last chapter, the overall conclusions and recommendation for the future studies of this research are given in chapter VI.

Finally, the samples of calculation for crystallite size, BET surface area and GC/MS spectrum are included in appendices at the end of this thesis.

CHA PTER II

LITERATURE REVIEWS

Recently has been reported that there are severally studies to synthesize ZnO nanoparticles, controlled morphologies and to investigate ZnO properties.

Zinc oxide (ZnO), excellent chemical and thermal stability (Li et al, 2005), and the electrical properties of a II-VI group compound semiconductor with a wide direct-band gap of 3.3 eV, might be a good potential candidate in several applications such as semiconductor, catalysis. The ZnO powder has a hexagonal zincite structure (Wang, 2003). It has been used for transparent conductive films, varistors, solar cell windows and bulk acoustic wave devices. ZnO powder with suitable dopants is used as a photoconductor in electrography, a varistor in ceramic technology and an additive in various ferrites. Morover, ZnO has a large exiton binding energy of 60 meV at room temperature and it can ensure an efficient UV emission at a room temperature under a low excitation energy (Lyu et al, 2002). ZnO has been introduced as additive to polymer to form the composite that can absorb and shield electromagnetic waves and eliminate static charge deposition in some electron devices.

One-dimension crystals such as nanorods, nanotubes (Xing et al, 2004), nanowires or nanowhiskers (Hu et al, 2001) have attracted much attention due to their specific physical properties and interesting applications in nanodevices. Nanometre-size inorganic rods exhibit a wide range of electrical and optical properties that depend sensitively on both shape and size (Lieber, 1998). Shape control has shown significant concern in the fabrication of semiconductor nanocrystals, metal nanocrystals and other inorganic materials. Qu et al (2004) found that the physical properties of the semiconductor quantum dots could be manipulated by changing their size and/or shape. To obtain ZnO powders with appropriate chemical, electrical and optical properties specifically for intended application, synthesis condition to control morphology, chemical composition and particle size is the most important (Xu et al, 2004). For the application of ZnO as pigment, the morphology and particle size are essential parameters (Music, 2002). Zhang et al (2004) reported that the key for

controlling shape and size is a level of supersaturation in thermal evaporation of zinc powders that control ZnO nucleation and growth.

The developments of nanoelectronic and nanooptoelectronic devices, nanoscaled ZnO materials with high surface area and quantum confinement effect is currently attracting considerable interest (Yang et al, 2004). ZnO nanorods have been produced by several techniques such as glycothermal synthesis, thermal decomposition, hydrothermal syntheses, sol-gel synthesis, chemical vapor deposition, spray pyrolysis, wet-chemical methods, and gas reaction method (Li et al, 2001), etc.

The thermal genesis of metal oxides from inorganics precursors has been widely adopted to obtain technologically important materials (Hussien, 1991). The physical and chemical characteristics of the precursor have great effects on the particle morphology and composition. Thermal decomposition of zinc salt such as $Zn(CH_3COO)_2$ is still powerful approach to obtain ZnO nanoscaled materials. Yang et al (2004) studied size control of ZnO nanoparticles via thermal decomposition of zinc acetate coated on organic additives. They used zinc acetate as precursor because its high solubility and low decomposition temperature (Gardner, 1984). Moreover, it has been reported that zinc acetate has been widely used as a precursor of thermal decomposition method such as work of Yang et al (2003). Beside zinc acetate, other chemicals have been introduced. Kim et al (2003) used zinc acetylacetonate hydrate as precursor of vapor deposition method while Saravanan (2004) used zinc (II) cupferron complex as precursor in thermal decomposition method.

Nanocrystalline material and nanocomposites are composed of ultrafine crystallite sizes (<50 nm). Nanoclusters are subject of current interest because of their unusual magnetic, optical, electronic properties, which are often different from their bulk properties. Nanostructures metal-oxide thin films are applied to be a gas sensor (NO_x, CO, CO_2, CH_4 and aromatic hydrocarbon) with highly efficient sensitivity and selectivity. Nanosize metallic powders have been used for the production of gas tight materials, dense parts and porous coating (Ahmed, 1999). Nanometer-size particles have different physical and chemical properties from bulk materials.

ZnO has received a considerable amount of attention over the fast few years. There have been many existing preparation techniques for this material. One of the interesting processes is the synthesis by using organic solvents. Inoue et al. has developed a new synthesis method for inorganic materials by using organic media at elevated temperature (200-300°C) under autogeneous pressure of organics for many years. It has been found that many oxides and mixed oxides can be crystallized in organic media at temperatures lower than that required by the hydrothermal reaction. They (Inoue et al, 1988) reported that the thermal reaction of gibbsite in ethylene glycol at 250°C yielded an ethylene glycol derivative of boehmite and they have found that microcrystalline χ-alumina is formed under quite mild condition. The synthetic process as mentioned above, the use of glycol (organic solvent) instead of water in the system is different method from the conventional methods. This method was called "Glycothermal method" and they (Inoue et al, 1992) also found that this reaction in inert organic solvents such as toluene, benzene and/or others can be occurred by thermal decomposition of AIP and yielded a product composed of 4 to 20 nm particles having the χ-alumina mixture. The χ-alumina was stable and maintained a surface area above100 m^2/g until its transformation at 1150 °C to be α-alumina. With this result, they applied this method for zirconia synthesis and reported that thermal decomposition of zirconium alkoxides in organic solvents yielded tetragonal zirconia, which had a large surface area and a fairly high thermal stability. However, zirconium n-alkoxides, which decomposed into glycols did not decompose at 300 °C in inert organic solvent (Inoue et al, 1993). Bae et al (1998) prepared Magnetite, Fe_3O_4, powder under glycothermal conditions in 1,4 butanediol by precipitation from metal nitrates with aqueous ammonium hydroxide. Fine powders were obtained in the temperature range 190 to 270°C. The average particle diameter of Fe_3O_4 increased with increasing reaction temperature and time. The specific surface areas of the synthesized Fe_3O_4 powders decreased with increasing reaction temperature.

Solvothermal synthetic methods have been developed by using organic solvents such as pyridine at 180°C (Li et al, 1999). The syntheses were accomplished at a relatively low temperature and pressure in a closed system and could be easily controlled. The most straightforward way to synthesize ZnSe and CdSe is a direct combination of elemental metal and selenium at very high temperature. Peng et al

(2001) studied solvothermal method provides us a new idea and greatly decrease the direct reaction temperature of elemental Zn (or Cd) and Se. They successfully synthesized ZnSe and CdSe at 180 °C for 24h without stirring. Many papers mentioned above explain the synthesis of several metal oxides and binary metal oxides in organic solvents. The product was produced by glycothermal method and solvothermal method has high thermal stability. This novel method may be a new route to prepare micro- and nanocrystalline metal oxides. And in this method, it can be control the morphologies of metal oxides.

Yin et al (2001) reported a new synthesis of ZnO nanorods by thermal decomposition of zinc acetate in organic solvents such as oleic acid, which produces relatively monodisperse ZnO nanorods (ZnO quantum rods) with diameters of 2 nm and lengths in the range 40-50 nm. Xu et al (2002) reported a simple and novel approach to fabricate ZnO nanorods with diameter of 10-60 nm and lengths of several micrometers by thermal decomposition of the precursor of ZnC_2O_4 obtained via chemical reaction between zinc acetate and oxalic acid in the presence of surfactant nonyl phenyl ether (9)/(5). At the same time, Xu et al successfully synthesized tin oxide nanorods by thermal decomposition of SnC_2O_4 precursor via chemical reaction between $SnCl_2{\cdot}2H_2O$ and $Na_2C_2O_4$ in the presence of same surfactant and NaCl flux. They found that the formation of the nanorods must be affected by the character of the starting material, such as the particle size. Only in this way can the ZnO and tin oxide nanorods be formed in the presence of the suitable NaCl and surfactant NP-9/5.

Hydrothermal synthesis, an important method for wet chemistry, has been employed for the preparation of ZnO materials in the last decade, and particles with narrow size distribution can be observed without microagglomeration or a little of microagglomeration. Moreover, well crystallization and phase homogeneity can be obtained by Sakagami(1990). This method is becoming popular because of environmental reason. Since water is used as the reaction solvent instead of organic solvent. The hydrothermal synthetic route (Yoshimura, 1998) has advantages to obtain high-crystallized powders with narrow grain size-distribution and high purity without heat treatment at high temperature (Chittofrti et al, 1990). The particle properties such as morphology and size can be controlled via the hydrothermal

process by adjusting the source species, reaction temperature and time, etc (Xu et al, 2004). Liu et al (2003) reported that they have been preparing single crystal ZnO for long time single crystal growth but the wet-chemical approaches still face problems of polydispersivity and difficulties in bringing the rod diameters down to sub-100nm regime. Xu et al, 2004 studied preparation of ZnO particles with various morphologies hydrothermal treatment of zinc acetate in pure water, KOH or ammonia aqueous solution and they found that the selected solvents play a different role in controlling the morphologies of the obtained powders. In pure water, the pencil-like are obtained while different concentration KOH solutions showed changing of morphologies from twinned pyramidal, shortened prismatic, sheet to prismatic-like. Ellipsoidal and long prismatic-like shapes were obtained when using various concentrated ammonia solution as solvent. Lu et al (2000) has successfully prepared by applying ammonia as the base source via hydrothermal at temperature ≥ 100°C. They reported that the increase of the reaction temperature slightly reduces particle size and production yield of ZnO powder. On the other hand, as a pH of starting solution increases from 9to12, the morphology of ZnO powder markedly varies from an ellipsoidal shape to a rod-like shape. Wei et al (2004) has been successfully prepared ZnO nanorods by hydrothermal synthesis using $Zn(OH)_4^{2-}$ precursor in alcohol solution with surfactant free. The results show that single crystalline ZnO nanorods grow from ZnO nuclei spontaneously, and +c-axis ((001) direction) is the fast growth direction.

Under the hydrothermal condition, the growth rate is significantly contrary to the controlled orientation. As the concentration of growth units increases, the growth rate will also increase, while the growth orientation tends to be more confused. To achieve high growth rate and good orientation simultaneously is the goal of many materialists (Sun et al, 2002). Li et al (2005) found that nanorod ZnO obtained various diameters to concentration of reactants, reaction temperature, and solution pH. The length of the ZnO nanorods is controlled by growth time and by the concentration of reagents in the aqueous solution. Cheng et al (2004) studied 1-D ZnO nanorods with different aspect ratios were synthesized by a one-step, hydrothermal method. In a typical procedure, solutions of zinc acetate dehydrate in methanol, ethanol and solutions of sodium hydroxide (NaOH) in methanol, ethanol with different

concentrations were prepared as stock solutions in advance. They found that the diameter of ZnO nanorods prepared in methanol is around 25 nm, the length is around 100 nm (aspect ratio 4:1) and the one in ethanol is around 40 nm and 500 nm (aspect ratio > 10:1), respectively. They studied 1-D ZnO growth along the *c*-axis under hydrothermal conditions is related to both its intrinsic crystal; its growth habit under hydrothermal condition. In general the growth rate of a plane will be controlled by a combination of internal, structurally-related factors (intermolecular boding preference or dislocations), and external factors (supersaturation, temperature, solvents and impurities) (Kubota, 2001). They inferred that the different aspect ratios of ZnO nanorods raised from different growth rates along the c-axis in different reaction media. *i.e.*, the growth rate along the c-axis in ethanol is higher than that in methanol.

Sol-gel synthesis, one of the major problems in using the sol-gel route for the synthesis of ZnO thin film is the insoluble nature of zinc alkoxides in most of alcohols.

Kamalasanan (1996) reported the preparation of high quality zinc oxide thin films from a sol prepared from zinc acetate, ethylene glycol and n-propyl alcohol and triethyl amine (TEA).

ZnO nanoparticles with different morphologies have been obtained by controlling different perameters of the precipitation process, pH and washing medium (Rodriguez-Paez et al, 2001). Meulenkamp found that aging of particles was governed by temperature, the water content, and the presence of reaction products. Water and acetate induced considerably accelerated particle growth.

Flame aerosol technology is widely employed for large-scale manufacture of carbon black and ceramics commodities such as fumed silica and titania and to a lesser extent, for special chemicals such as zinc oxide and alumina powders (Pratsinis, 1998). The spray pyrolysis process differs from spray drying in the use of a solution, the consequent process of precipitation or condensation within a droplet, and the use of a significantly higher temperature (usually>300°C). The key challenges of spray pyrolysis are control over the morphology and composition of product particles. Zhao

(1998) studied spray pyrolysis from solution of zinc acetate dehydrate and they successfully synthesized pure ZnO ultrafine powders with a uniform size of 20-30nm.

Xing et al (2004) reported (001) direction is fastest growth face of ZnO crystals at the nanotube walls tend to grow along the c-axis and the (100) facet is mostly exposed. Jeyagowry (2002) reported, in normal precipitation conditions, ZnO nanorods have been grown along the c-axis of the crystal (wurtzite structure) while the C_6 symmetry is strictly maintained for their external crystal facets. The growth axes are pendicular to the highest symmetrical crystallographic planes of the crystals. ZnO nanorods in a novel aqueous solution method (Li et al, 2005) are found to grow along (0001) direction. Li et al. (1999) concluded that the direction of the crystal face with the corner of the coordination polyhedron occurring at the interface has the fastest growth rate; the direction of the crystal face with the edge of the coordination polyhedron occurring at the interface has the second fastest growth rate; the direction of the crystal face with the face of the coordination polyhedron occurring at the interface has the slowest growth rate.

CHAPTER III

THEORY

Nanoparticles can be considers solid structures with nanometer-scale dimensional repeat distances between the different phases that constitute the structure. Nanostructure phases present in nanocomposites as zero-dimensional (e.g., embedded cluster), 1D (one dimensional; e.g., nanotubes), 2D (nanoscale coatings), and 3D (embedded networks). In general, nanomaterials can demonstrate different mechanical, electrical, optical, electrochemical, catalytic, and structural properties than those of each individual component. (Ajayan et al, 2003)

3.1 Zinc oxide (ZnO)

ZnO, an n-type II–VI compound semiconductor with a wide direct-band gap of 3.3 eV. The bandgap of ZnO can be tuned via divalent substitution on the cation site. It has attracted more and more attention over the past few years because it can find applications in various fields, such as photosensitization, field emission display, gas sensors, varistors and transducers, etc. The large ZnO exciton binding energy of 60 mV makes this material an attractive candidate for room-temperature lasing and low dimensional nanostructured ZnO offers the possibility of further improving lasing conditions due to quantum confinement effects.

ZnO is unique because it exhibits dual semiconducting and piezoelectric properties. ZnO normally forms in the hexagonal (wurtzite) crystal structure with a = 3.25 Å and c = 5.12 Å, as shown in Figure 3.1. The Zn atoms are tetrahedrally coordinated to four O atoms, where the Zn d-electrons hybridize with the O p-electrons. The wurtzite structure family has a few important members, such as ZnO, GaN, AlN, ZnS, and CdSe, which are important materials for applications in optoelectronics, lasing, and piezoelectricity. Some of the physical properties of ZnO are listed in Table 3.1. Of great importance is the fact that it completely absorbs ultraviolet light below 366 nm and, thus, is unique among white pigments. It high

refractive indexes make it a good white pigment where its mean diameter for maximum light scattering is 0.25 μm. Variously doped oxides are used for photocopying, catalysts and phosphors.

Primary zinc oxide is manufactured by oxidizing zinc vapor in burner wherein the concentration of zinc vapor and the flow of air is controlled so as to develop the desired particle size and shape. The purity of the zinc oxide depend upon the source of the zinc vapor.

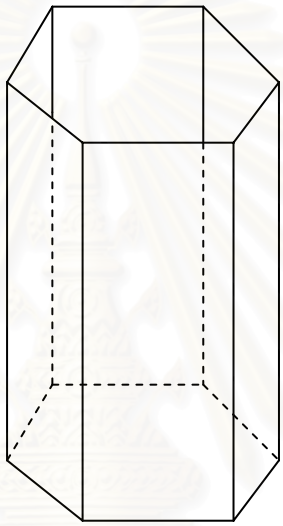

Figure 3.1 Crystal structure of zinc oxide.

Table 3.1 The physical properties of zinc oxide

Properties	
Melting point, °C	1,975
Color	white
Refractive index	2.015, 2.068
Exciton binding energy, meV	60
Density, g/cm^3	5.606
Specific gravity	5.68
Heat capacity, J/(mol. °C)	40.26
Enthalpy, kJ/mol	-356.1
Entropy, kJ/mol	43.65
Coefficient of expansion, ×10-6/°C	4.0
Conductivity(n-type), S/cm	10^{-7}-10^3
Crystal structure	hexagonal, wurtzite
Dimension, Å ; a c	3.24 5.19

3.2 Preparation procedure

Zinc oxide powders have been prepared by several methods. The physical and chemical properties of zinc oxide are quite different by the process of preparation.

3.2.1 Hydrothermal method (West, 1997)

The method involves heating the reactants in water/steam at high pressures and temperatures. The water performs two roles, as a pressure-transmitting medium and as a solvent, in which the solubility of the reactants is pressure and temperature dependent. In addition, some or all of the reactance are partially soluble in the water under pressure and this enables reaction to take place in, or with the aid of, liquid and/or vapor phases. Under these conditions, reactions may occur that, in the absence of water, would occur only at much high temperatures. The method is therefore

particularly suited for the synthesis of phases that are unstable at higher temperatures. It is also a useful technique for growth of single crystals. By arranging for a suitable temperature gradient to be present in the reaction vessel, dissolution of the starting material may occur at the hot end and reprecipitation at the cooler end.

Since hydrothermal reactions must be carried out in closed vessels. The pressure- temperature relations of water at constant volume are important. The critical temperature of water is 374°C. Below 374°C, two fluid phases, liquid and vapor, can coexist. Above 374°C only one fluid phase, supercritical water ever exists. At pressures below saturated steam curve liquid water is absent and the vapor phase is not saturated with respect to steam.

The design of hydrothermal equipment is basically a tube, usually of steel, closed at one end. The other end has a screw cap with a gasket of soft copper to provide a seal. Alternatively, the bomb may be connected directly to an independent pressure source, such as a hydraulic ram: this is known as the “cold seal” method. The reaction mixture and an appropriate amount of water are placed inside the bomb which is then sealed and placed inside an oven at the required temperature.

Hydrothermal methods have been used successfully for the synthesis of many materials. A good example is the family of calcium silicate hydrates, many of which are important components of set cement and concrete. Typically, lime, CaO and quartz, SiO_2, are heated with water at temperatures in the range 150 to 500°C and pressure of 0.1 to 2 kbar. Each calcium silicate hydrate has, for its synthesis, optimum preferred conditions of composition of starting mix, temperature, pressure and time. For example, xonolite, $Ca_6Si_6O_{17}(OH)_2$, may be prepared by heating equimolar mixtures of CaO and SiO_2 at saturated stream pressures in the range150 to 350°C.

For the growth of single crystals by hydrothermal methods it is often necessary to add mineralizer. A mineralizer is any compound added to the aqueous solution that speeds up its crystallization. It usually operates by increasing the solubility of the solute through the formation of soluble species that would not usually

be in the water. For instance, the solubility of quartz in water at 400°C and 2 kbar is to small to permit the recrystallization of quartz, in a temperature gradient, within a reasonable space of time. On addition of NaOH as a mineralizer, however, large quartz crystals may be readily grown. Using the following condition, crystals of kilogram size have been grown: quartz and 1.0 M NaOH solution are held at 400°C and 1.7 kBar: at this temperature some of the quartz dissolves. A temperature gradient is arranged to exist in the reaction vessel and at 360 °C the solution is supersaturated with respect to quartz which precipitates onto a seed crystal.

3.2.2 Glycothermal and solvothermal method

Glycothermal and solvothermal method have been developed for synthesis of metal oxide and binary metal oxide by using glycol and solvent as the reaction medium, respectively. The use of glycol or solvent instead of water in the hydrothermal method produced the different form of intermediate phase and the stability of such intermediate phase was not strong. Instability of the intermediate phase gives a large driving force to the formation of product under quite mild condition. The syntheses were accomplished at a relatively low temperature and pressure in a closed system and could be easily controlled, but the organic solvent is usually harmful to the environment and not appropriate for use on a large scale (Peng, 2001).

The solvothermal synthesis consists in modifying the physico-chemical properties of the solvent in order to reach a critical behavior. Then, finely divided microcrystallites of various materials can be elaborated through this process(Verdon et al, 1995). The solvothermal process can be used in different ways according to:

(i) The nature of the solute (liquid or solid),

(ii) The chemical reaction (oxidation or reduction) involved during the process.

Considering the interaction between the solvent and the solute, three main synthesis routes can be concerned:

(1) The solvothermal precipitation - the material precursor is insoluble and therefore the solute and the solvent are initially in the same liquid phase.

(2) The solvothermal decomposition - the material precursor is insoluble in the solvent. In this case, the critical temperature of the selected solvent is adjusted to the decomposition temperature of the precursor.

(3) The solvothermal recrystallization - the finely divided precursor has the same chemical composition as the final material, but is amorphous or poorly crystallized. (Verdon et al, 1995)

The preparation method is described in the experimental section, Chapter IV.

3.2.3 Thermal spray pyrolysis

Spray pyrolysis (SP) is a type of aerosol process for the synthesis of ultrafine powder that develops on the basis of spray drying. The SP process is similar to spray drying in many aspects, but it differs from spray drying in the use of a solution, the consequent process of precipitation or condensation within a droplet, and the use of a significantly higher temperature (usually>300°C). The SP process has great application prospects for the preparation of pure uniform ultrafine particles.

Thermal spray processing is a commercially relevant, proven technique for processing nanostructureed coating. Thermal spray techniques are effective because agglomerated nanocrystalline powders are melted, accelerated against a substrate, and quenched very rapidly in a single step. This rapid melting and solidification promotes the retention of a nanocrystalline phase and even amorphous structure. Retention of the nanocrystalline structure leads to enhanced wear behavior, greater hardness, and sometimes a reduced coefficient of friction compared to conventional coatings. (Pulikel et al, 2003)

The ability to maintain the nanocrystalline structure during processing and upon consolidation is critical to improving its properties because it is the nanoscale microstructure that leads to the unique properties. Several parameters are critical: (a)

the thermal stability of the agglomerated powders: nanocrystalline materials can experience grain growth at temperatures well below the temperatures observed for conventional materials. The high surface area drives this growth. (b) The degree of melting that occurs in flight: this can be controlled by the spray distance, the temperature of the jet, and the velocity of the jet, and optimal parameters are determined primarily by experiment. (c) The cooling rate: a high cooling rate leads to high nucleation and slow grain growth, which promotes the formation of nanocrystalline grains. The systems that tend to maintain their nanocrystallne structure even at elevated temperature are apt to have impurities or a second phase that stabilize the grain structure.

3.2.4 Precipitation method

Precipitation method involves the growth of crystals from a solvent of different composition to the crystal. The solvent may be one of the constituents of the desired crystals, e.g., crystallization of salt hydrate crystals using water as the solvent, or the solvent may be entirely separate liquid element or compound in which the crystals of interest are partially soluble, e.g., SiO_2 and various high melting silicates may be precipitated from low melting borate or halide melts. In these cases, the solvent melts are sometimes referred to as fluxed since the effectively reduce the melting point of the crystals by a considerable amount.

A variety of particle sizes and shapes can be produced, depending on the reaction conditions. Moreover, the particles can be agglomerates of much finer primary particles.

3.2.5 Sol-gel method

Sol-gel chemistry is based on inorganic polymerization reaction. When ultrafine colloidal dispersions lose fluid they can turn into a highly viscous mass. Such a mass is called a gel. When chemical methods are used to turn solution of metal compounds into gels, we are dealing with sol-gel process. Highly reactive and pure ceramic powders can be prepared from such gels. Two routes are usually described in

the literature depending on whether the precursor is an aqueous solution of an inorganic salt or an alkoxide in an organic solvent.

3.3 Single crystal (McGraw-Hill encyclopedia of science & technology, 1997)

In crystalline solids the atoms or molecules are stacked in a regular manner, forming a three-dimensional pattern, which may be obtained by a three-dimensional repetition of a certain pattern unit called a unit cell. When the periodicity of the pattern extends throughout the certain piece of material, one speaks of a single crystal. A single crystal is formed by the growth of a crystal nucleus without secondary nucleation or impingement on other crystal.

3.3.1 Growth techniques

Among the most common methods of growing single crystals are those of P. Bridgeman and J. Czochralski. In the Bridgeman method the material is melted in a vertical cylindrical vessel, which tapers conically to a point at the bottom. The vessel then is lowered slowly into a cold zone. Crystallization begins in the tip and continues usually by growth from the first formed nucleus. In the Czochralski method a small single crystal (seed) is introduced into the surface of the melt and then drawn slowly upward into a cold zone. Single crystals of ultrahigh purity have been grown by zone melting. Single crystals are also often grown by bathing a seed with a supersaturated solution, the supersaturation being kept lower than necessary for sensible nucleation.

When grown from a melt, single crystals usually take the form of their container. Crystals grown from solution (gas, liquid, or solid) often have a well-defined form, which reflects the symmetry of the unit cell. For example, rock salt or ammonium chloride crystals often grow from solutions in the form of cubes with faces parallel to the 100 planes of the crystal, or in the form of octahedrons with faces parallel to the 111 planes. The growth form of crystals is usually dictated by kinetic factors and does not correspond necessarily to the equilibrium form.

3.3.2 Physical properties

Ideally, single crystals are free from internal boundaries. They give rise to a characteristic x-ray diffraction pattern. For example, the Laue pattern of a single crystal consists of a single characteristic set of sharp intensity maxima.

Many types of single crystal exhibit anisotropy, that is, a variation of some of their physical properties according to the direction along which they are measured. For example, the electrical resistivity of a randomly oriented aggregate of graphite crystallites is the same in all directions. The resistivity of a graphite single crystal is different, however, when measured along crystal axes. This anisotropy exist both for structure-sensitive properties, which are strongly affected by crystal imperfections (such as cleavage and crystal growth rate), and structure-insensitive properties, which are not affected by imperfections (such as elastic coefficients).

CHAPTER IV

EXPERIMENT

The synthesis of zinc oxide samples using organic solvent explains in this chapter. The chemicals, catalyst preparation and characterization are explained in following section.

4.1 Chemicals

These synthesis are prepared with the following reagent:

1. Zinc acetate ($Zn(CH_3COO)_2$) available from Sigma-Aldrich, 99.99%
2. 1,3 Propanediol (1,3-PG, $HO(CH_2)_3OH$) available from Aldrich, 98%
3. 1,4 Butanediol (1,4-BG, $HO(CH_2)_4OH$) available from Aldrich, 99%
4. 1,5 Pentanediol (1,4-PeG, $HO(CH_2)_5OH$) available from Merck, 99%
6. 1,6 Hexanediol (1,4-HG, $HO(CH_2)_6OH$) available from Aldrich
7. 1-Butanol ($CH_3(CH_2)_3OH$) available from Analytical Univar Reagent
8. 1-Hexanol ($CH_3(CH_2)_5OH$) available from Aldrich, 98%
9. 1-Octanol ($CH_3(CH_2)_7OH$) available from Aldrich, 99%
10. 1-Decanol ($CH_3(CH_2)_9OH$) available from Aldrich, 99%
11. Toluene ($C_6H_5CH_3$) available from Analytical Univar Reagent
12. Benzene (C_6H_6) available from Merck.
13. O-Xylene ($C_6H_4(CH_3)_2$) available from Aldrich, 97%

Table 4.1 Reagents used for the synthesis of zinc oxide.

Reagents	Weight/Volume
Zinc acetate (various starting material concentrations)	10, 15, 20 g
Organic solvents (1,3-PG, 1,4-BG, 1,5-PeG, 1,6-HG, 1-Butanol, 1-Hexanol, 1-Octanol, 1-Decanol, Toluene, Benzene, Xylene)	
- In the synthesis mixtures	100 cm^3
- In the gap	30 cm^3

4.2 Equipment

All equipment using for the catalyst consisted of:

4.2.1 Autoclave reactor

- Made from stainless steel
- Volume of 1000 cm^3
- 10 cm inside diameter
- Maximum temperature of 350^oC
- Pressure gauge in the range of 0-140 bar
- Relief valve used to prevent runaway reaction
- Iron jacket was used to reduce the volume of autoclave to be 300 cm^3
- Test tube was used to contain the reagent and glycol

The autoclave reactor is shown in Figure 4.1

4.2.2 Temperature program controller

A temperature program controller CHINO DB1000F was connected to a thermocouple with 0.5 mm diameter attached to the reagent in the autoclave.

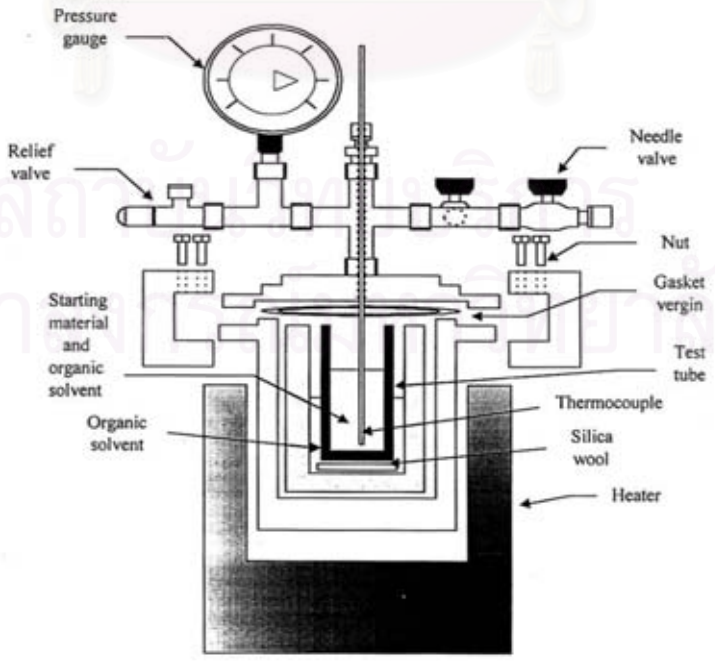

Figure 4.1 Autoclave reactor.

4.2.3 Electrical furnace (Heater)

Electrical furnace supplied the required heat to the autoclave for the reaction.

4.2.4 Gas controlling system

Nitrogen was set with a pressure regulator (0-150 bar) and needle valves are used to release gas from autoclave.

The diagram of the reaction equipment is shown in Figure 4.2

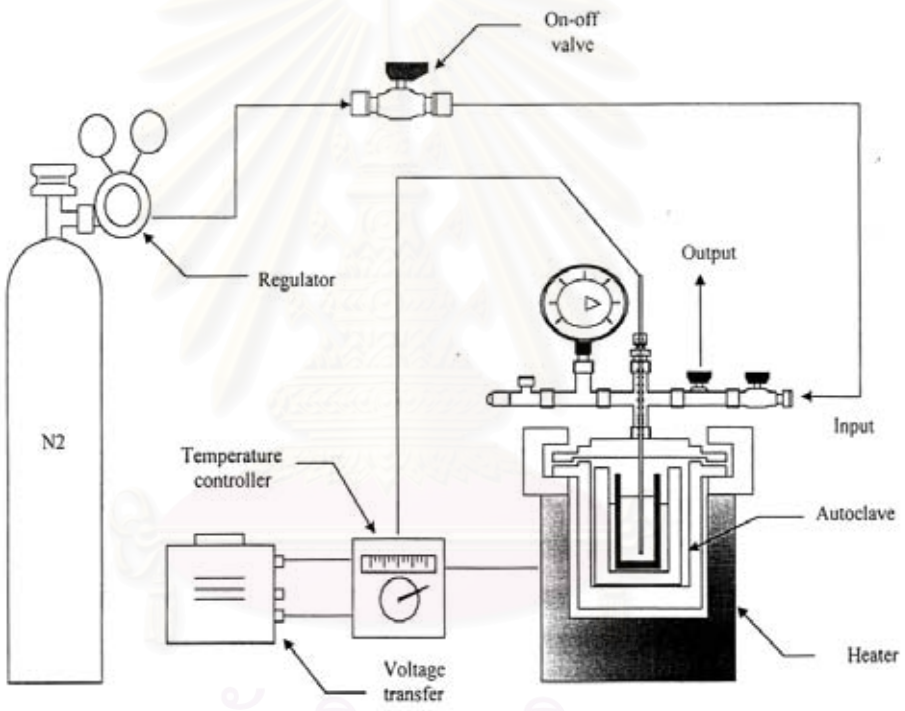

Figure 4.2 Diagram of the reaction equipment for the catalyst preparation.

4.3 Preparation of Zinc oxide

Zinc oxide was prepared by using zinc acetate for starting material. The starting material were suspended in 100 ml of solvent and in the test tube, and then set up in an autoclave. In the gap between the test tube and autoclave wall, 30 ml of solvent was added. After the autoclave was completely purged with nitrogen, the autoclave was heated to desired temperature (200^{o}C-300^{o}C) at the rate of 2.5°C min^{-1} and held at that temperature for 2 hours. Autogeneous pressure during the reaction

gradually increased as the temperature was raised. After the reaction, the autoclave was cooled to room temperature. The resulting powders were collected after repeated washing with methanol by centrifugation. They were then air-dried.

4.4 Characterization studies

4.4.1 X- Ray Diffraction analysis (XRD)

The crystallinity and X-ray diffraction (XRD) patterns of zinc oxide were performed by a X-ray diffractometer SEIMENS D5000 connected with a personal computer with Diffract AT version 3.3 program for fully control of the XRD analyzer at Center of Excellences on Catalysis and Catalytic Reaction Engineering, Chulalongkorn University. The experiments were carried out by using CuKα radiation with Ni filter and the operating condition of measurement is shown as below:

2θ range of detection	:	20 – 80 ^{o}
Resolution	:	0.04 ^{o}
Number of Scan	:	10

The functions of based line subtraction and smoothing were used in order to get the well formed XRD spectra.

4.4.2 Scanning Electron Microscopy (SEM)

The morphology and crystallite size of secondary particles of prepared zinc oxide were observed by using JEOL JSM6400 Scanning Electron Microscope (SEM) at the Scientific and Technological Research Equipment Centre, Chulalongkorn University (STREC).

4.4.3 Transmission Electron Microscope (TEM)

Morphology and crystallite size of primary particles of prepared zinc oxide were observed by using JEOL JEM1220 Transmission Electron Microscope (TEM) which operated at 80 kV at Kasetsart University Research and Development Institute.

The specimens for TEM were prepared by putting the as-grown products in ethanol and immersing them in an ultrasonic bath for 15 min, then dropping a few drops of the resulting suspension containing the synthesized materials onto a TEM grid.

4.4.4 Selected area electron diffraction (SAED)

The selected area electron diffraction (SAED) was performing by using a JEOL JEM-2010 which operated at 200 kV at National Metal and Materials Technology Center (MTEC).

The specimens for TEM were prepared by putting the as-grown products in ethanol and immersing them in an ultrasonic bath and sonicated for 15 min. A drop of this well-dispersed suspension was placed on a carbon-coated 200-mesh copper grid, followed by drying the sample under ambient condition before it was placed in the sample holder of the microscope.

4.4.5 BET surface area measurement

Physical adsorption isotherms are measured near the boiling point of a gas (e.g., nitrogen, at -196^{o}C). From these isotherms the amount of gas needed to form a monolayer can be determined. If the area occupied by each adsorbed gas molecule is known, the surface area can be determined for all finely divided solids, regardless of their chemical composition.

The specific surface area of samples was calculated using the Brunauer-Emmett-Teller single point method on the basis of nitrogen uptake measured at liquid-nitrogen boiling point temperature equipped with a gas chromatograph.

4.4.5.1 BET apparatus

The reaction apparatus of BET surface area measurement consisted of two feed lines of helium and nitrogen. The flow rate of the gases was adjusted by means of fine-metering valve on the gas chromatograph. The sample cell made from Pyrex glass.

The operation condition of gas chromatograph (GOW-MAC) is shown in Table 4.2.

Table 4.2 Operating condition of gas chromatograph (GOW-MAC)

Model	**GOW-MAC**
Detector	TCD
Helium flow rate	30 ml/min
Detector temperature	80 °C
Detector current	80 mA

4.4.5.2 Procedure

The mixture gas of helium and nitrogen was flown through the system at the nitrogen relative pressure of 0.3. The catalyst sample was placed in the sample cell, ca. 0.3-0.5 g, which was then heated up to 200^{o}C and held at that temperature for 2 h. Then the catalyst sample was cooled down to room temperature and the specific surface area was measured. There were three steps to measure the specific surface area.

Adsorption step: The catalyst that set in the sample cell was dipped into the liquid nitrogen. Nitrogen gas that was introduced into the system was adsorbed on the surface of the catalyst sample until equilibrium was reached.

Desorption step: The sample cell with nitrogen gas-adsorbed catalyst sample was dipped into a water bath at room temperature. The adsorbed nitrogen gas was desorbed from the surface of the catalyst sample. This step was completed when the integrator line was back in the position of the base line.

Calibration step: 1 ml of nitrogen gas at atmospheric pressure was injected through the calibration port of the gas chromatograph and the area was measured. The area was the calibration peak. The calculation method is explained in Appendix B.

4.4.6 UV-visible absorbtion

UV-visible absorbtion spectroscopy measurement was carried out in a UV-vis-NIR spectroscopy, UV Varian Cary 500.

4.4.7 Thermogravimetric and differential thermal analysis (TG/DTA)

TG/DTA was used to determine the weight loss of precursor and ZnO during heat treatment. About 4-6 mg of each sample was analyzed by the thermogravimetric and differential thermal analysis, PerkinElmer Thermal Analysis Diamond TG/DTA at Center of Excellences on Catalysis and Catalytic Reaction Engineering, Chulalongkorn University. The furnace was heated from 50 °C to 320 °C at a constant rate of 10 °C min^{-1} and then cooled naturally. The whole TG/DTA measurement was made under gas nitrogen at gas flow rate of 100 mL min^{-1}.

4.4.8 Fourier transform Infrared (FT-IR)

Transmittance spectra of particles were determined by FT-IR using Nicolet model Impact 400. Each sample was mixed with KBr with ratio of sample: KBr equal to 1:100 and then pressed into a thin wafer. Infrared spectra were recorded between 400 and 4000 cm^{-1} on a microcomputer.

4.4.9 Gas Chromatography and Mass Spectrometry

The composition of remaining liquid was analyzed by Gas Chromatography and Mass Spectrometry (Agelient Technologies, Network 5793) at Department of science service (Ministry of science and technology). The spectrum of GC/MS explained in Appendix C.

CHAPTER V

RESULTS AND DISCUSSION

The nanocrystalline zinc oxide (ZnO) obtained in this work were synthesized by thermal reaction of Zinc acetate ($Zn(CH_3COO)_2$) with various organic solvents, in an autoclave under autogenous pressure. The procedure was so-call solvothermal method. The physical properties of ZnO products were characterized and investigated.

In this chapter, the results and discussion are divided into 4 sections. First, the effect of reaction temperature on the properties ZnO nanoparticles is presented in section 5.1. Second, the effect of the amount of starting material on the properties ZnO nanoparticles is presented in section 5.2; follow by the effect of organic solvent on the properties of ZnO nanoparticles in section 5.3 and the crystallization mechanism of ZnO nanoparticles synthesized by solvothermal method in last section

5.1 The effect of reaction temperature on the properties of ZnO nanoparticles.

Zinc oxide powder has been synthesized in 1,4 butanediol, 1-octanol and 1-decanol at various reaction temperatures 200 °C to 300 °C for 2 h by using zinc acetate 15 g. The XRD patterns of ZnO nanoparticles synthesized in 1,4 butanediol, 1-octanol and 1-decanol at various reaction temperature are shown in Figure 5.1, 5.2 and 5.3, respectively. All diffraction peaks of thus-obtained products were corresponding to the hexagonal wurtzite structure of ZnO with lattice parameters *a* and *c* of 3.24 and 5.19 Å, respectively. No diffraction peaks of impurities or secondary phase were observed. The strong intensity of ZnO diffraction peaks indicates that resulting product have high purity of ZnO wurtzite phase (normalized to (101) reflection about 36.6 of 2θ position in Figure 5.1 which is usually the most intense feature in the ZnO zincite diffraction pattern). This result suggested that ZnO was successfully synthesized by solvothermal reaction in 1,4 butanediol, 1-octanol and 1-decanol.

Figure 5.4 to 5.14 shows SEM images of the as-synthesized ZnO in 1,4 butanediol, 1-octanol and 1-decanol at various reaction temperatures. Aggregation of fine particles were observed by the reaction in 1,4 butanediol, while the nanorods of ZnO were revealed by the reaction in 1-octanol and 1-decanol.

The primary particles of as-synthesized ZnO prepared in 1,4 butanediol, 1-octanol and 1-decanol at various reaction temperatures are shown as TEM images in Figure 5.15 to 5.25. The morphology of thus-obtained ZnO seemed to be nanorods with relatively straight, non porous and their surfaces were smooth. The average diameter and length size of ZnO nanoparticles were calculated by TEM. The diameter and length size distributions based on these images are depicted in the histograms as Fig. 5.26 to 5.36, obtained from analysis of more than 70 particles per sample. It was found that as-synthesized ZnO showed the narrow sizes distribution. The average diameter sizes of ZnO showed the narrowly distribution, found as was deduced from the histogram. It can be seen that most of the rod have a nanosized diameter.

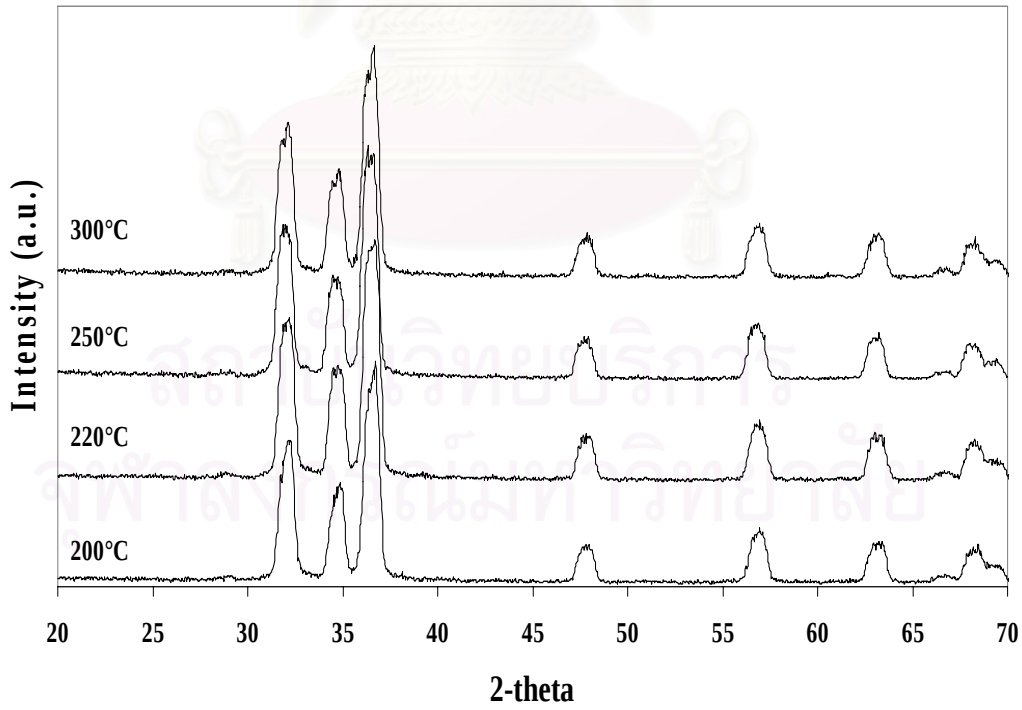

Figure 5.1 XRD patterns of ZnO nanoparticles that synthesized in 1,4 butanediol at various reaction temperatures for 2 h by using zinc acetate 15g.

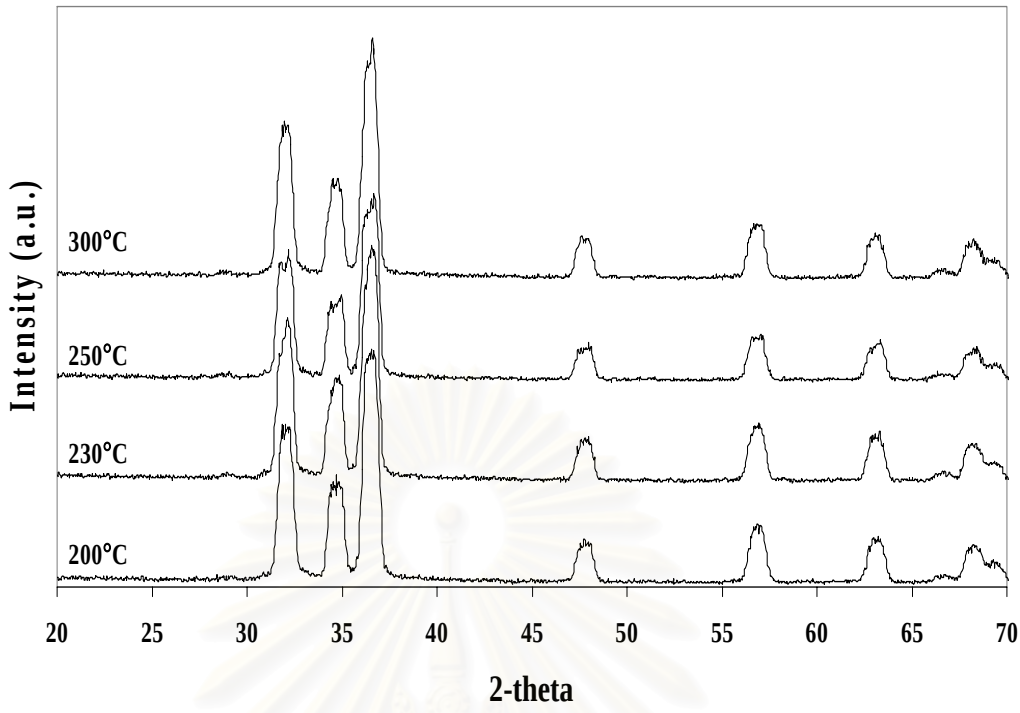

Figure 5.2 XRD patterns of ZnO nanoparticles that synthesized in 1-octanol at various reaction temperatures for 2 h by using zinc acetate 15g.

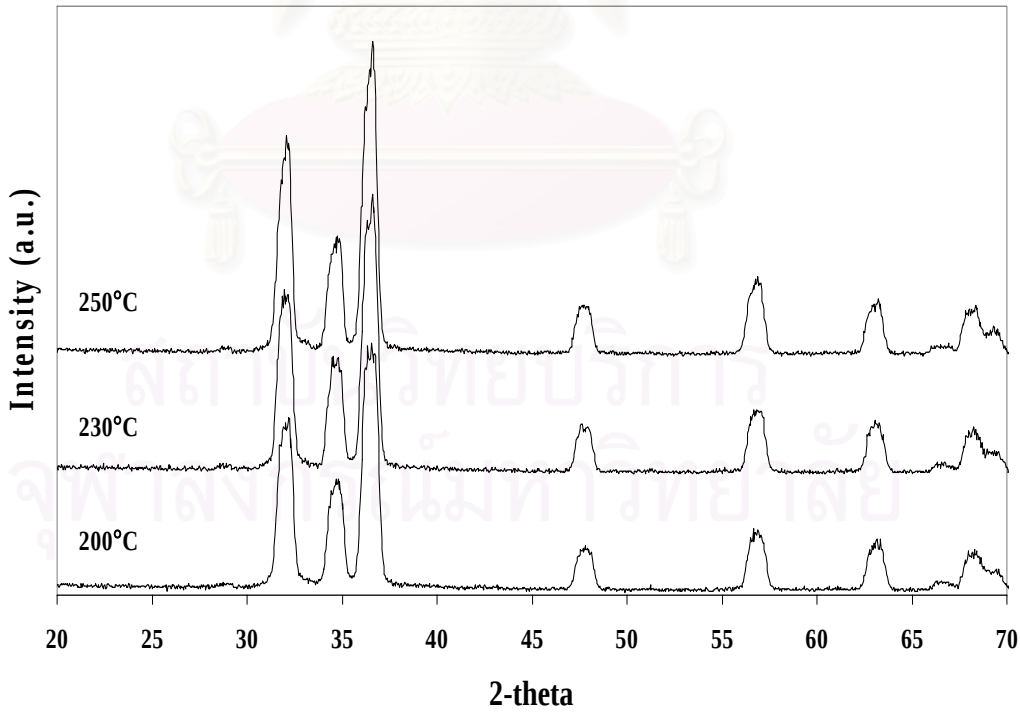

Figure 5.3 XRD patterns of ZnO nanoparticles that synthesized in 1-decanol at various reaction temperatures for 2 h by using zinc acetate 15g.

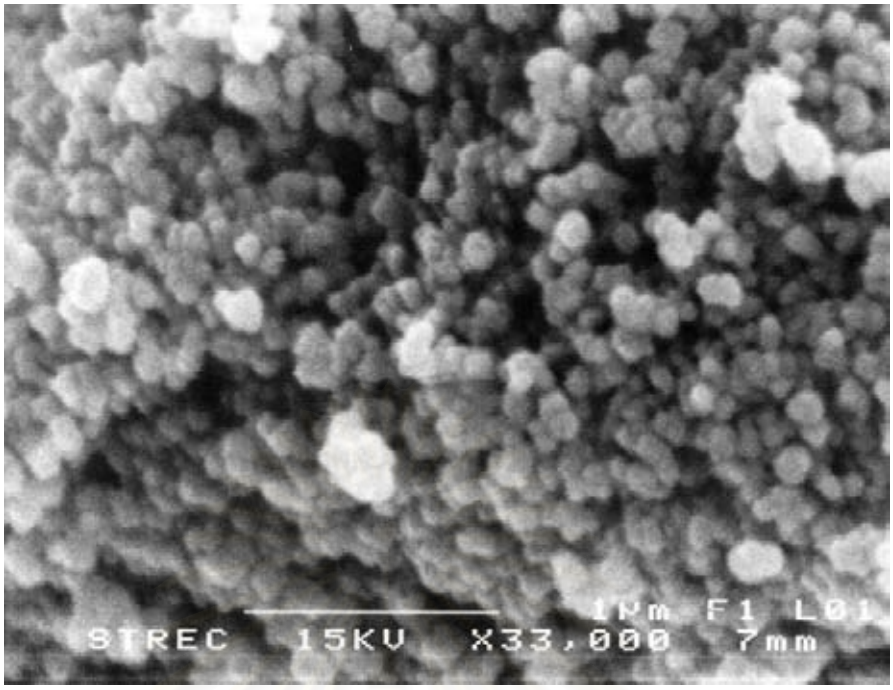

Figure 5.4 SEM images of ZnO nanoparticles as-synthesized in 1,4 butanediol at 200 °C for 2 h by using zinc acetate 15 g.

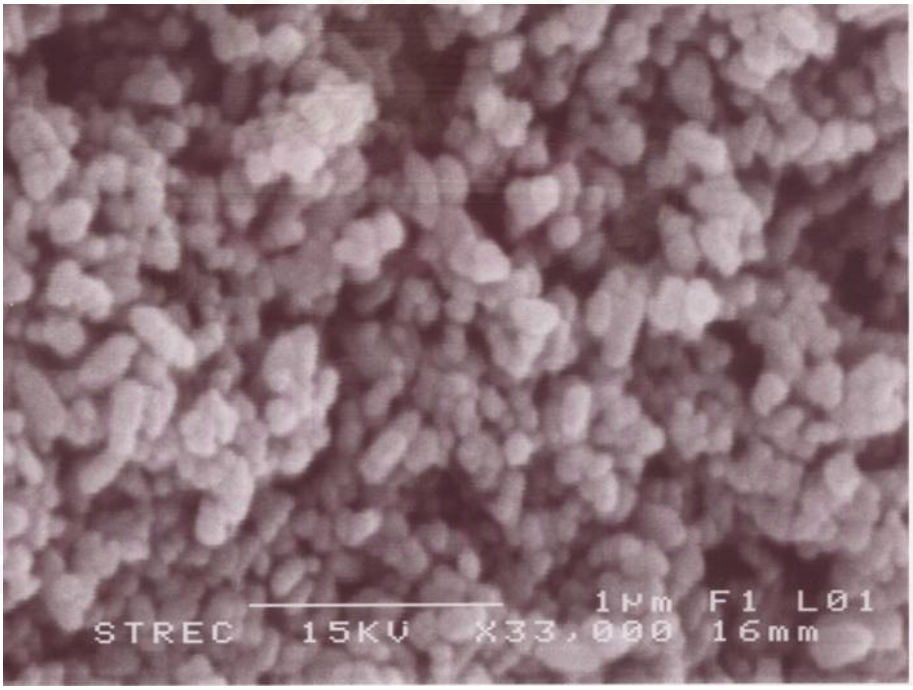

Figure 5.5 SEM images of ZnO nanoparticles as-synthesized in 1,4 butanediol at 220 °C for 2 h by using zinc acetate 15 g.

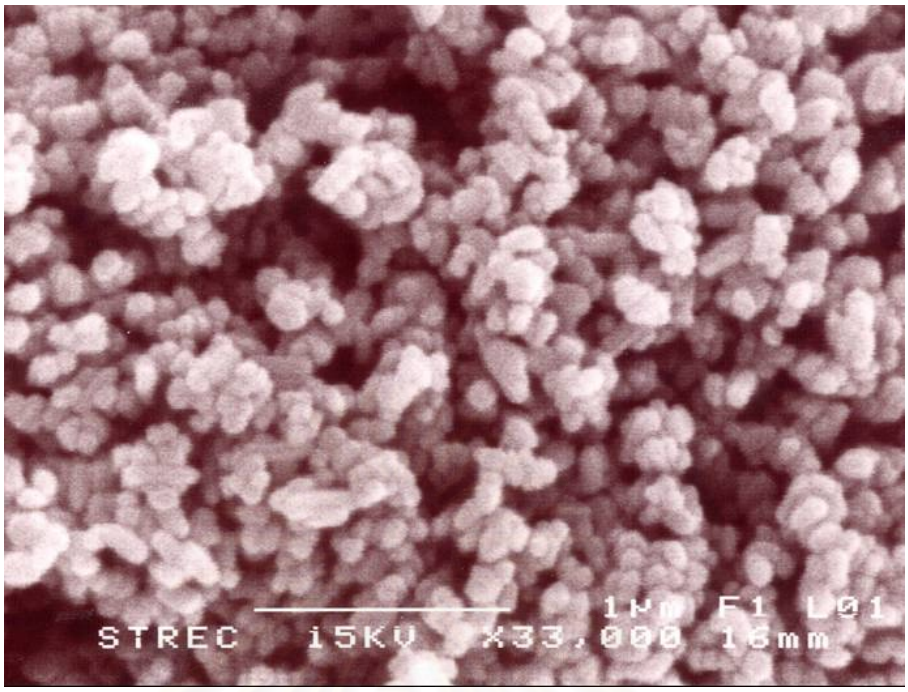

Figure 5.6 SEM images of ZnO nanoparticles as-synthesized in 1,4 butanediol at 250 °C for 2 h by using zinc acetate 15 g.

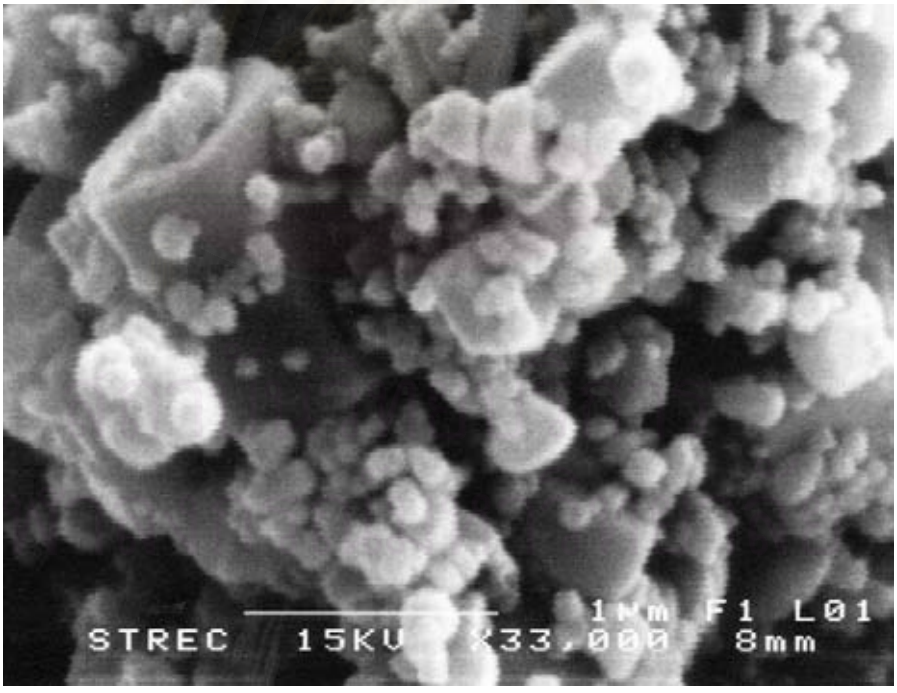

Figure 5.7 SEM images of ZnO nanoparticles as-synthesized in 1,4 butanediol at 300 °C for 2 h by using zinc acetate 15 g.

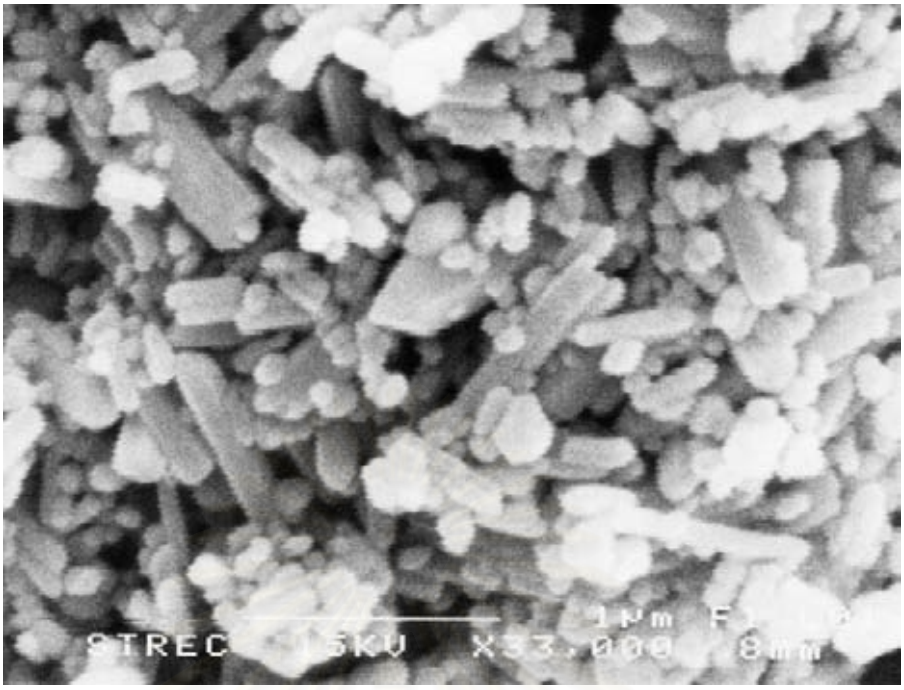

Figure 5.8 SEM images of ZnO nanoparticles as-synthesized in 1-octanol at 200 °C for 2 h by using zinc acetate 15 g.

Figure 5.9 SEM images of ZnO nanoparticles as-synthesized in 1-octanol at 230 °C for 2 h by using zinc acetate 15 g.

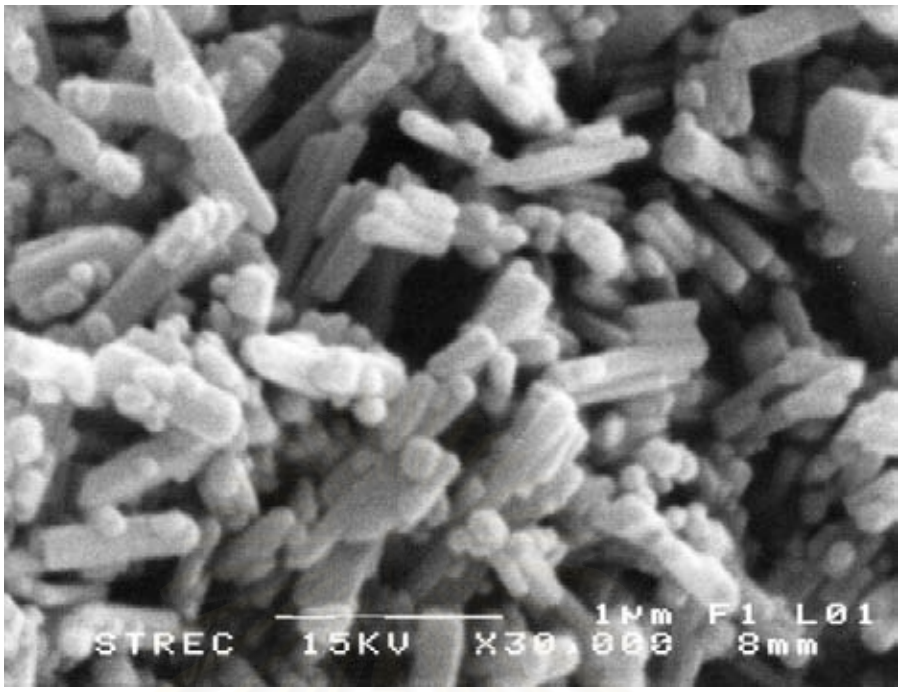

Figure 5.10 SEM images of ZnO nanoparticles as-synthesized in 1-octanol at 250 °C for 2 h by using zinc acetate 15 g.

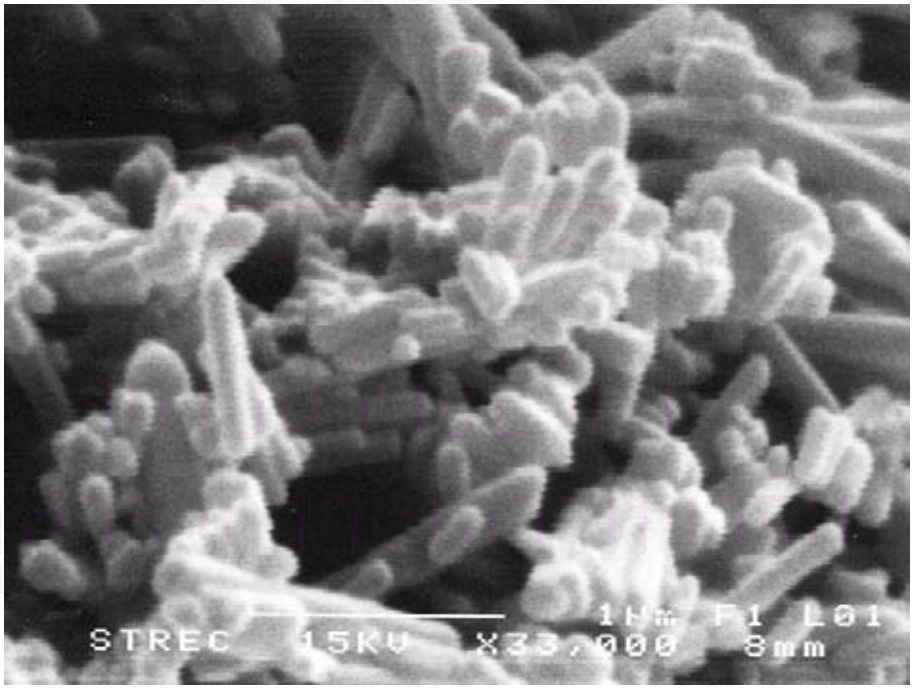

Figure 5.11 SEM images of ZnO nanoparticles as-synthesized in 1-octanol 300 °C for 2 h by using zinc acetate 15 g.

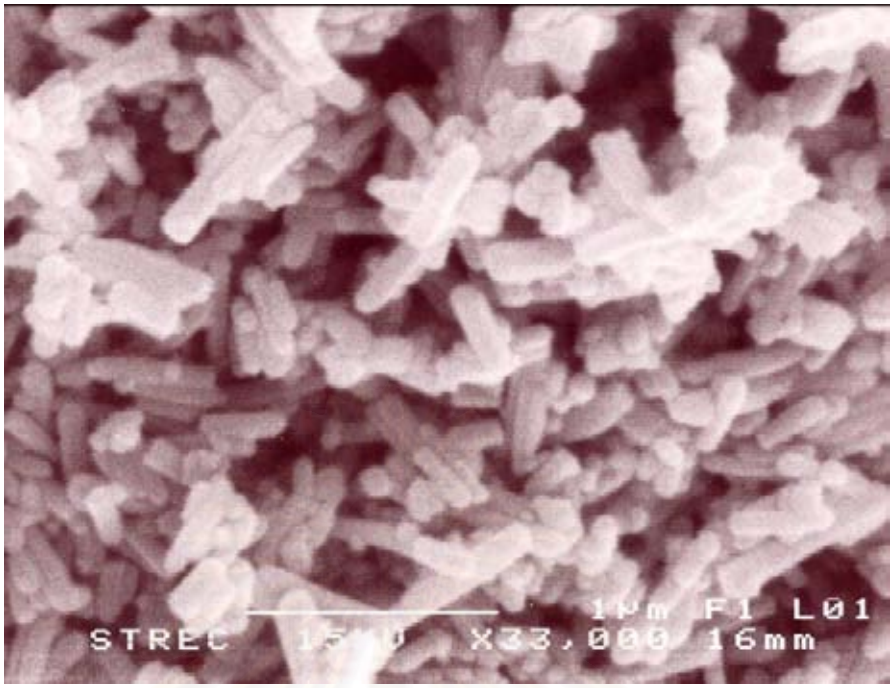

Figure 5.12 SEM images of ZnO nanoparticles as-synthesized in 1-decanol at 200 °C for 2 h by using zinc acetate 15 g.

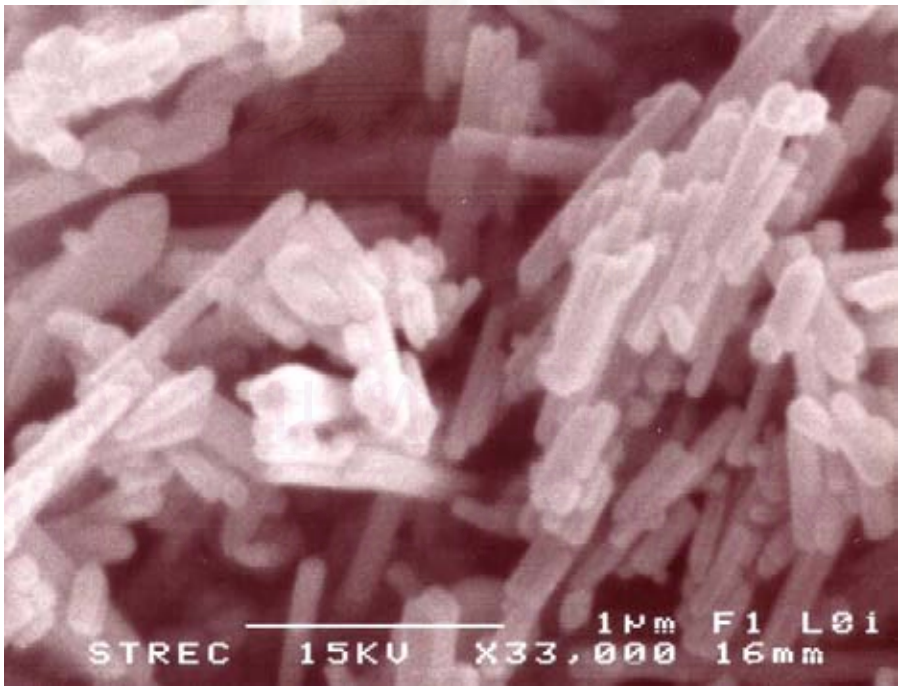

Figure 5.13 SEM images of ZnO nanoparticles as-synthesized in 1-decanol at 230 °C for 2 h by using zinc acetate 15 g.

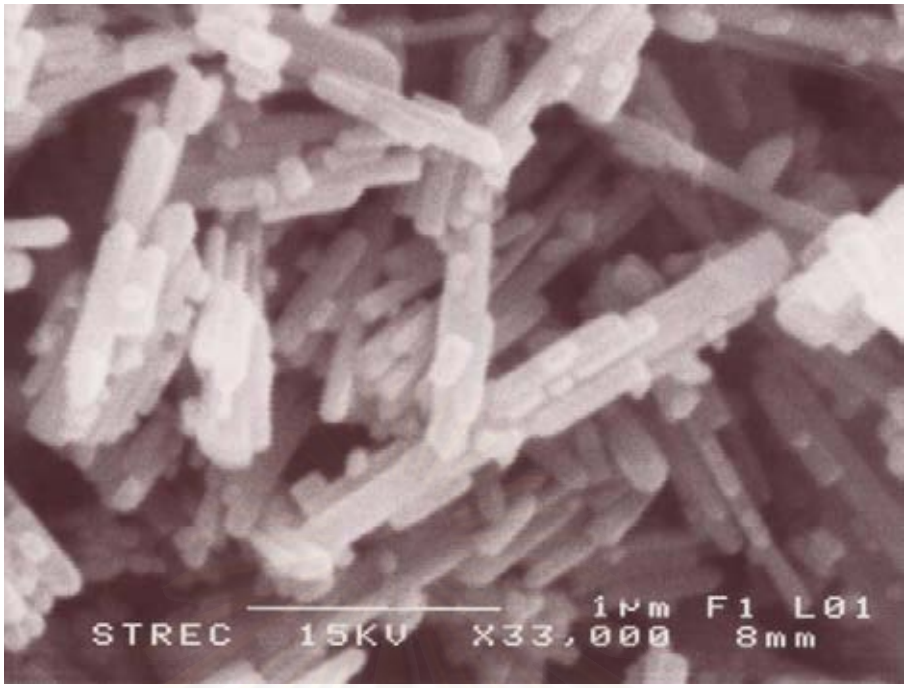

Figure 5.14 SEM image of ZnO nanoparticles as-synthesized in 1-decanol at 250 °C for 2 h by using zinc acetate 15 g.

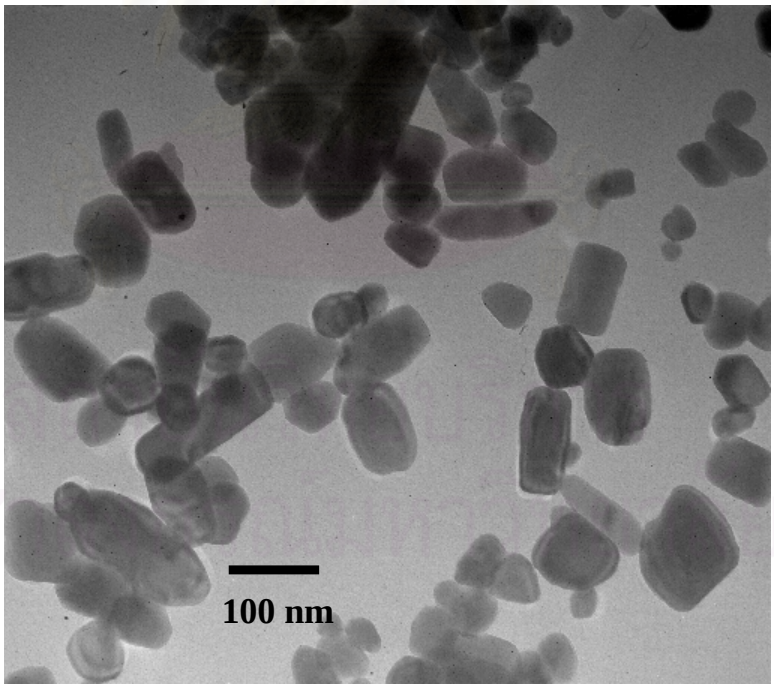

Figure 5.15 TEM images of ZnO nanoparticles as-synthesized in 1,4 butanediol at 200 °C for 2 h by using zinc acetate 15 g.

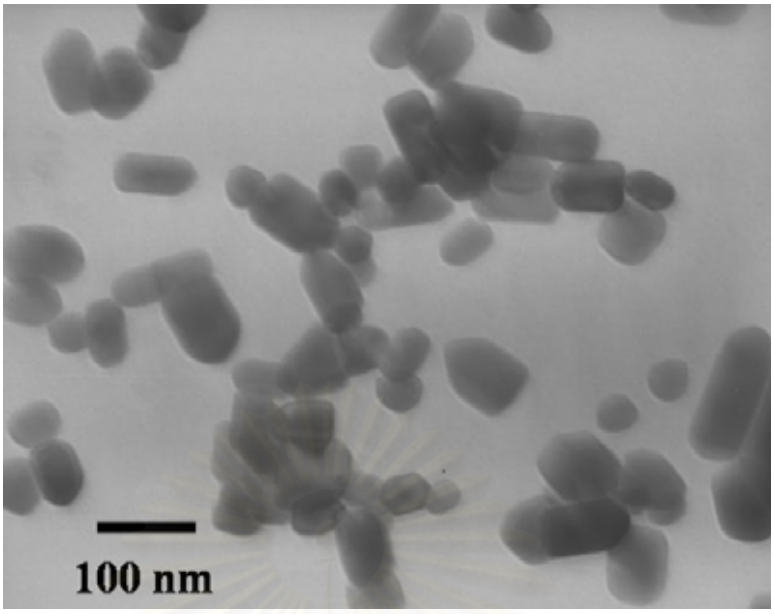

Figure 5.16 TEM images of ZnO nanoparticles as-synthesized in 1,4 butanediol at 230°C for 2 h by using zinc acetate 15 g.

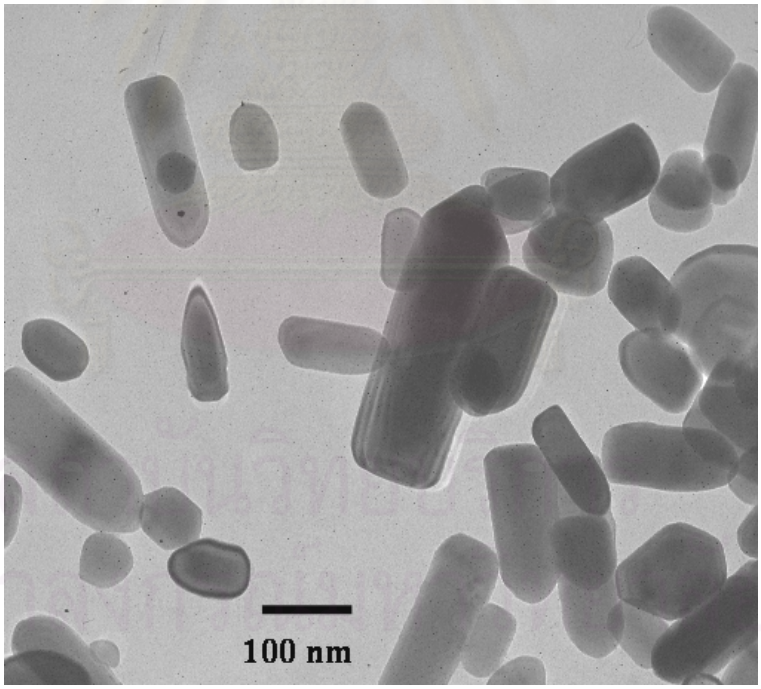

Figure 5.17 TEM images of ZnO nanoparticles as-synthesized in 1,4butanediol at 250 °C for 2 h by using zinc acetate 15 g.

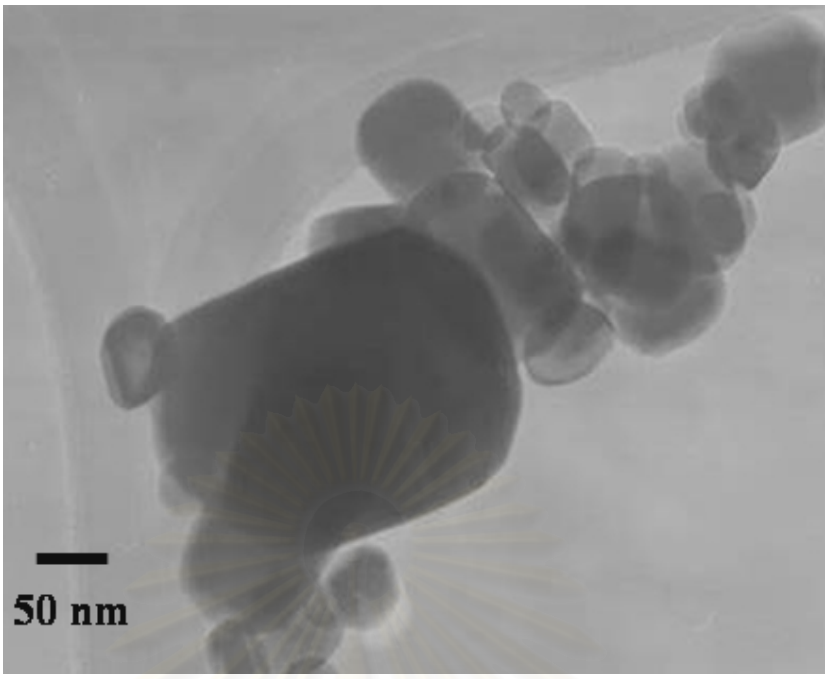

Figure 5.18 TEM images of ZnO nanoparticles as-synthesized in 1,4butanediol at 300°C for 2 h by using zinc acetate 15 g.

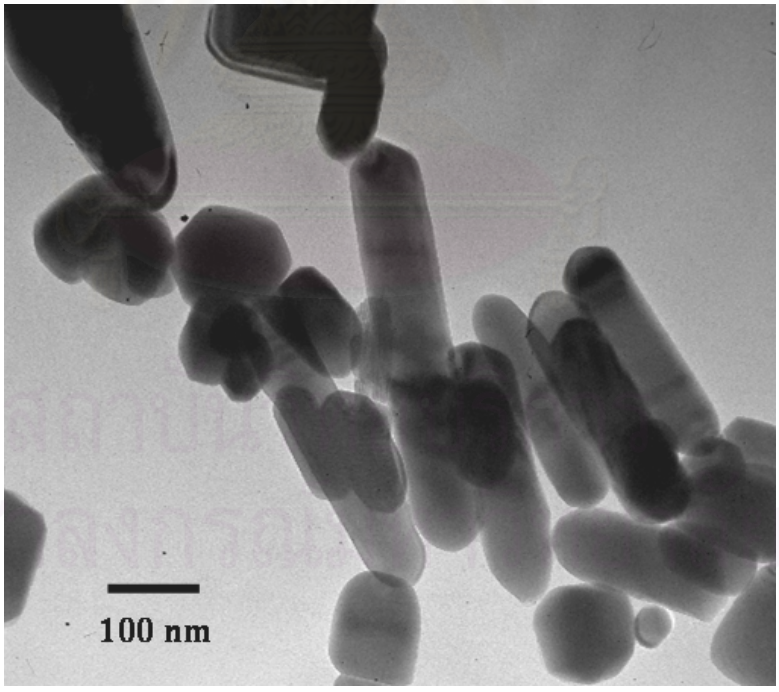

Figure 5.19 TEM images of ZnO nanoparticles as-synthesized in 1-octanol at 200 °C for 2 h by using zinc acetate 15 g.

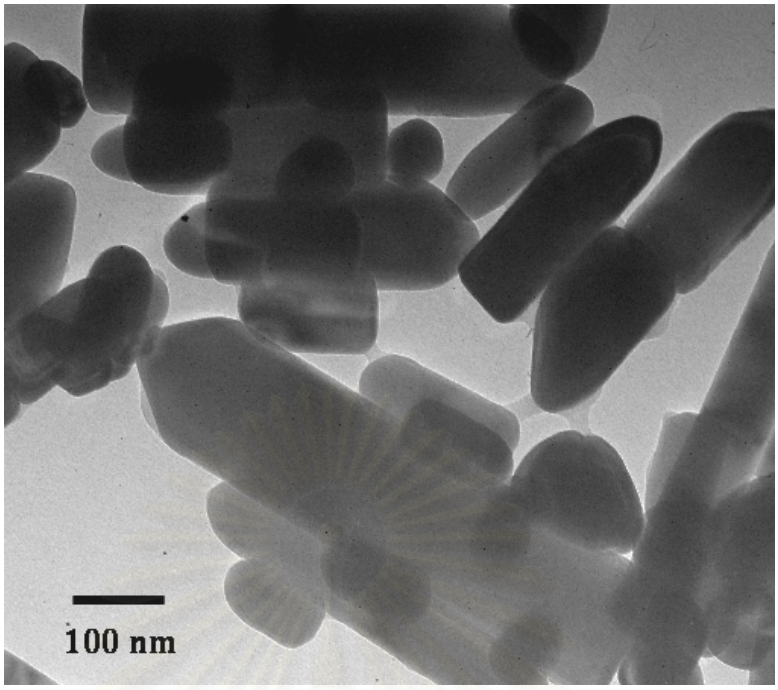

Figure 5.20 TEM images of ZnO nanoparticles as-synthesized in 1-octanol at 230°C for 2 h by using zinc acetate 15 g.

Figure 5.21 TEM images of ZnO nanoparticles as-synthesized in 1-octanol at 250 °C for 2 h by using zinc acetate 15 g.

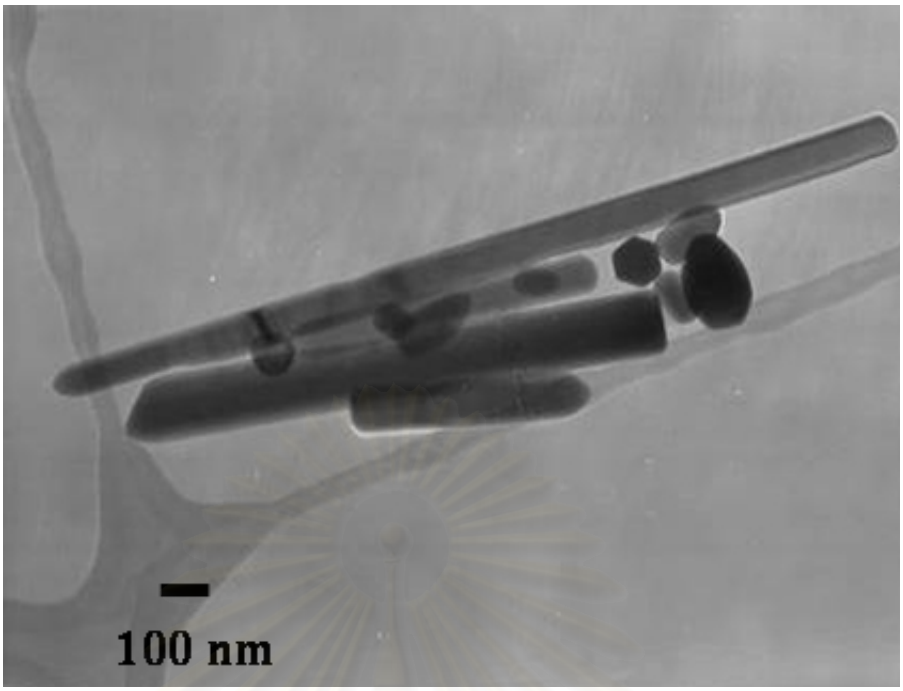

Figure 5.22 TEM images of ZnO nanoparticles as-synthesized in 1-octanol at 300°C for 2 h by using zinc acetate 15 g.

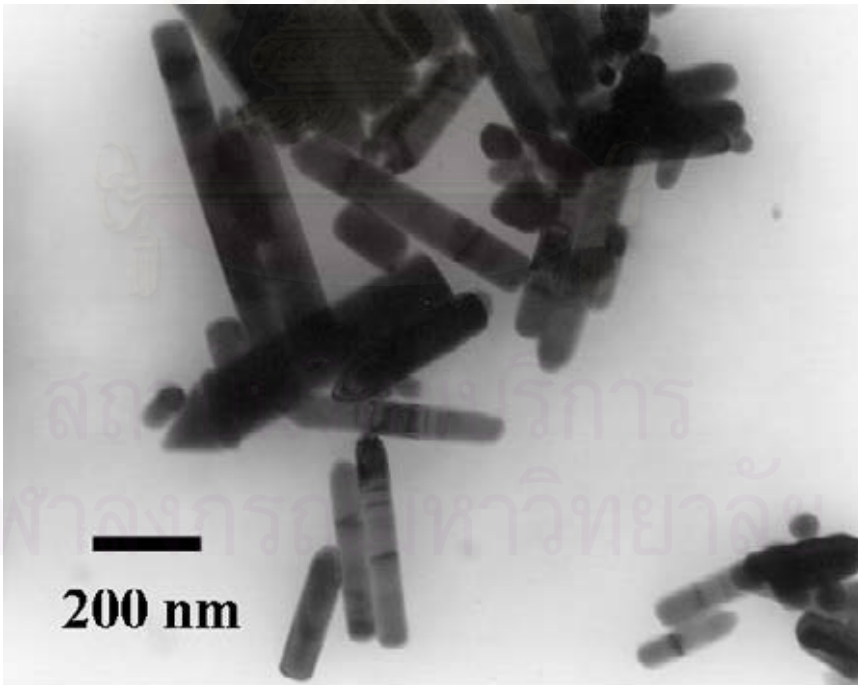

Figure 5.23 TEM images of ZnO nanoparticles as-synthesized in 1-decanol at 200 °C for 2 h by using zinc acetate 15 g.

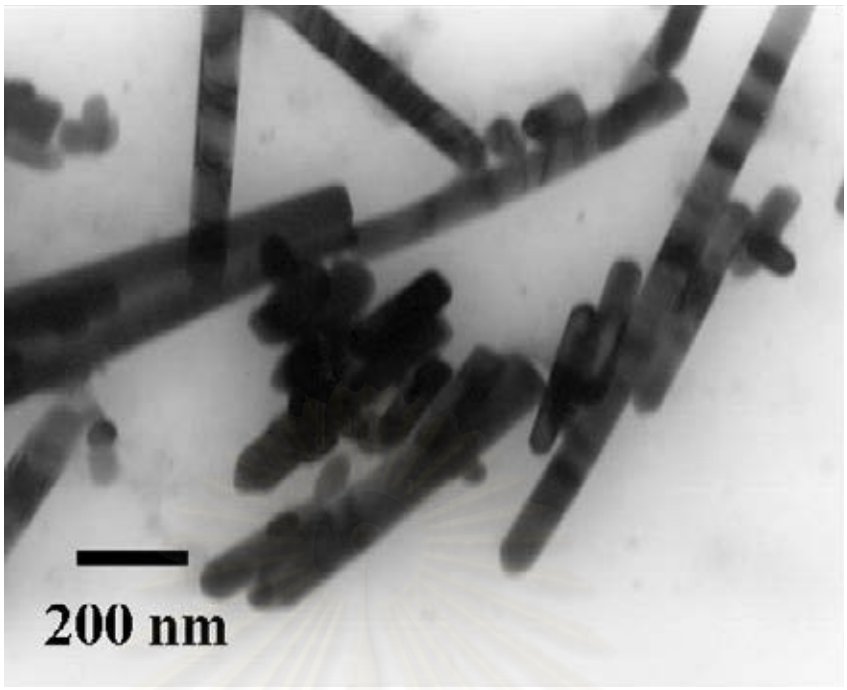

Figure 5.24 TEM images of ZnO nanoparticles as-synthesized in 1-decanol at 230°C for 2 h by using zinc acetate 15 g.

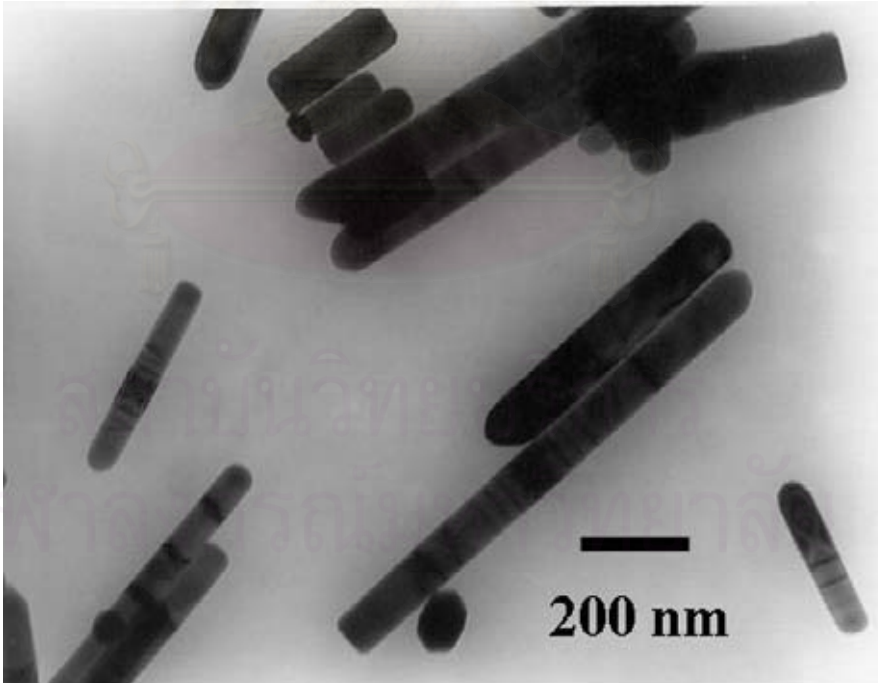

Figure 5.25 TEM image of ZnO nanoparticles as-synthesized in 1-decanol at 250 °C for 2 h by using zinc acetate 15 g.

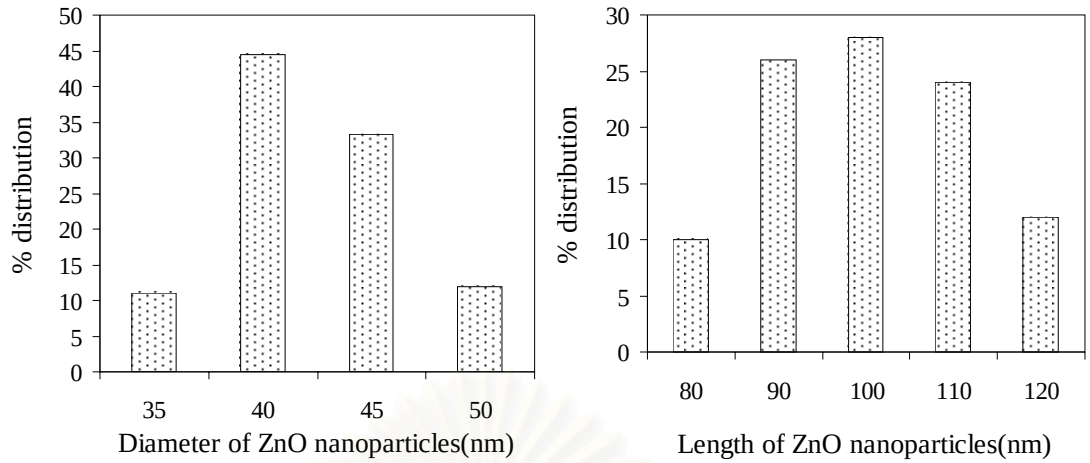

Figure 5.26 Histograms of the diameter and length size distributions obtained from TEM images for ZnO prepared in 1,4 butanediol at 200°C for 2h by using zinc acetate 15 g.

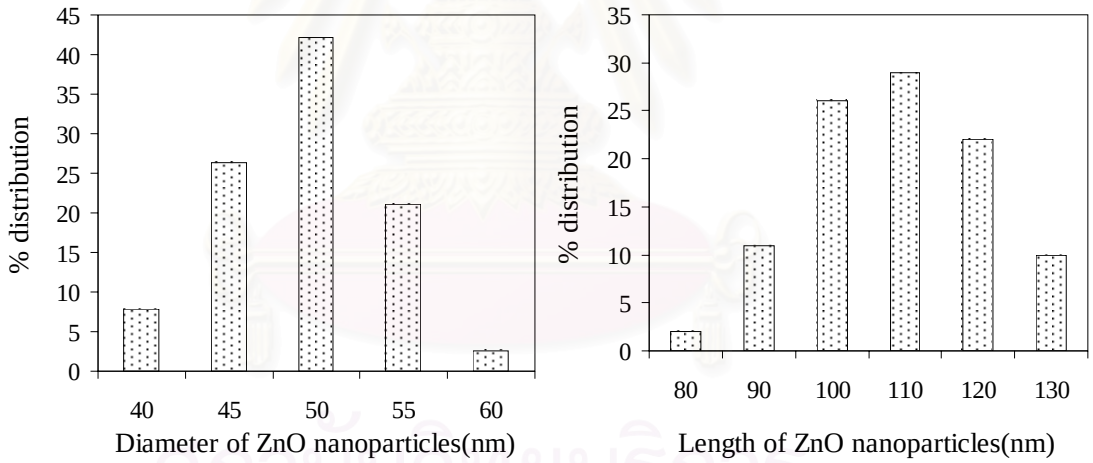

Figure 5.27 Histograms of the diameter and length size distributions obtained from TEM images for ZnO prepared in 1,4 butanediol at 220°C for 2h by using zinc acetate 15 g.

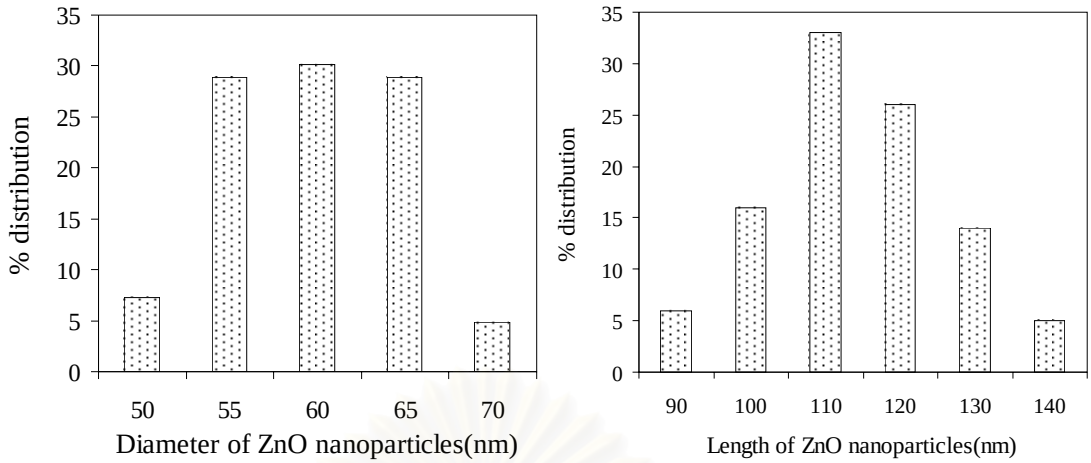

Figure 5.28 Histograms of the diameter and length size distributions obtained from TEM images for ZnO prepared in 1,4 butanediol at 250°C for 2h by using zinc acetate 15 g.

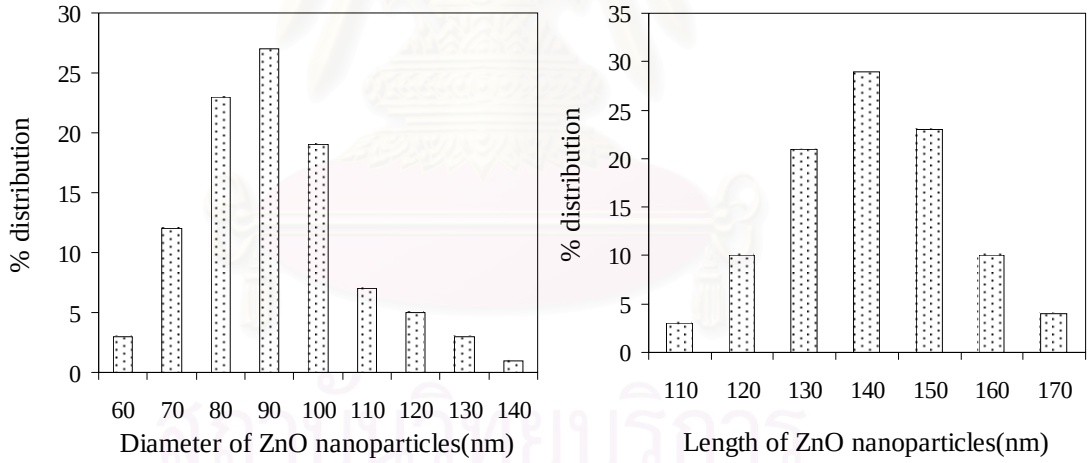

Figure 5.29 Histograms of the diameter and length size distributions obtained from TEM images for ZnO prepared in 1,4 butanediol at 300°C for 2h by using zinc acetate 15 g.

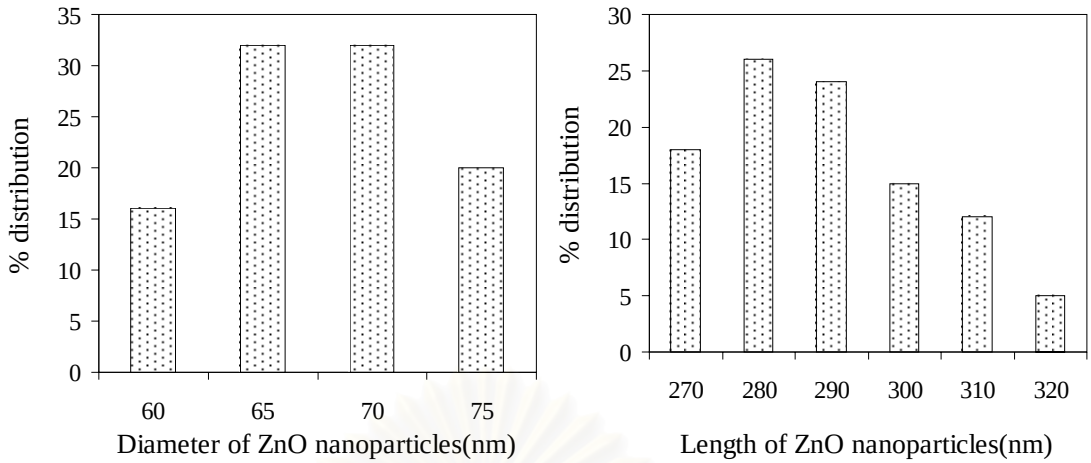

Figure 5.30 Histograms of the diameter and length size distributions obtained from TEM images for ZnO prepared in 1-octanol at 200°C for 2h by using zinc acetate 15 g.

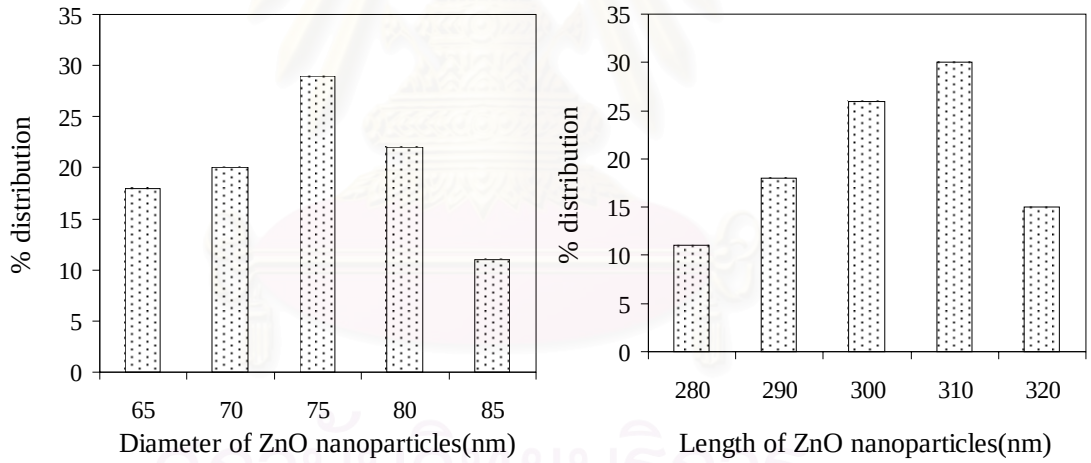

Figure 5.31 Histograms of the diameter and length size distributions obtained from TEM images for ZnO prepared in 1-octanol at 230°C for 2h by using zinc acetate 15 g.

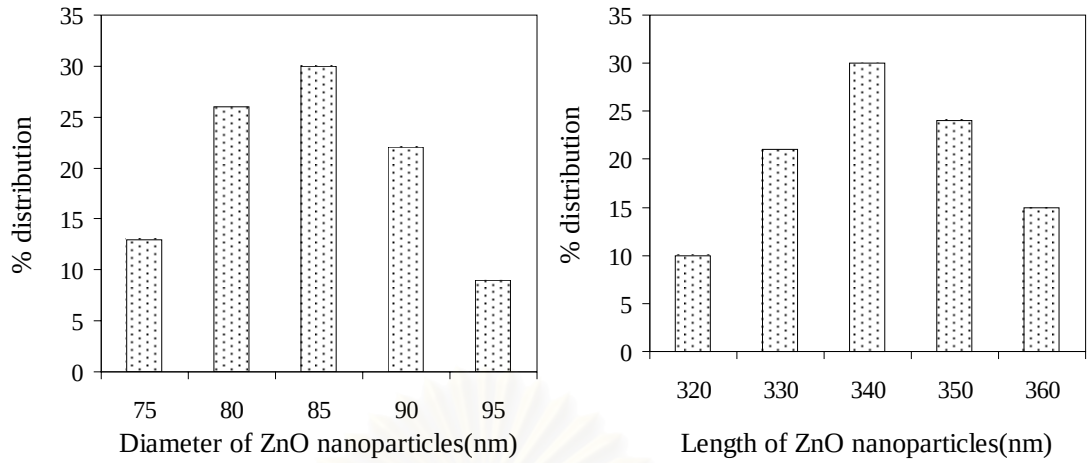

Figure 5.32 Histograms of the diameter and length size distributions obtained from TEM images for ZnO prepared in 1-octanol at 250°C for 2h by using zinc acetate 15 g.

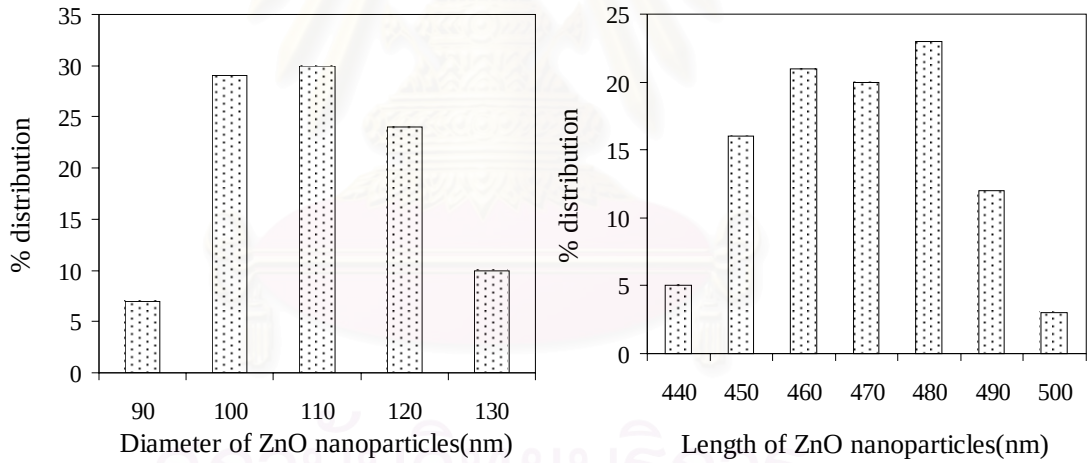

Figure 5.33 Histograms of the diameter and length size distributions obtained from TEM images for ZnO prepared in 1-octanol at 300°C for 2h by using zinc acetate 15 g.

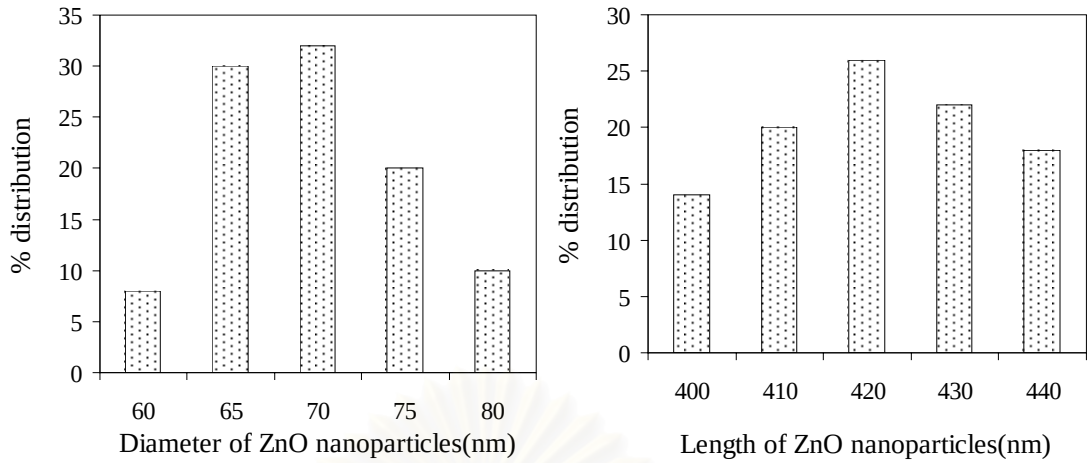

Figure 5.34 Histograms of the diameter and length size distributions obtained from TEM images for ZnO prepared in 1-decanol at 200°C for 2h by using zinc acetate 15 g.

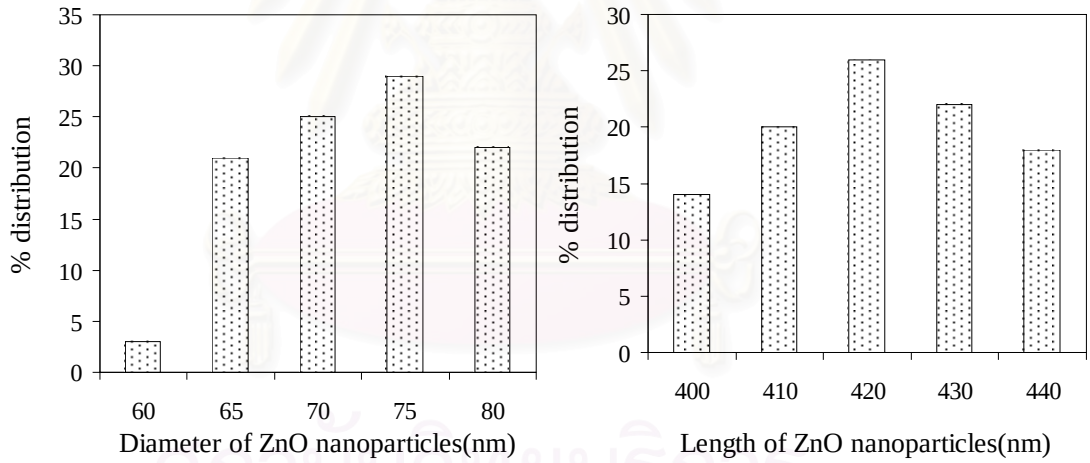

Figure 5.35 Histograms of the diameter and length size distributions obtained from TEM images for ZnO prepared in 1-decanol at 230°C for 2h by using zinc acetate 15 g.

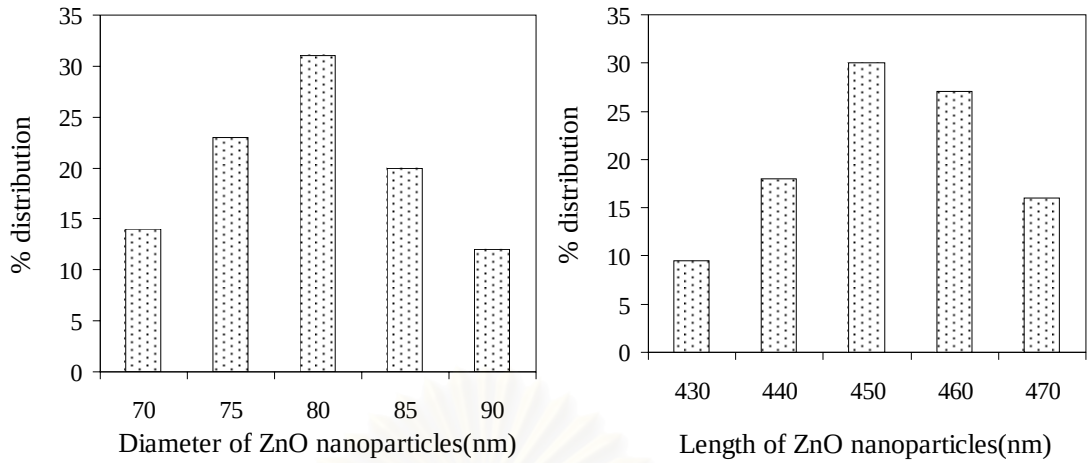

Figure 5.36 Histograms of the diameter and length size distributions obtained from TEM images for ZnO prepared in 1-decanol at 250°C for 2h by using zinc acetate 15 g.

Table 5.1 summarizes the average particles size and aspect ratios of thus-obtained ZnO synthesized in 1,4 butanediol, 1-octanol and 1-decanol. Aspect ratios of particles were evaluated as the ratio of length to diameter. The reaction temperature in 1,4 butanediol and 1-octanol was varied from 200-300^{o}C. The crystal diameter size of ZnO increased from 64 to 101 nm and 46 to 88 nm, corresponding with the temperature increased from 200-300^{o}C in 1-octanol and 1,4 butanediol, respectively. In 1-decanol the average diameter size were increase from 69 to 81 nm by various reaction temperatures from 200-250 ^{o}C, respectively. It can be explained by the sintering at higher reaction temperature. However the aspect ratios of particles were still same in each solvent. It suggests that the temperature was not affected on the growing rate ratio between planes in ZnO crystal.

Table 5.1 The physical properties of ZnO were prepared in 1,4 butanediol, 1-octanol and 1-decanol at various reaction temperatures for 2h by using zinc acetate 15 g.

Solvent	Temperature as-synthesized (°C)	Average diameter (nm)	Average length (nm)	Aspect ratio	BET surface area (m^2/g)
1,4 Butanediol	200	46	100	2.17	11.9
1,4 Butanediol	220	49	108	2.20	10.4
1,4 Butanediol	250	58	115	1.98	9.87
1,4 Butanediol	300	88	144	1.63	7.29
1-Octanol	200	67	284	4.23	11.13
1-Octanol	230	75	308	4.11	9.72
1-Octanol	250	84	343	4.08	8.87
1-Octanol	300	110	472	4.29	7.18
1-Decanol	200	69	392	5.68	8.41
1-Decanol	230	74	419	5.66	7.83
1-Decanol	250	81	455	5.62	7.09

5.2 The effect of the amount of starting material on the properties of ZnO nanoparticles

ZnO has been synthesized in 1,4 butanediol, 1-octanol, 1-decanol and toluene, by various amount of starting material. In toluene, the zinc acetate contents were varied from 10-25 g. by synthesized at 300 °C for 2h and in 1,4 butanediol, 1-octanol, and 1-decanol from 10-20 g. were prepared at 250 °C for 2h

The XRD patterns of ZnO nanoparticles synthesized in 1,4 butanediol, 1-octanol, 1-decanol and toluene are shown in Figure 5.37, 5.38, 5.39 and 5.40, respectively. Most of the ZnO product peaks can be indexed to the hexagonal wurtzite structure. No diffraction peak of zinc acetate or other impurities have been found in our samples. The strong intensity of ZnO diffraction peaks indicates that resulting product have high purity of ZnO wurtzite phase. This result suggests that ZnO is successfully synthesized by solvothermal reaction in 1,4 butanediol, 1-octanol, 1-decanol and toluene.

SEM images of the as-synthesized ZnO in 1,4 butanediol, 1-octanol, 1-dacanol and toluene with various amounts of starting precursors are shown in Figure 5.41 to 5.51 and SEM images of ZnO prepared in 1,4 butanediol, 1-octanol and 1-decanol at 250 °C by using zinc acetate 15 g have already shown in Figure 5.6, 5.10 and 5.14, respectively. SEM images of as-synthesized ZnO powders in 1-octanol, 1-decanol and toluene were the aggregation of nanorods crystal while aggregation of fine particles were observed by the reaction in 1,4 butanediol. It is obvious that the samples consist of large quantities of smooth solid hexagonal rods. The diameter and length of the rods increased as the amount of zinc acetate increased.

TEM micrographs of thus obtained powders prepared in 1,4 butanediol, 1-octanol and 1-decanol at 250 °C by using various amounts of zinc acetate are shown in Figure 5.17, 5.21, 5.25, and 5.52 to 5.62. The morphology of thus-obtained ZnO seemed to be nanorods with relatively straight and their surfaces were smooth. The particles size and size distribution were studies with TEM. The diameter and length distributions based on these images, which obtained from analysis of more than 70

particles per sample are depicted in the histograms as Fig. 5.28, 5.32, 5.36, and 5.63 to 5.73. The average diameter sizes of ZnO showed the narrowly distribution, found as was deduced from the histogram. It can be seen that most of the rod have a nanosized diameter.

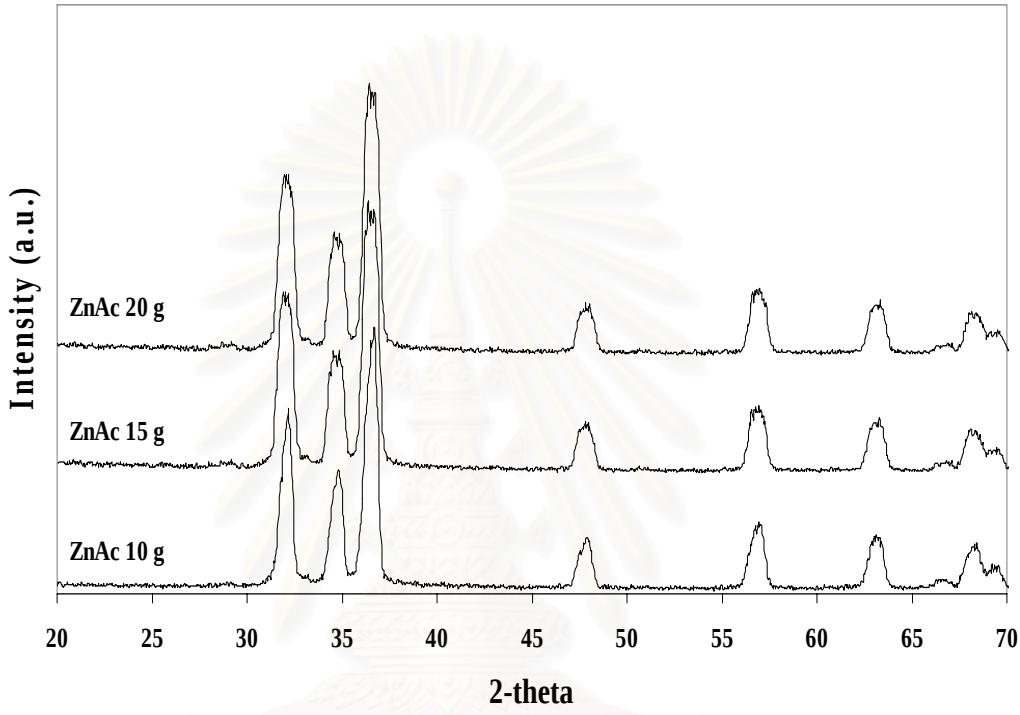

Figure 5.37 XRD patterns of ZnO nanoparticles that synthesized in 1,4 butanediol at 250 °C for 2 h by various amount of zinc acetate.

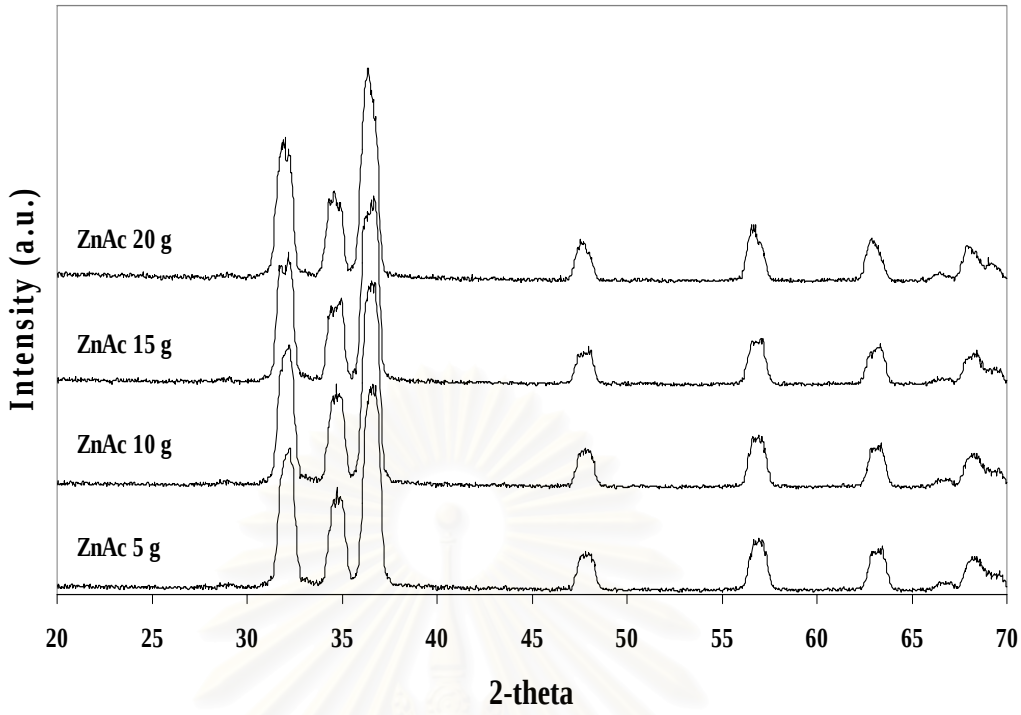

Figure 5.38 XRD patterns of ZnO nanoparticles that synthesized in 1-octanol at 250 °C for 2 h by various amount of zinc acetate.

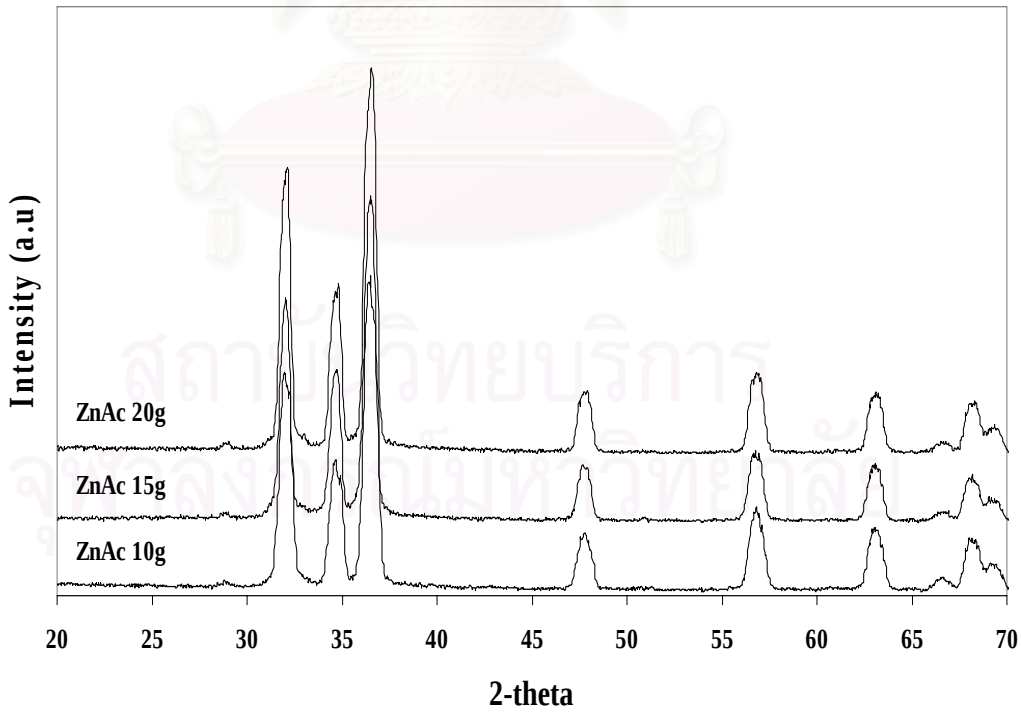

Figure 5.39 XRD patterns of ZnO nanoparticles that synthesized in 1-decanol at 250 °C for 2 h by various amount of zinc acetate.

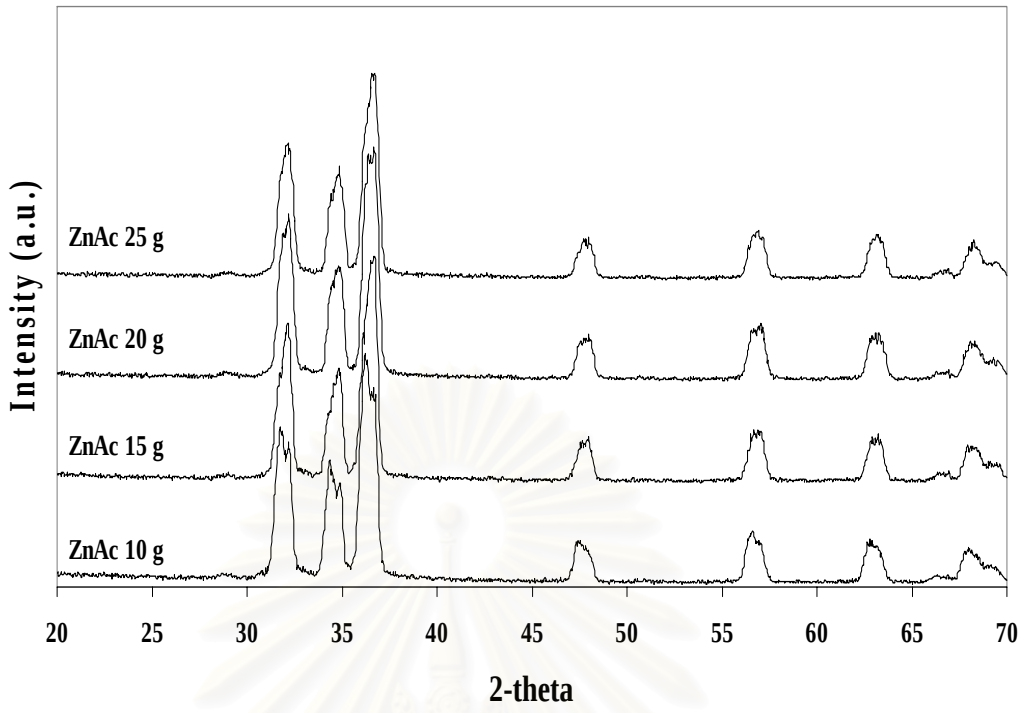

Figure 5.40 XRD patterns of ZnO nanoparticles that synthesized in toluene at 300 °C for 2 h by various amount of zinc acetate.

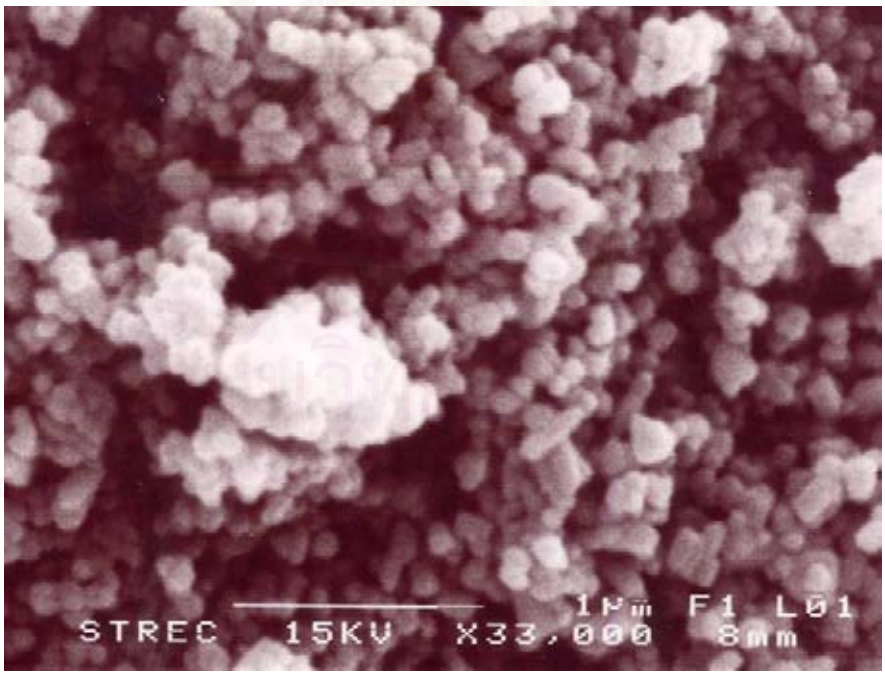

Figure 5.41 SEM images of ZnO nanoparticles as-synthesized in 1,4 butaindiol at 250 °C for 2 h by using zinc acetate 10 g.

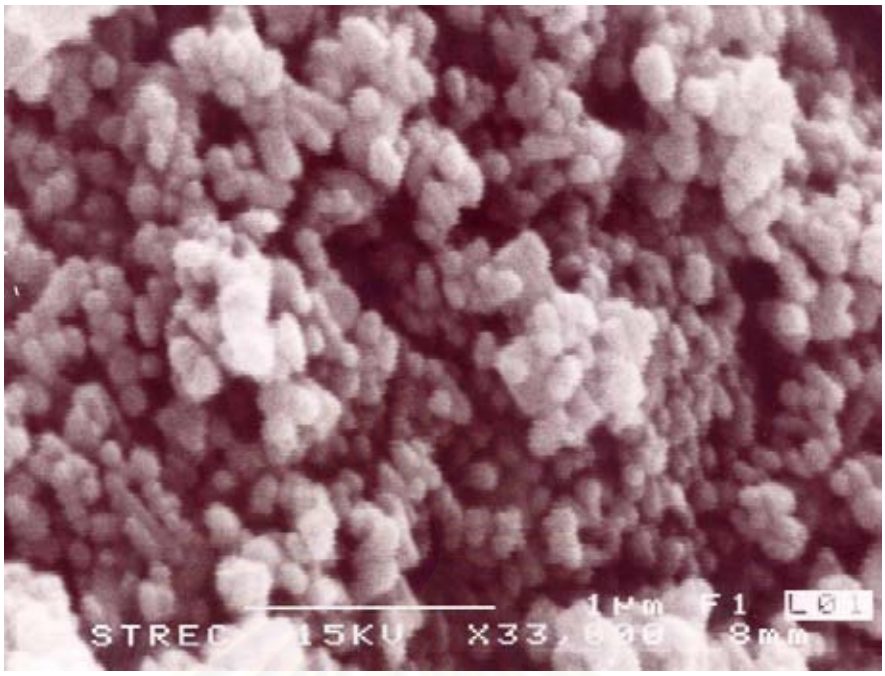

Figure 5.42 SEM image of ZnO nanoparticles as-synthesized in 1,4 butaindiol at 250 °C for 2 h by using zinc acetate 20g.

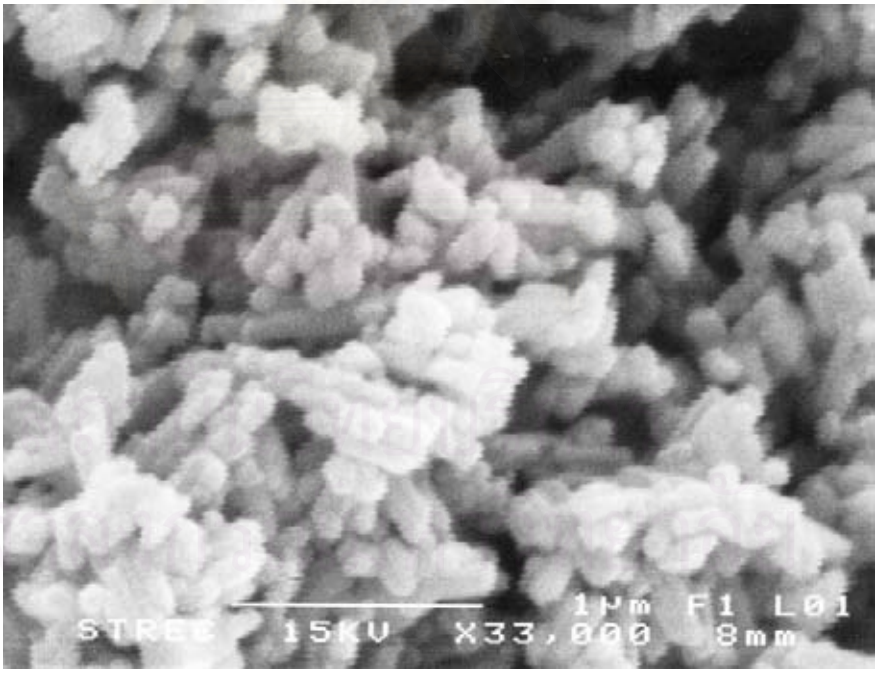

Figure 5.43 SEM image of ZnO nanoparticles as-synthesized in 1-octanol at 250 °C for 2 h by using zinc acetate 5 g.

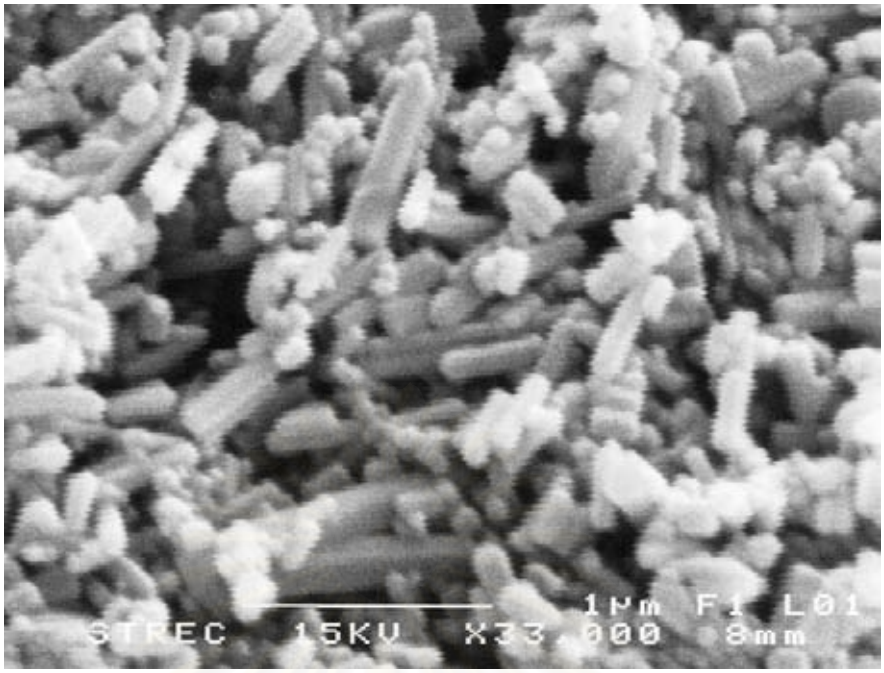

Figure 5.44 SEM image of ZnO nanoparticles as-synthesized in 1-octanol at 250 °C for 2 h by using zinc acetate 10 g.

Figure 5.45 SEM images of ZnO nanoparticles as-synthesized in 1-octanol at 250 °C for 2 h by using zinc acetate 20 g.

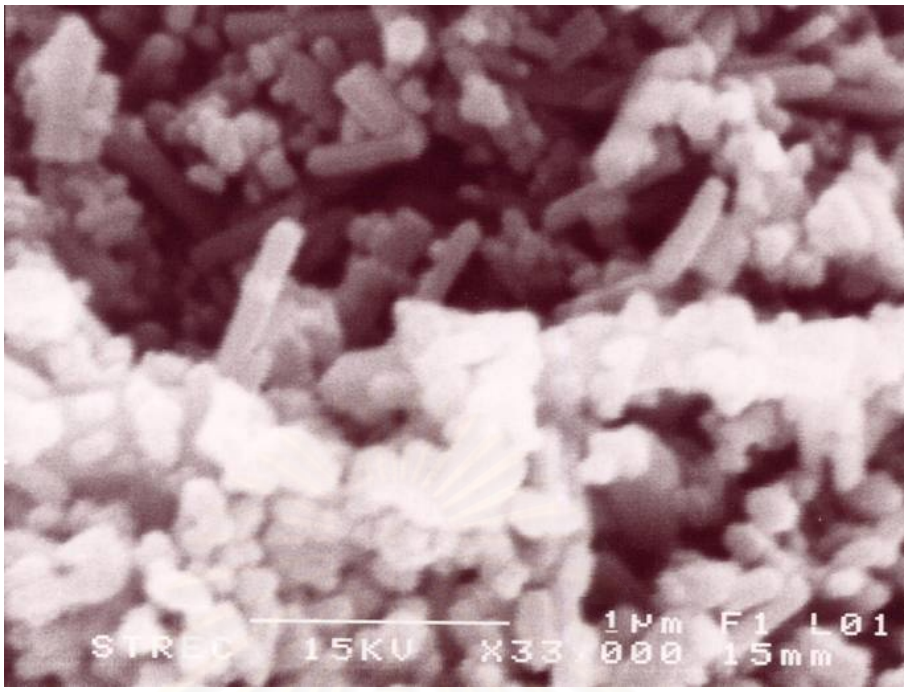

Figure 5.46 SEM images of ZnO nanoparticles as-synthesized in 1-decanol at 250 °C for 2 h by using zinc acetate 10 g.

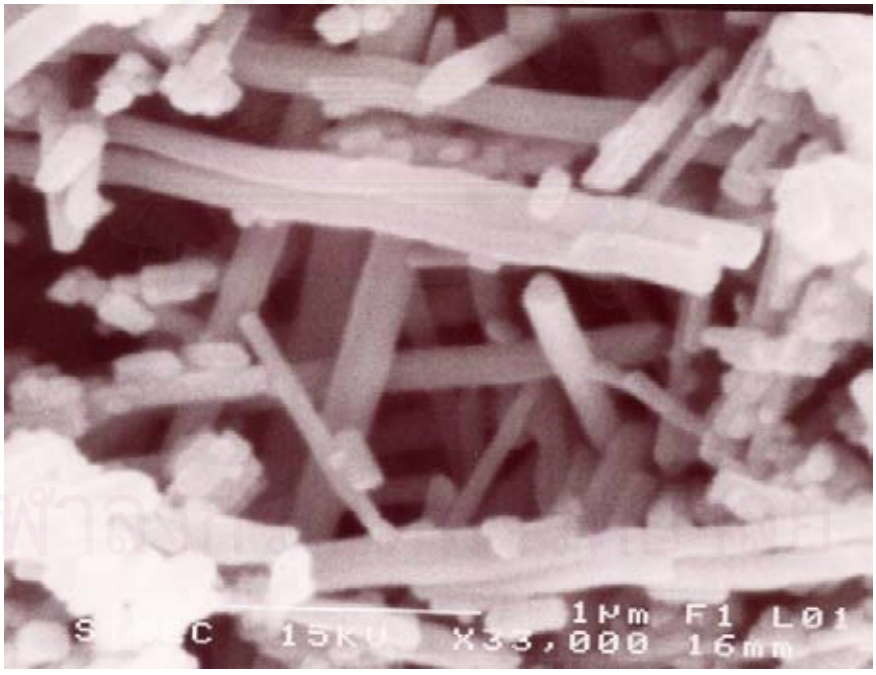

Figure 5.47 SEM images of ZnO nanoparticles as-synthesized in 1-decanol at 250 °C for 2 h by using zinc acetate 20 g.

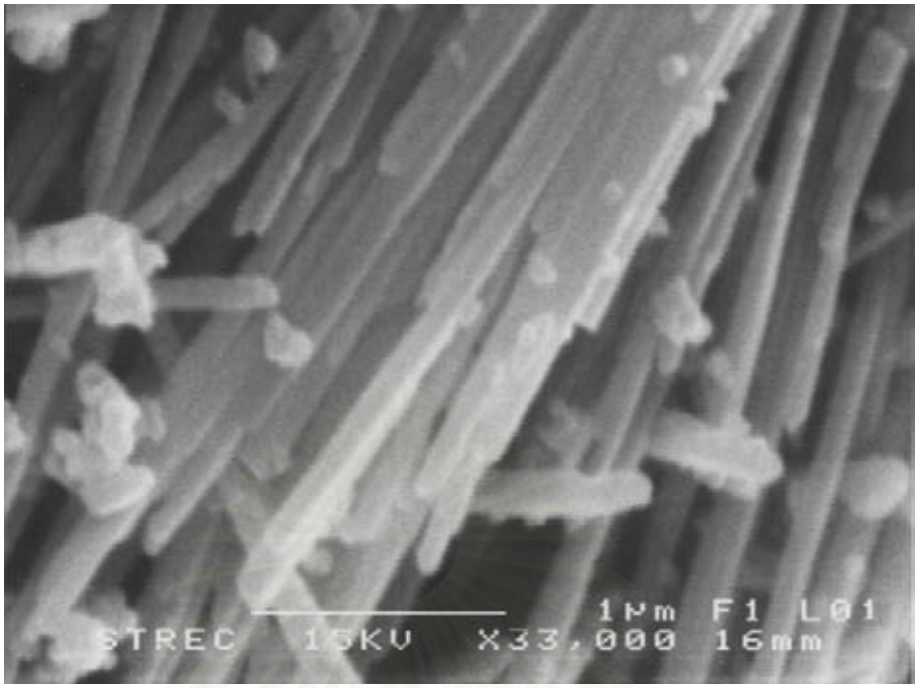

Figure 5.48 SEM images of ZnO nanoparticles as-synthesized in toluene at 300 °C for 2 h by using zinc acetate 10 g.

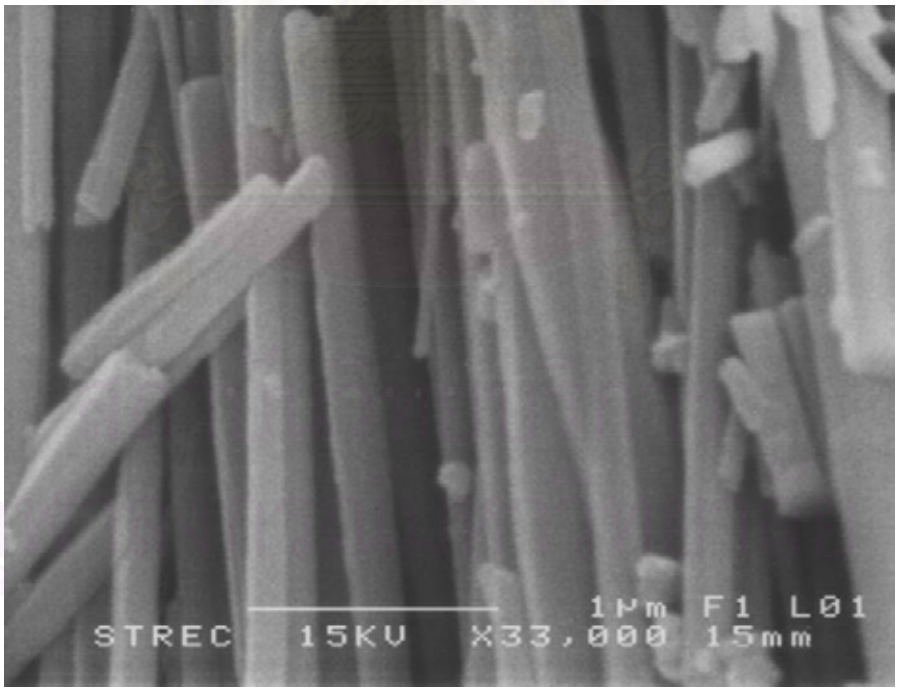

Figure 5.49 SEM images of ZnO nanoparticles as-synthesized in toluene at 300 °C for 2 h by using zinc acetate 15 g.

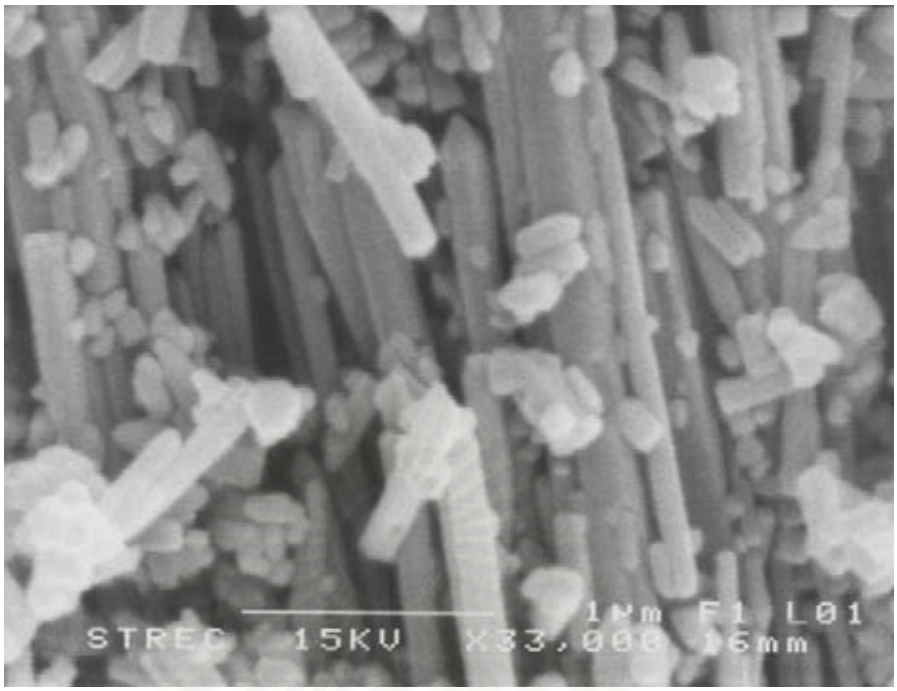

Figure 5.50 SEM images of ZnO nanoparticles as-synthesized in toluene at 300 °C for 2 h by using zinc acetate 20 g.

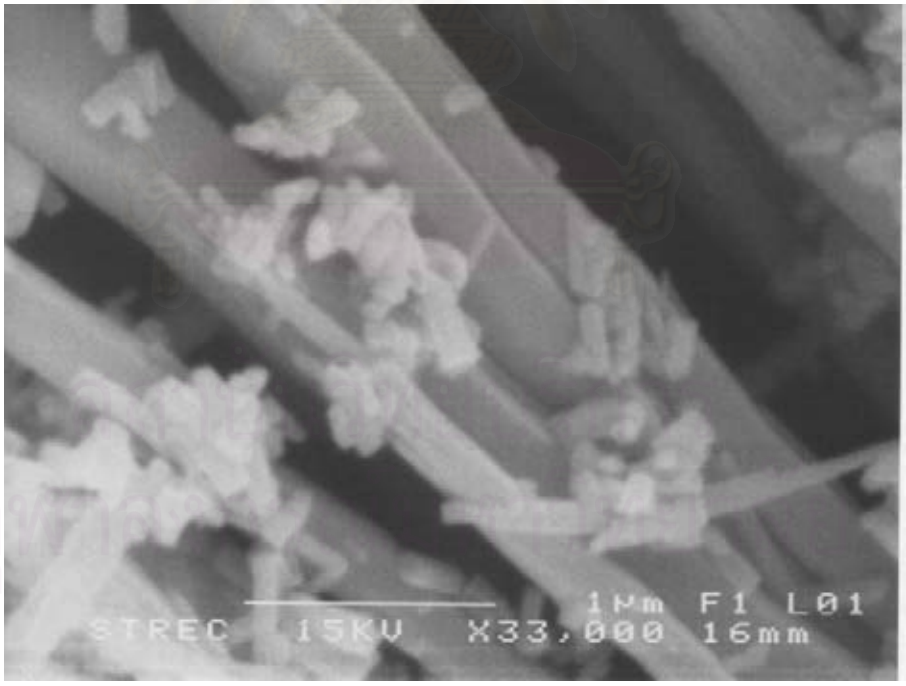

Figure 5.51 SEM images of ZnO nanoparticles as-synthesized in toluene at 300 °C for 2 h by using zinc acetate 25 g.

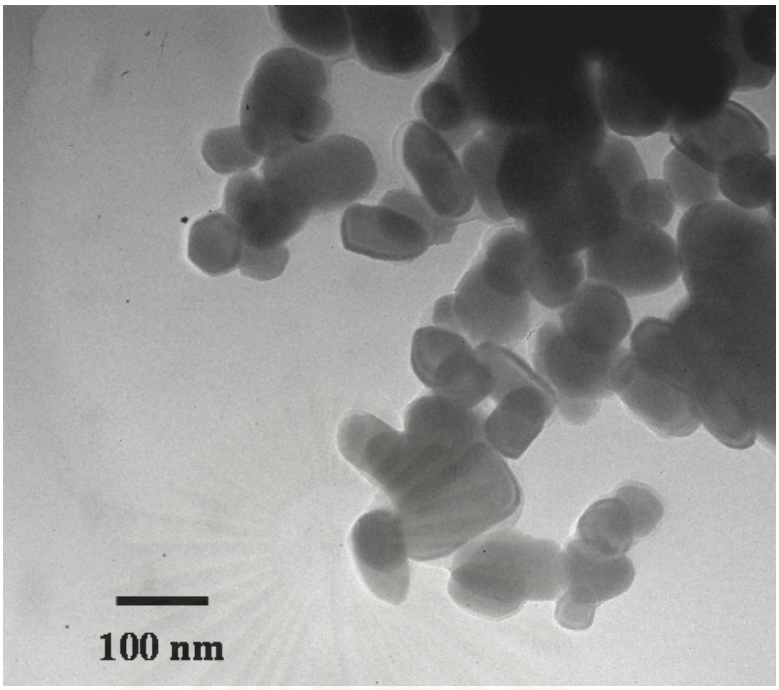

Figure 5.52 TEM images of ZnO nanoparticles as-synthesized in 1,4 butanediol at 250°C for 2 h by using zinc acetate 10 g.

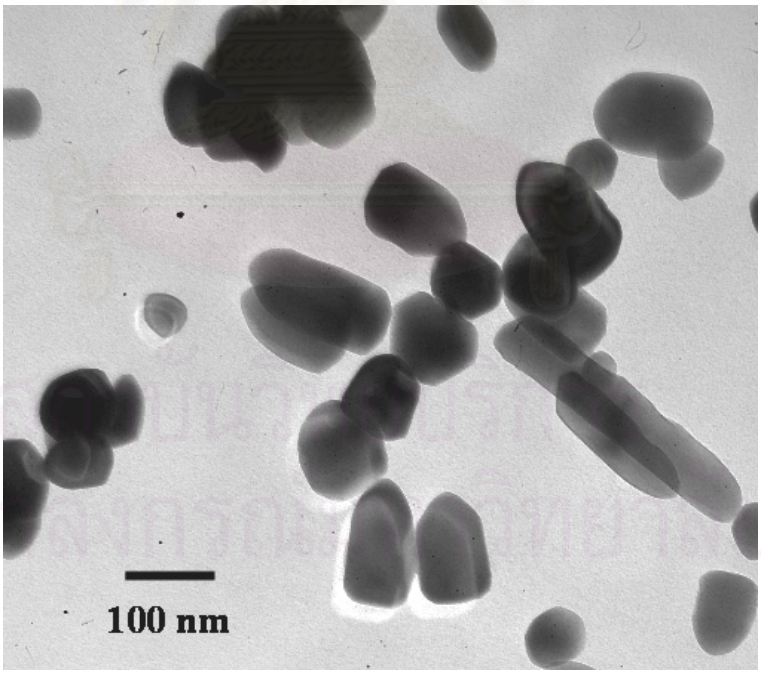

Figure 5.53 TEM image of ZnO nanoparticles as-synthesized in 1,4 butanediol at 250°C for 2 h by using zinc acetate 20 g.

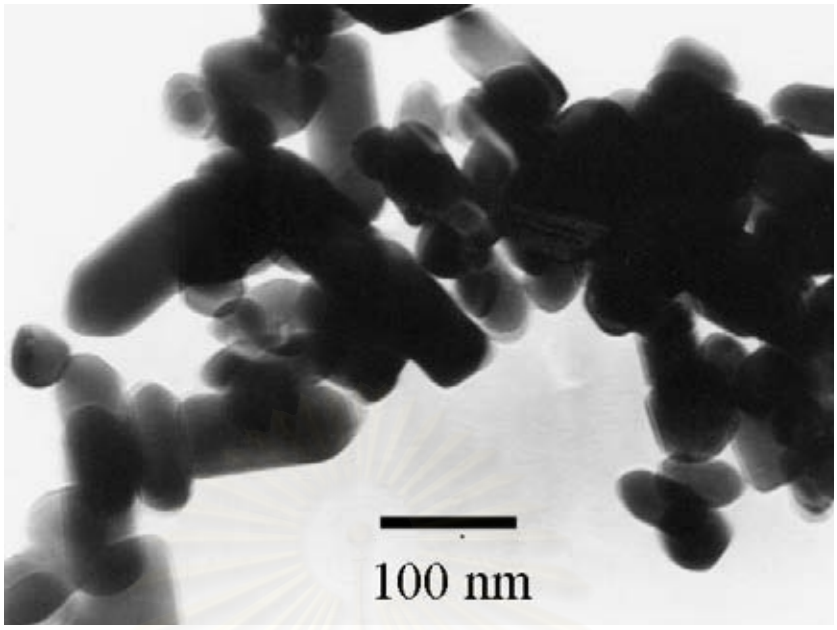

Figure 5.54 TEM image of ZnO nanoparticles as-synthesized in 1-octanol at 250°C for 2 h by using zinc acetate 5 g.

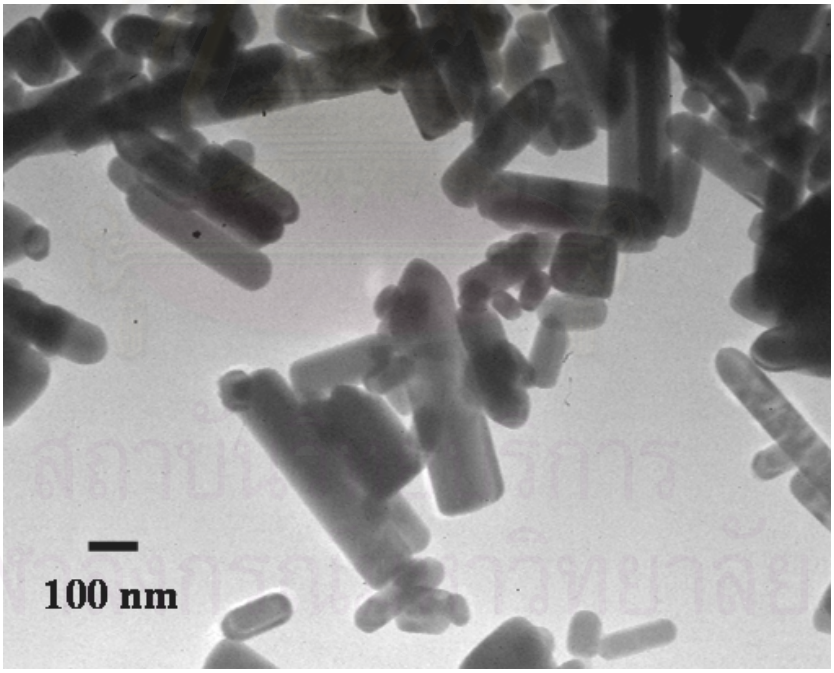

Figure 5.55 TEM image of ZnO nanoparticles as-synthesized in 1-octanol at 250°C for 2 h by using zinc acetate 10 g.

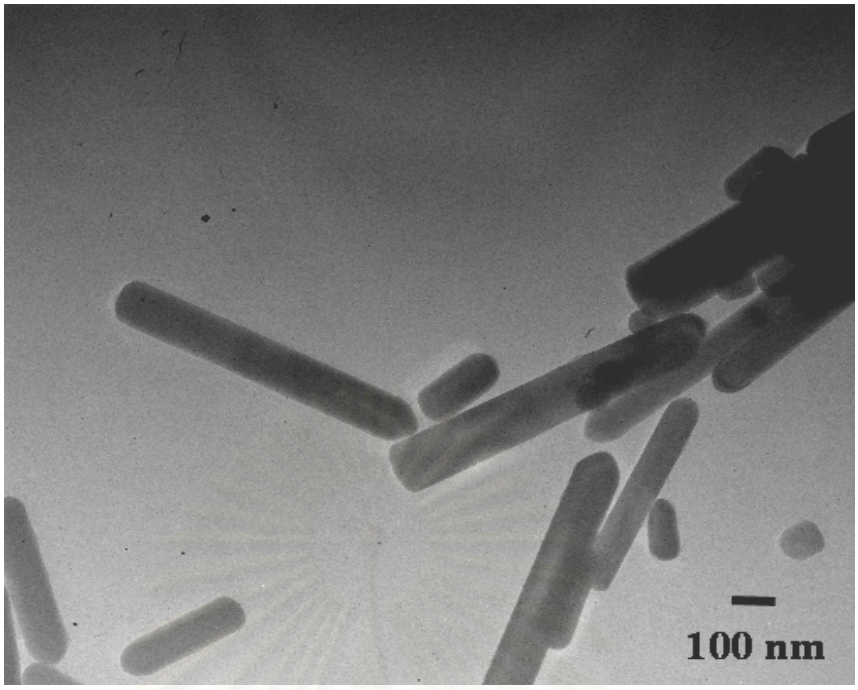

Figure 5.56 TEM image of ZnO nanoparticles as-synthesized in 1-octanol at 250°C for 2 h by using zinc acetate 20 g.

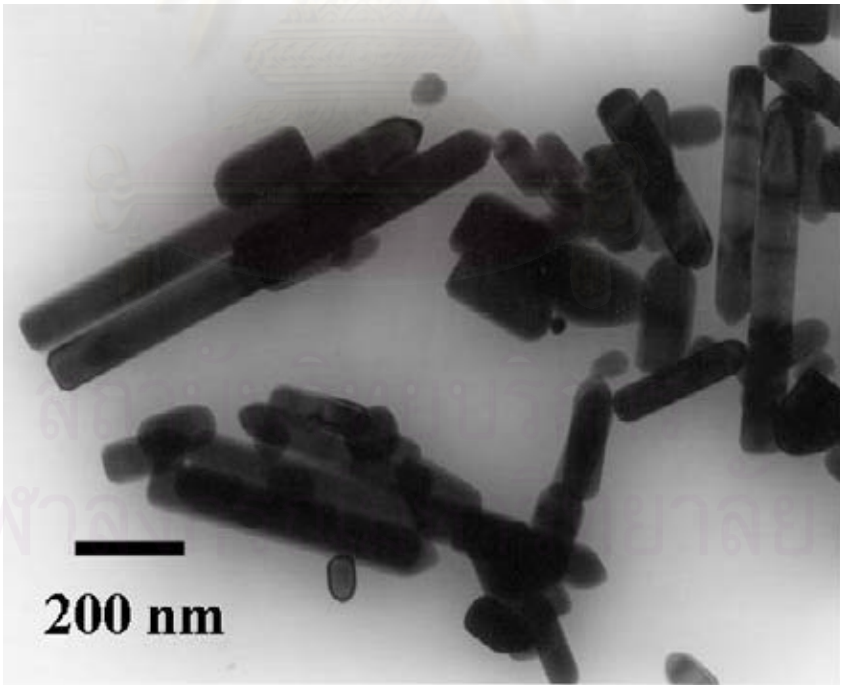

Figure 5.57 TEM image of ZnO nanoparticles as-synthesized in 1-decanol at 250°C for 2 h by using zinc acetate 10 g.

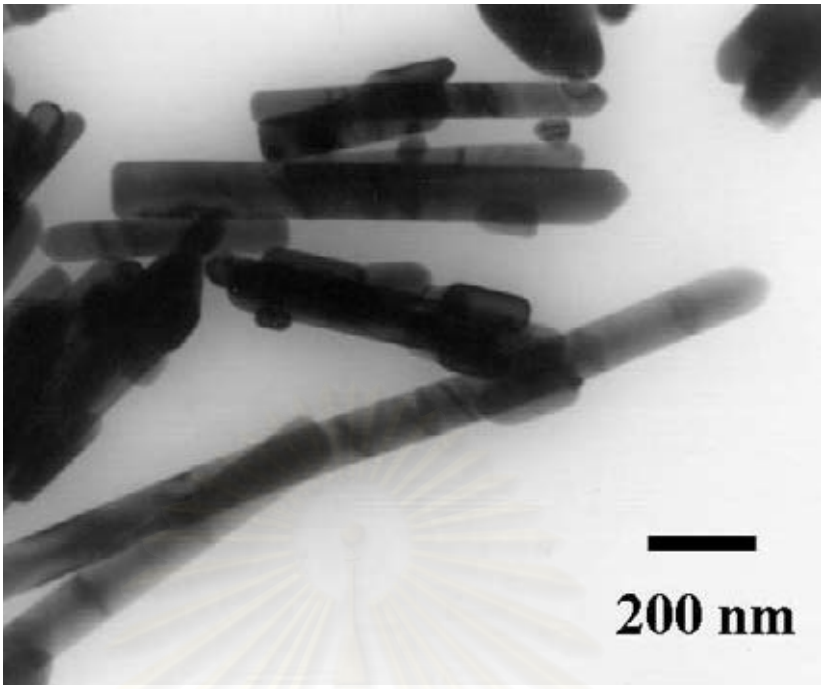

Figure 5.58 TEM image of ZnO nanoparticles as-synthesized in 1-decanol at 250°C for 2 h by using zinc acetate 20 g.

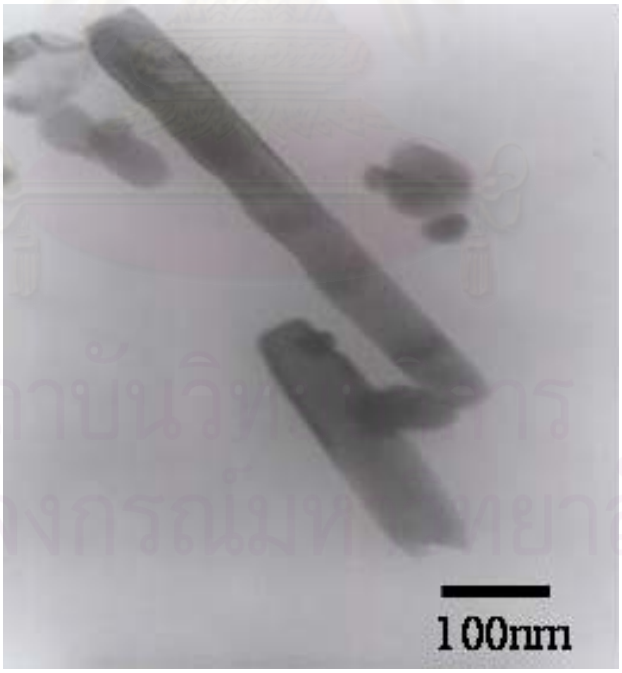

Figure 5.59 TEM image of ZnO nanoparticles as-synthesized in toluene at 300°C for 2 h by using zinc acetate 10 g.

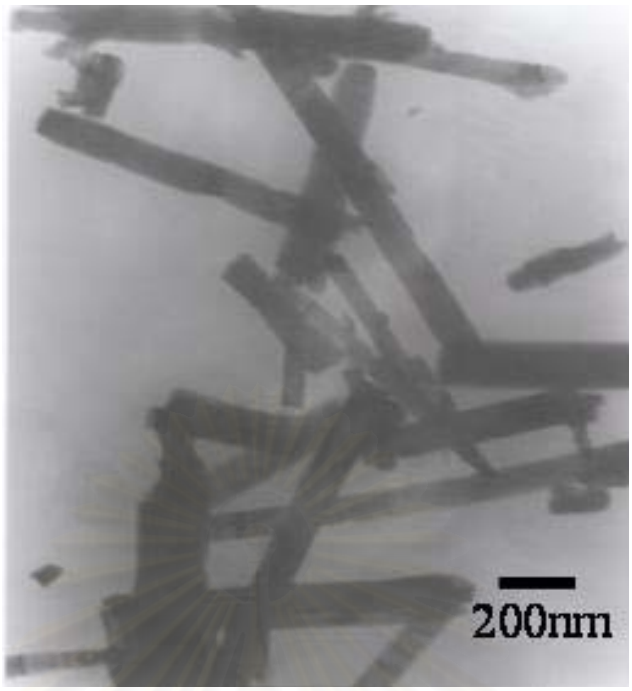

Figure 5.60 TEM image of ZnO nanoparticles as-synthesized in toluene at 300°C for 2 h by using zinc acetate 15 g.

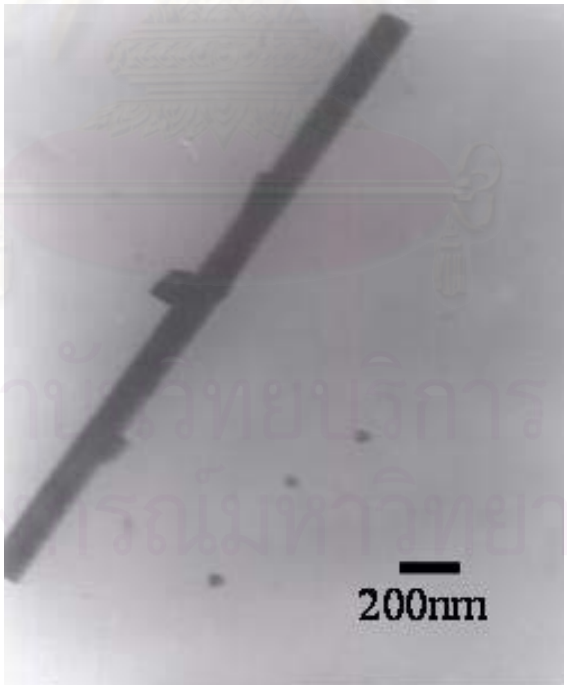

Figure 5.61 TEM image of ZnO nanoparticles as-synthesized in toluene at 300°C for 2 h by using zinc acetate 20 g.

Figure 5.62 TEM image of ZnO nanoparticles as-synthesized in toluene at 300°C for 2 h by using zinc acetate 25 g.

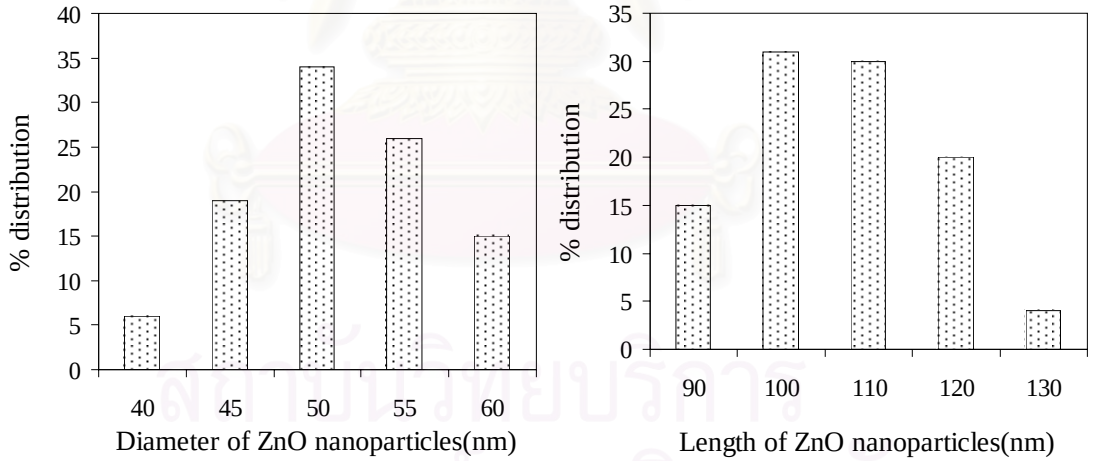

Figure 5.63 Histograms of the diameter and length size distributions obtained from TEM images for ZnO prepared in 1,4 butanediol at 250°C for 2h by using zinc acetate 10 g.

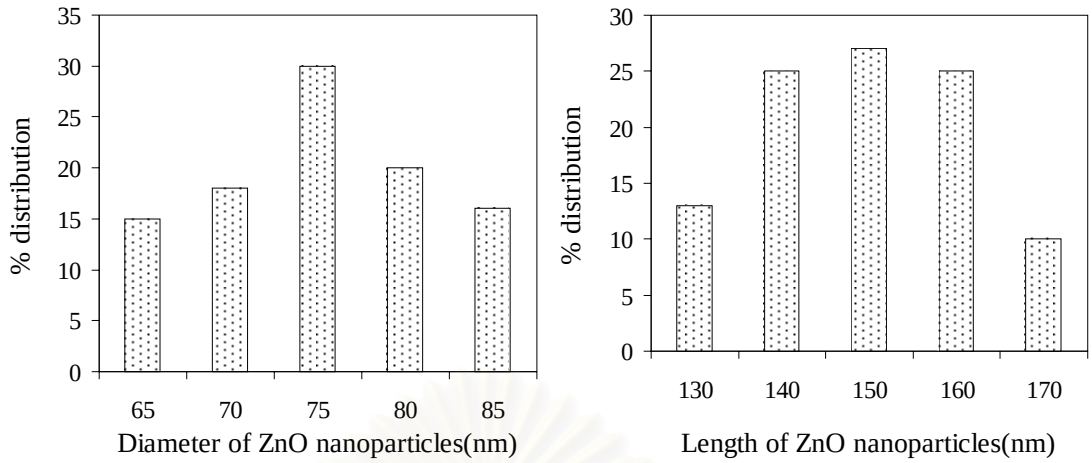

Figure 5.64 Histograms of the diameter and length size distributions obtained from TEM images for ZnO prepared in 1,4 butanediol at 250°C for 2h by using zinc acetate 20 g.

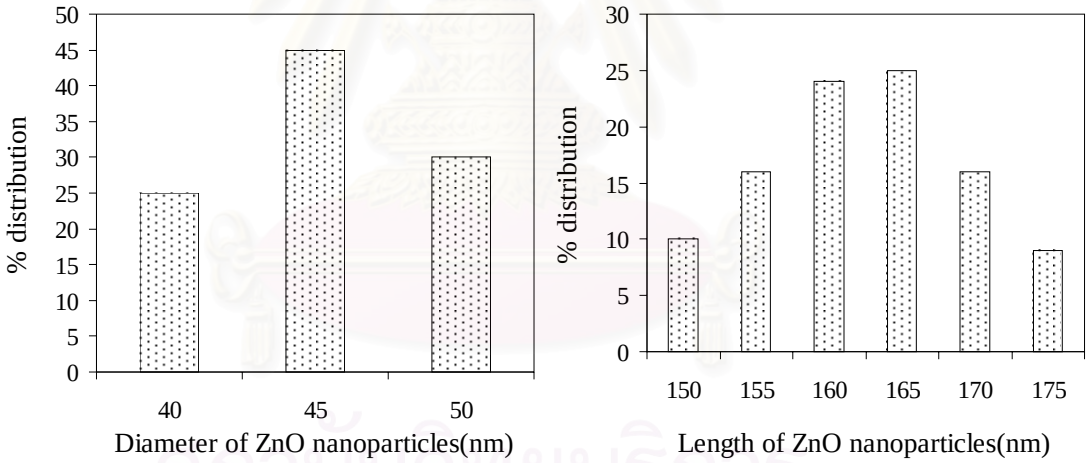

Figure 5.65 Histograms of the diameter and length size distributions obtained from TEM images for ZnO prepared in 1-octanol at 250°C for 2h by using zinc acetate 5 g.

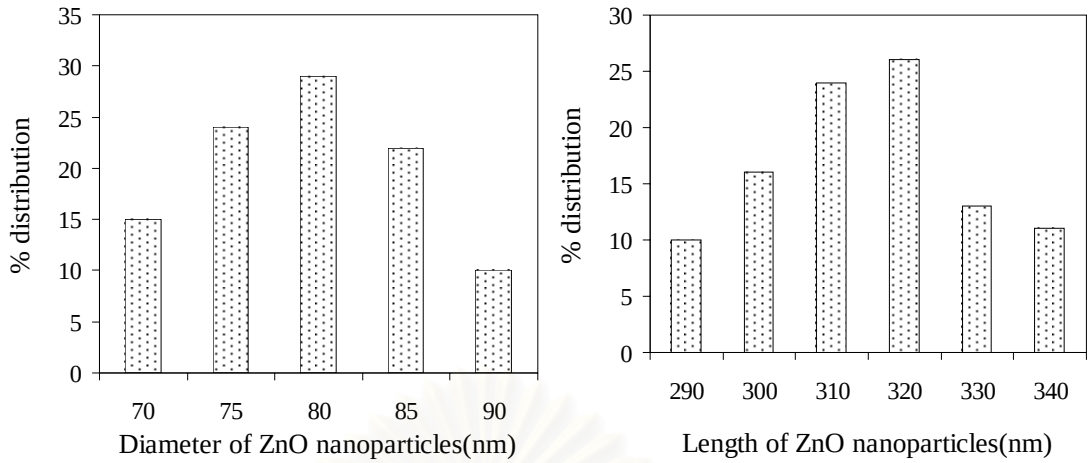

Figure 5.66 Histograms of the diameter and length size distributions obtained from TEM images for ZnO prepared in 1-octanol at 250°C for 2h by using zinc acetate 10 g.

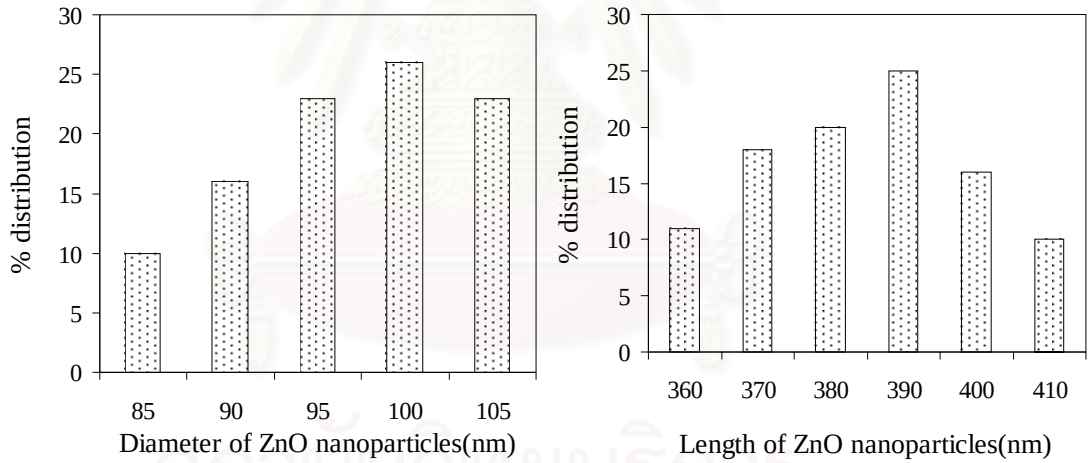

Figure 5.67 Histograms of the diameter and length size distributions obtained from TEM images for ZnO prepared in 1-octanol at 250°C for 2h by using zinc acetate 20 g.

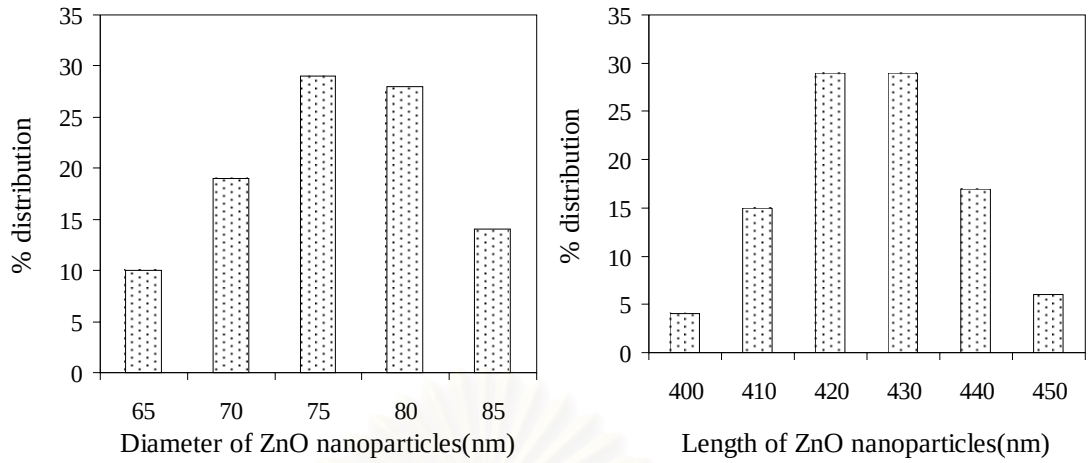

Figure 5.68 Histograms of the diameter and length size distributions obtained from TEM images for ZnO prepared in 1-decanol at 250°C for 2h by using zinc acetate 10 g.

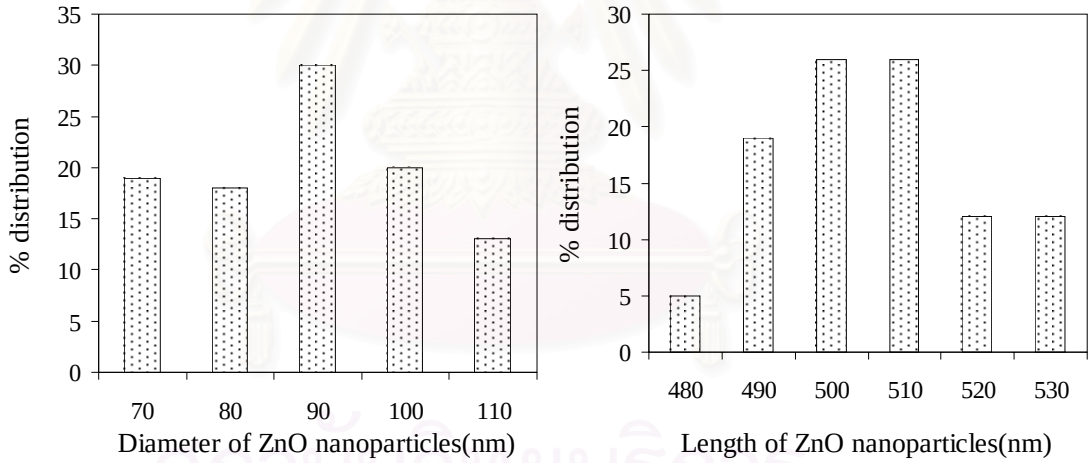

Figure 5.69 Histograms of the diameter and length size distributions obtained from TEM images for ZnO prepared in 1-decanol at 250°C for 2h by using zinc acetate 20 g.

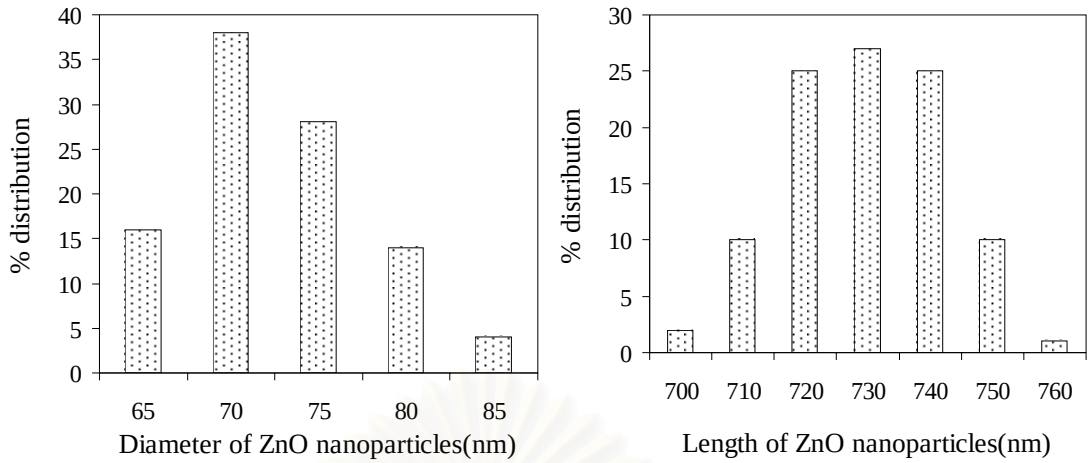

Figure 5.70 Histograms of the diameter and length size distributions obtained from TEM images for ZnO prepared in toluene at 300°C for 2h by using zinc acetate 10 g.

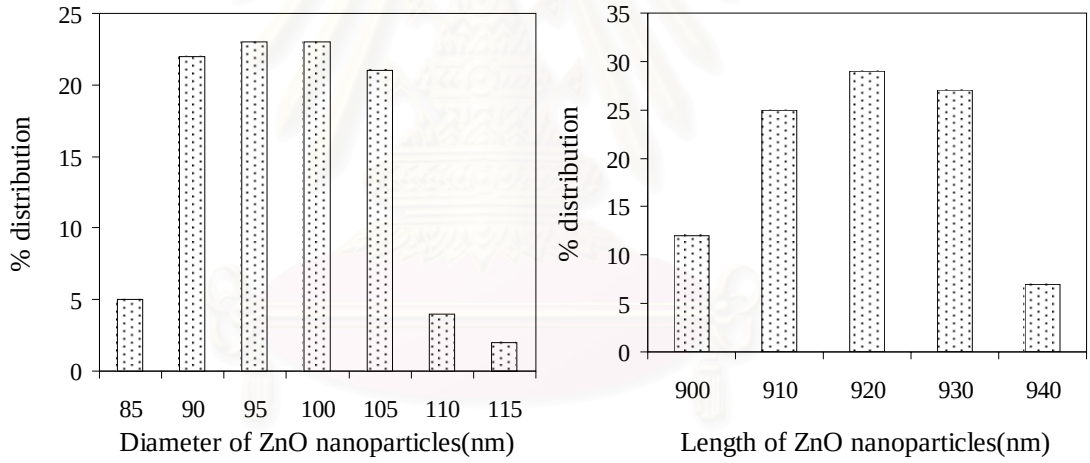

Figure 5.71 Histograms of the diameter and length size distributions obtained from TEM images for ZnO prepared in toluene at 300°C for 2h by using zinc acetate 15 g.

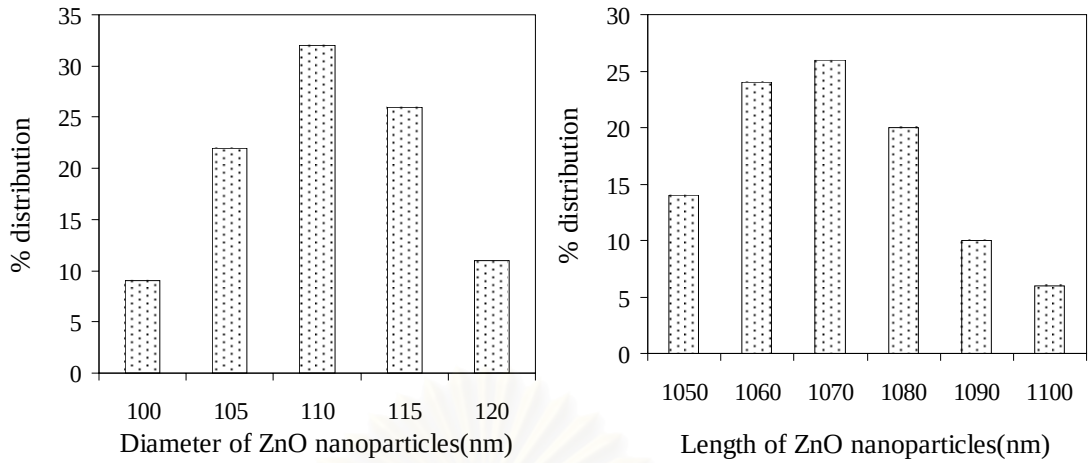

Figure 5.72 Histograms of the diameter and length size distributions obtained from TEM images for ZnO prepared in toluene at 300°C for 2h by using zinc acetate 20 g.

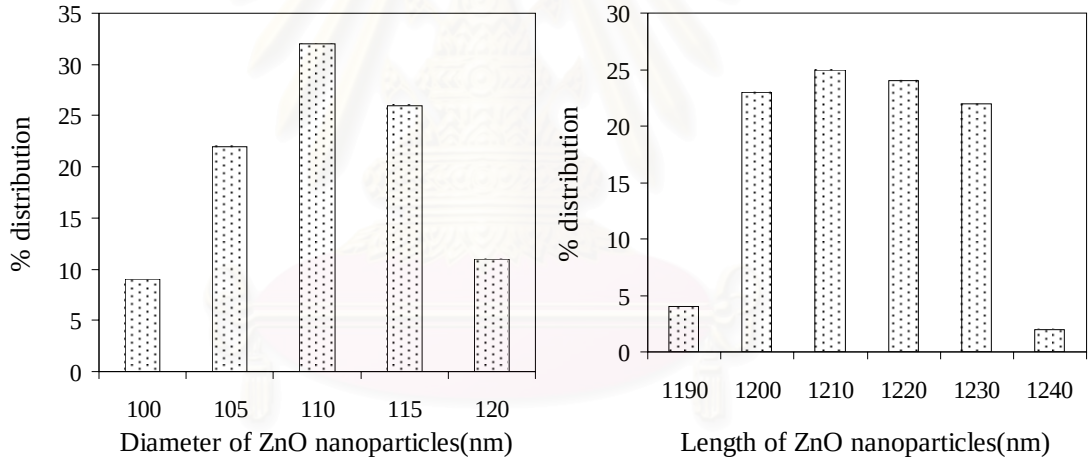

Figure 5.73 Histograms of the diameter and length size distributions obtained from TEM images for ZnO prepared in toluene at 300°C for 2h by using zinc acetate 25 g.

In case of reaction in toluene, the zinc acetate contents were varied from 10 to 25 g. As shown in Table 3, the average diameter sizes increased from 73 to 110 nm, corresponding to the increasing of the zinc acetate from 10 to 25g, respectively. It due to the fact that, the nucleation sites increased as the increasing of zinc acetate concentration. In case of reaction in 1,4 butanediol and 1-decanol, the average diameter size increased from 52 to 75 nm and 76 to 91 nm when the amount of zinc acetate increase from 10 to 20 g, respectively. The average diameter sizes increased from 43 to 97 nm of 1-octanol, corresponding to the increasing of the zinc acetate from 5 to 20g. Wei et al (2005) were reported that the diameter of the nanorods and the aspect ratios are decreased by decreasing the amount of precursor in hydrothermal method. However, in this thesis, the aspect ratios of particles were still same in each solvent which synthesized via solvothermal method by various amounts of starting material in 1,4 butanediol ,1-octanol and 1-decanol around 2, 4 and 5.6, respectively. The length and the aspect ratio of products obtained in toluene were highest and the aspect ratios around 10. The aspect ratio of ZnO nanoparticles is found to same by various amounts of zinc acetate in each solvent. It is suggested that the concentration of starting material via solvithermal metod was not affected on the growing rate ratio between plane in ZnO crystal. Table 5.2 summarized the particles size and physical properties of thus-obtained ZnO synthesized via solvothermal reaction.

Table 5.2 The physical properties of ZnO were prepared in 1,4 butanediol, 1-octanol, 1-decanol and toluene at various reaction temperatures for 2h by various amount of zinc.

Solvent	Temperature as-synthesized (°C)	Amount of zinc acetate (g)	Average diameter (nm)	Average length (nm)	Aspect ratio	BET surface area (m^2/g)
1,4 Butanediol	250	10	52	105	2.02	10.09
1,4 Butanediol	250	15	58	115	1.98	9.87
1,4 Butanediol	250	20	75	151	2.01	8.66
1-Octanol	250	5	43	162	3.76	11.4
1-Octanol	250	10	79	299	3.78	9.45
1-Octanol	250	15	84	343	4.08	8.87
1-Octanol	250	20	97	385	3.97	8.12
1-Decanol	250	10	76	423	5.56	7.76
1-Decanol	250	15	81	455	5.62	7.09
1-Decanol	250	20	91	506	5.56	6.24
Toluene	300	10	73	730	10.0	7.64
Toluene	300	15	98	920	9.39	6.89
Toluene	300	20	105	1070	10.19	6.44
Toluene	300	25	110	1216	11.05	6.07

5.3 The effect of organic solvents on the properties of ZnO nanoparticles

Zinc oxide was synthesized in various organic solvents (alcohol, and glycol) by using zinc acetate 15 g at 250°C for 2 h and zinc oxide was synthesized in benzene, toluene and xylene by using zinc acetate 15 g at 300°C for 2h.

5.3.1 ZnO nanoparticles prepared in various glycol

The ZnO nanoparticles were synthesized by glycothemal reaction in 1,3 propanediol (PG-ZnO), 1,4 butanediol (BG-ZnO), 1,5 pentanediol (PeG-ZnO) and 1,6 hexanediol (HG-ZnO) under the same conditions. Figure 5.74 shows the XRD patterns identifying the phases formed with ZnO nanocrystals obtained in different glycol. Most of the ZnO products peaks can be indexed to the hexagonal wurtzite structure. No characteristic peaks of impurities or secondary phases were observed. The strong intensity of ZnO diffraction peaks indicates that resulting product have high purity of ZnO wurtzite phase. This suggests suggested that ZnO was successfully synthesized by glycothermal reaction in 1,3 propanediol, 1,4 butanediol, 1,5 pentanediol and 1,6 hexanediol.

The ZnO products synthesized in 1,3 propanediol, 1,4 butanediol, 1,5 pentanediol and 1,6 hexanediol were characterized by SEM for analyzing morphology of the products as shown in Figure 5.75, 5.6, 5.76 and 5.77, respectively. Aggregations of fine particles were observed by the reaction in glycol. The images indicate that the surface of ZnO is smooth solid. SEM results indexed to the morphology of the secondary particle which diameter size and length are increased by changing the organic solvent.

TEM images of primary particles ZnO synthesized in 1,3 propanediol, 1,4 butanediol, 1,5 pentanediol and 1,6 hexanediol are presented in Figure 5.78, 5.17, 5.79 and 5.80, respectively,. The morphology of thus-obtained ZnO seemed to be nanorods with smooth surfaces. The diameter and length distribution based on these images are depicted in the histograms as Figure 5.89-5.91 and 5.28. The average diameter sizes of ZnO showed the narrowly distribution, found as was deduced from the histogram. It can be seen that most of fine particles have a nanosize diameter.

Physical properties of as-synthesized ZnO nanocrystals are summarized in Table 5.3. Aspect ratios of ZnO nanorods increased form 1.7 to 2.3 corresponding to the solvents change from 1,3 pentanediol to 1,6 hexanediol.

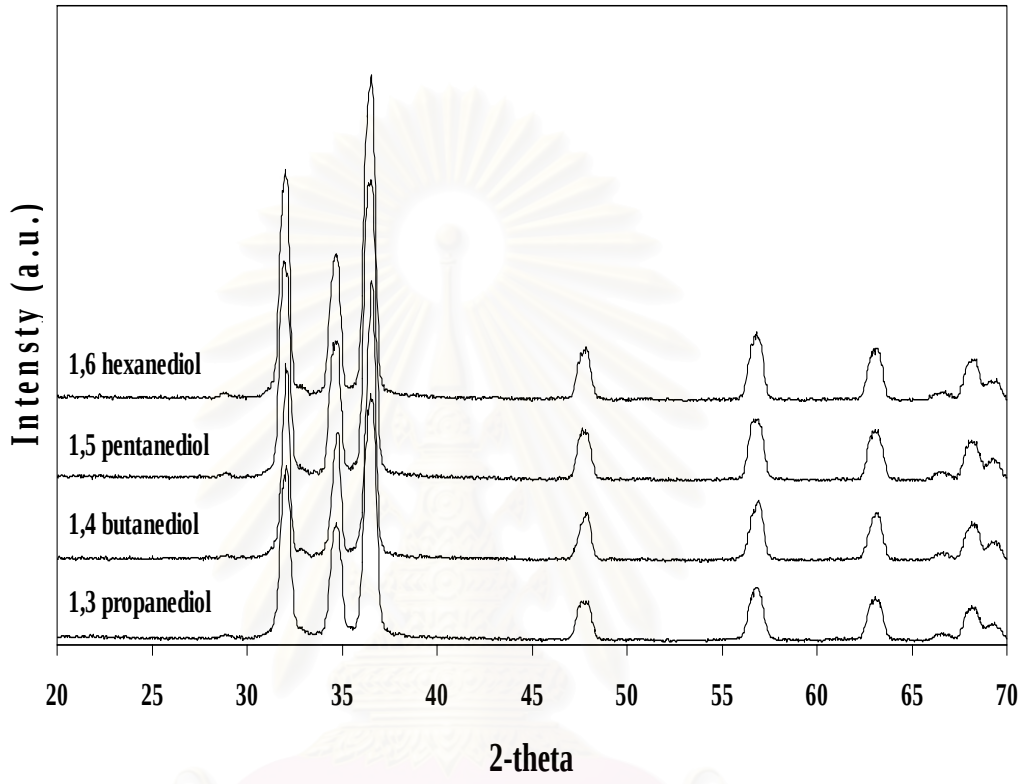

Figure 5.74 XRD patterns of ZnO nanoparticles that synthesized in glycol at 250°C for 2 h by using zinc acetate 15g.

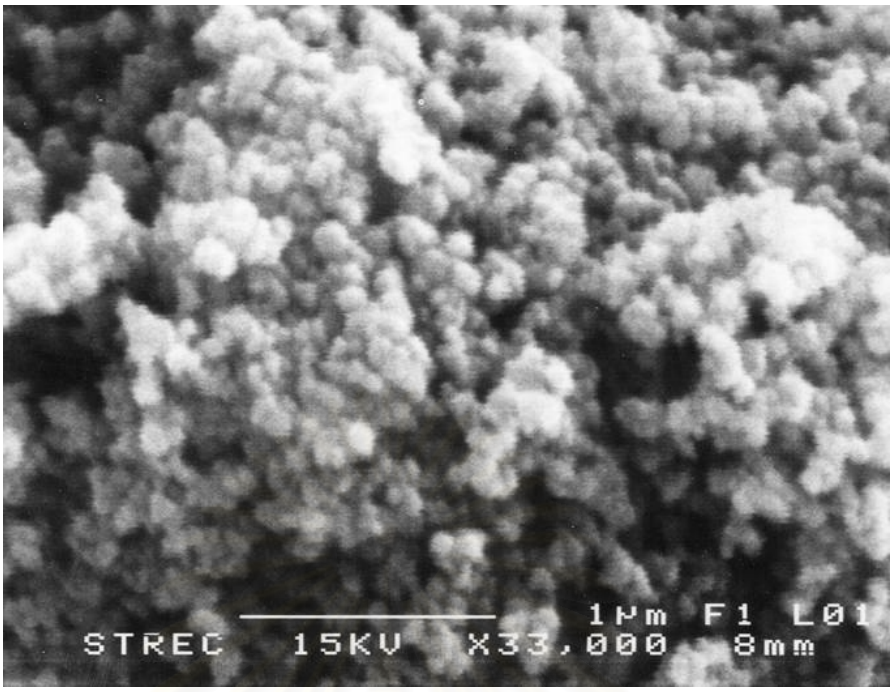

Figure 5.75 SEM image of ZnO nanoparticles as-synthesized in 1,3 propanediol at 250°C for 2 h by using zinc acetate 15 g.

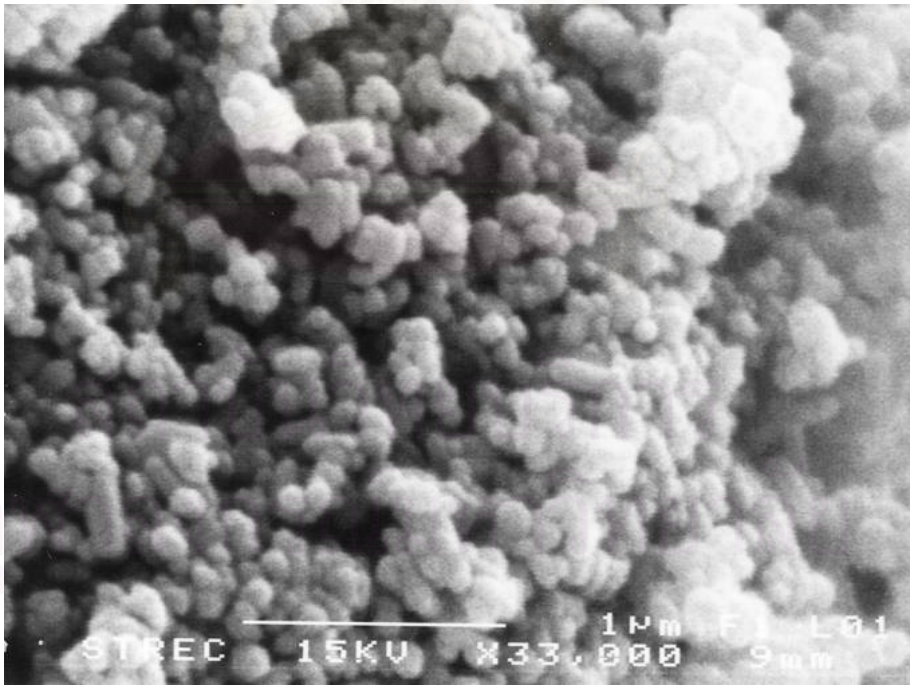

Figure 5.76 SEM image of ZnO nanoparticles as-synthesized in 1,5 pentanediol at 250°C for 2 h by using zinc acetate 15 g.

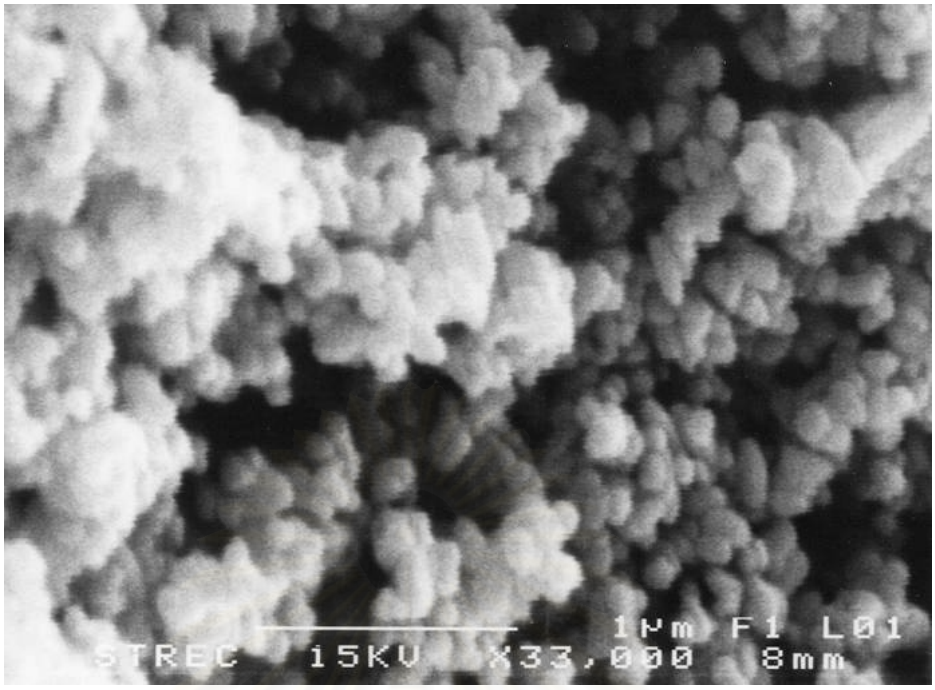

Figure 5.77 SEM image of ZnO nanoparticles as-synthesized in 1,6 hexanediol at 250°C for 2 h by using zinc acetate 15 g.

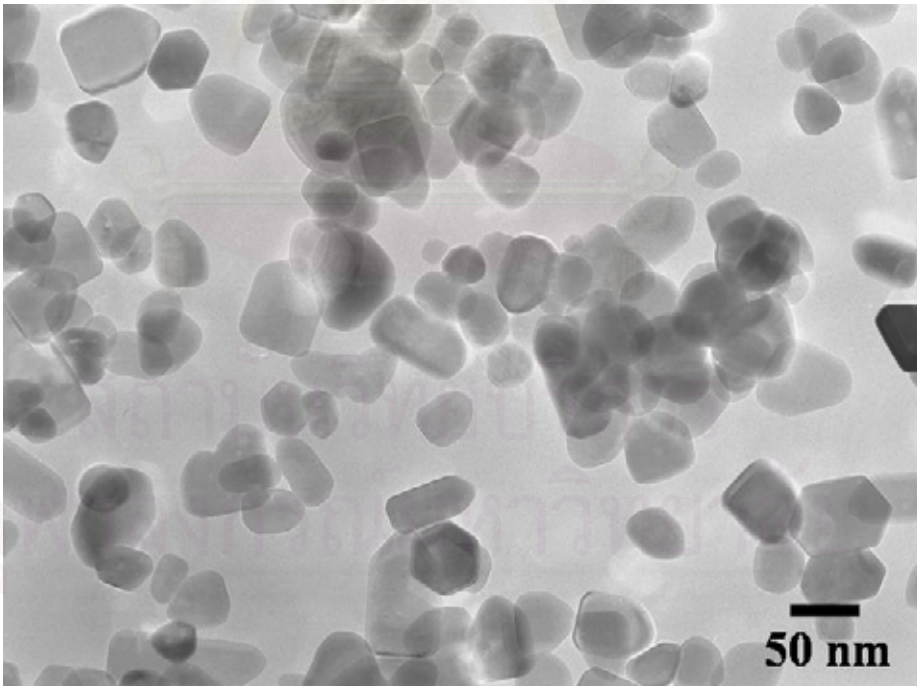

Figure 5.78 TEM image of ZnO nanoparticles as-synthesized in 1,3 propanediol at 250°C for 2 h by using zinc acetate 15 g.

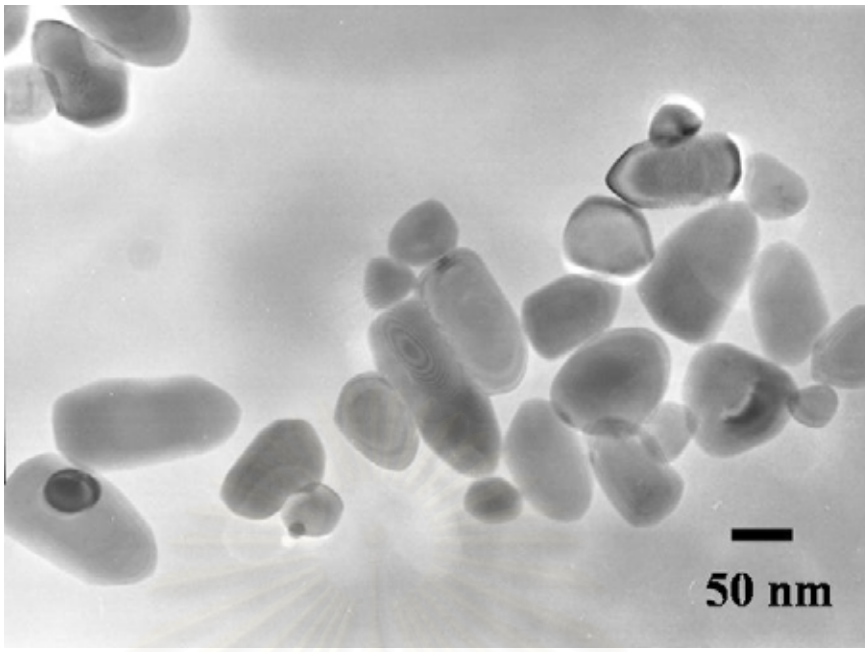

Figure 5.79 TEM image of ZnO nanoparticles as-synthesized in 1,3 pentanediol at 250°C for 2 h by using zinc acetate 15 g.

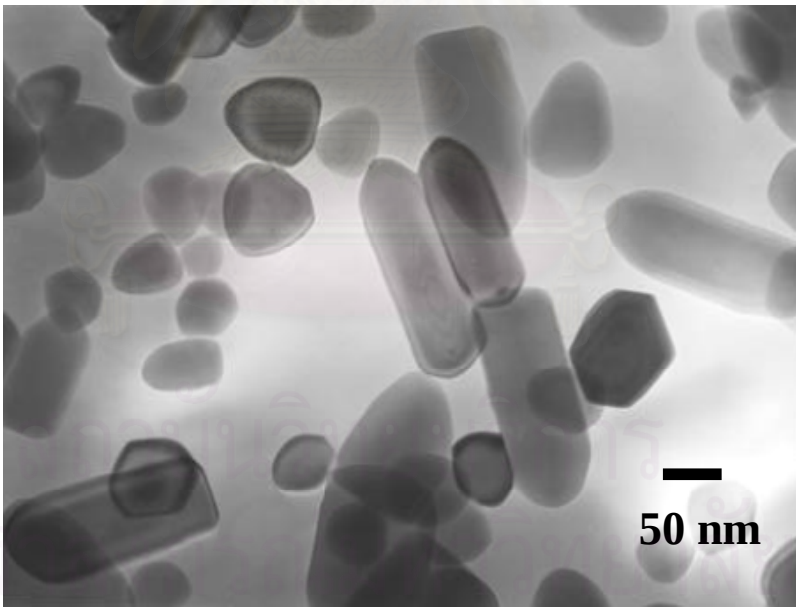

Figure 5.80 TEM image of ZnO nanoparticles as-synthesized in 1,6 hexanediol at 250°C for 2 h by using zinc acetate 15 g.

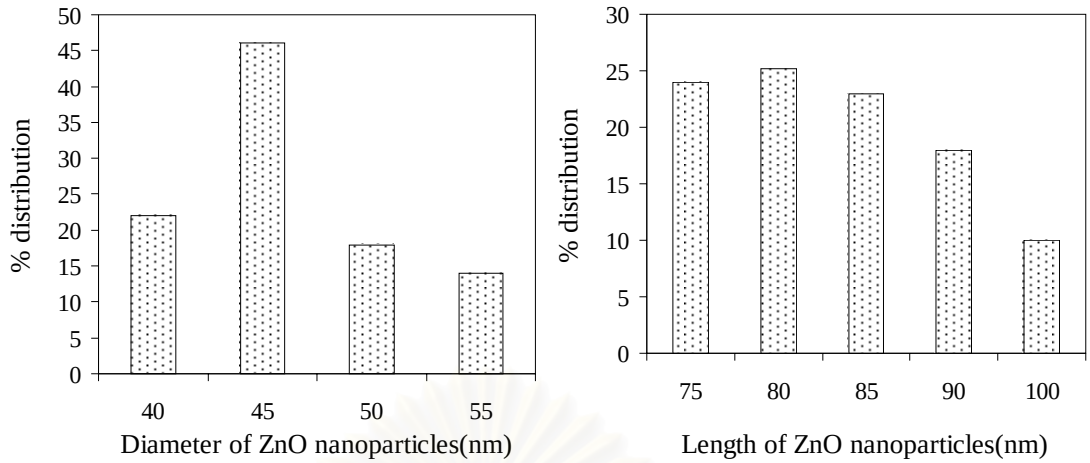

Figure 5.81 Histograms of the diameter and length size distributions obtained from TEM images for ZnO prepared in 1,3 propanediol at 250°C for 2h by using zinc acetate 15 g.

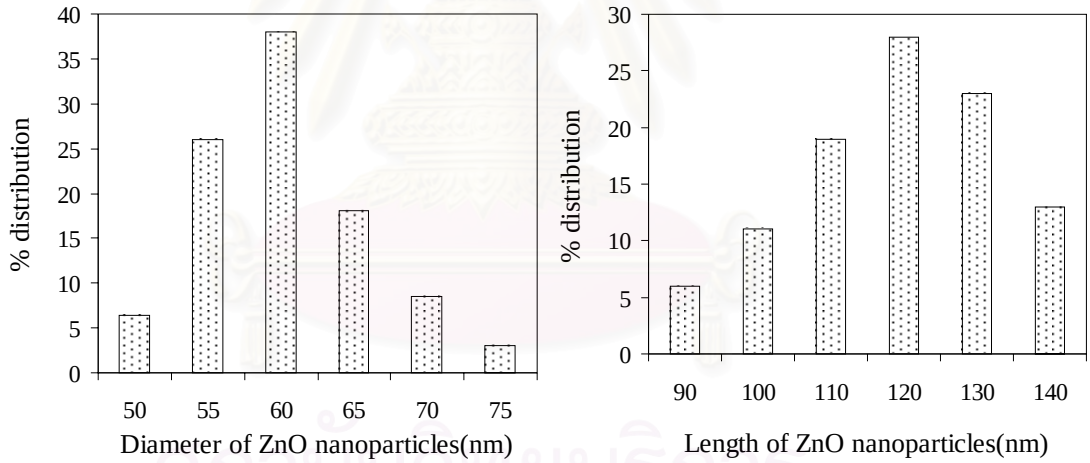

Figure 5.82 Histograms of the diameter and length size distributions obtained from TEM images for ZnO prepared in 1,5 pentanediol at 250°C for 2h by using zinc acetate 15 g.

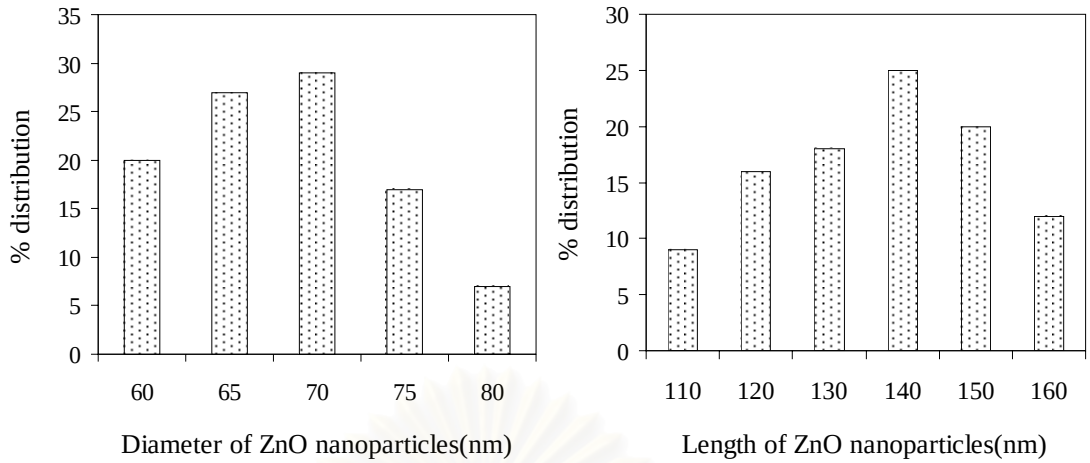

Figure 5.83 Histograms of the diameter and length size distributions obtained from TEM images for ZnO prepared in 1,6 hexanediol at 250°C for 2h by using zinc acetate 15 g.

5.1.2 ZnO nanoparticles prepared in various alcohols

The as-synthesized nanocrystalline ZnO products were prepared in 1-butanol (B-ZnO), 1-hexanol (H-ZnO), 1-octanol (O-ZnO) and 1-decanol (D-ZnO) at 250°C for 2h by using zinc acetate 15g. The typical XRD patterns for the ZnO powders obtained in different alcohol are shown in Figure 5.84. Most of the ZnO product peaks can be indexed to the hexagonal wurtzite structure. No peak from any else phases of ZnO and impurities were observed. The strong intensity of ZnO diffraction peaks indicates that resulting product have high purity of ZnO wurtzite phase. This result suggested that ZnO was successfully synthesized by solvothermal reaction in 1-butanol, 1-hexanol, 1-octanol and 1-decanol

The ZnO products synthesized in 1-butanol, 1-hexanol, 1-octanol and 1-decanol were characterized by SEM for analyzing morphology of the products as shown in Figures 5.85, 5.86, 5.10 and 5.87, respectively. ZnO nanorods were obtained by the reaction in long-chain alcohols. As can be seen the Figures 5.85-5.87 and 5.10, the samples were smooth solid hexagonal rods. SEM results indicate that the

morphology of the secondary particle which length and aspect ratio increased with changing the alcohol from 1-butanol, 1-hexanol, 1-octanol to 1-decanol.

The primary particles are shown as TEM images in Figure 5.88, 5.89, 5.21 and 5.90. The morphology of thus-obtained ZnO seemed to be nanorods with relatively straight and their surfaces were smooth. The diameter distributions and length distribution based on these images are depicted in the histograms as Figure 5.91, 5.92, 5.32 and 5.93. The average diameter sizes of ZnO showed the narrowly distribution, found as was deduced from the histogram. It can be seen that most of the rod have a nanosize diameter. The physical properties of as-synthesized ZnO nanocrystals are summarized in Table 5.3.

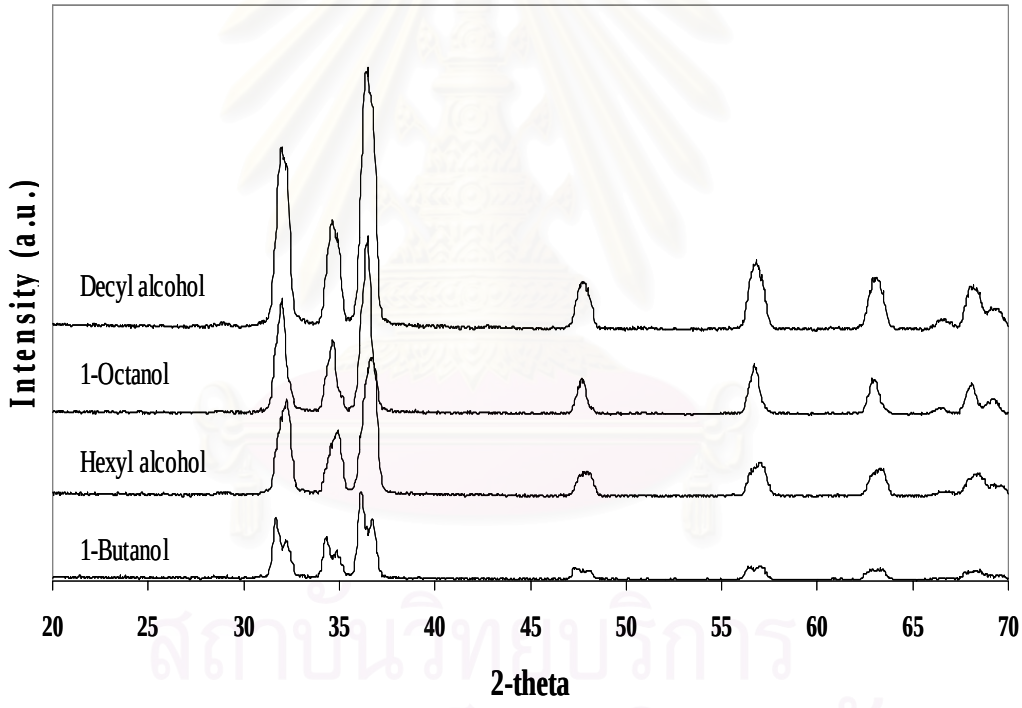

Figure 5.84 XRD patterns of ZnO nanoparticles that synthesized in alcohol at 250°C for 2 h by using zinc acetate 15g.

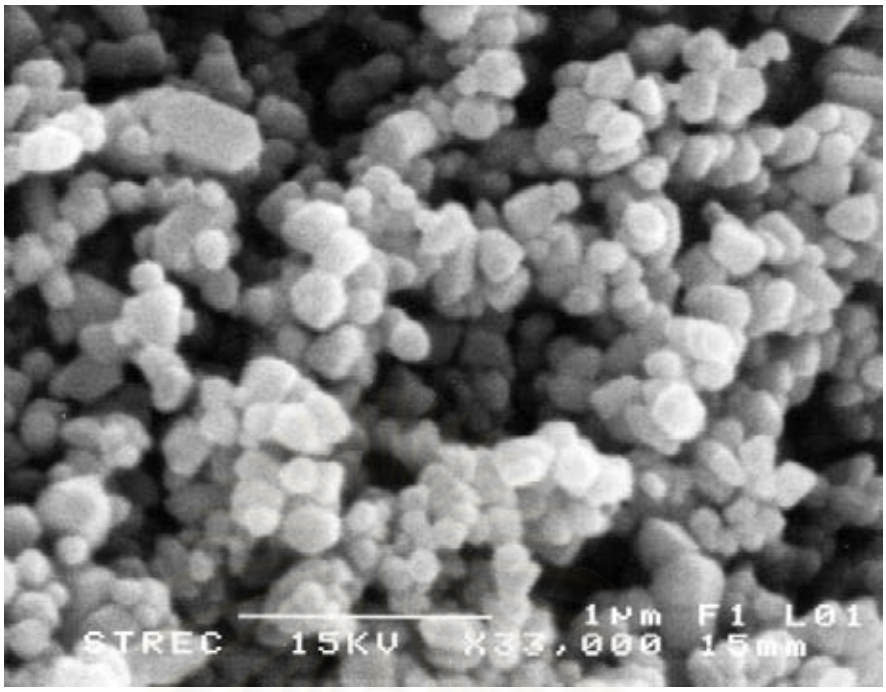

Figure 5.85 SEM image of ZnO nanoparticles as-synthesized in 1-butanol at 250°C for 2 h by using zinc acetate 15 g.

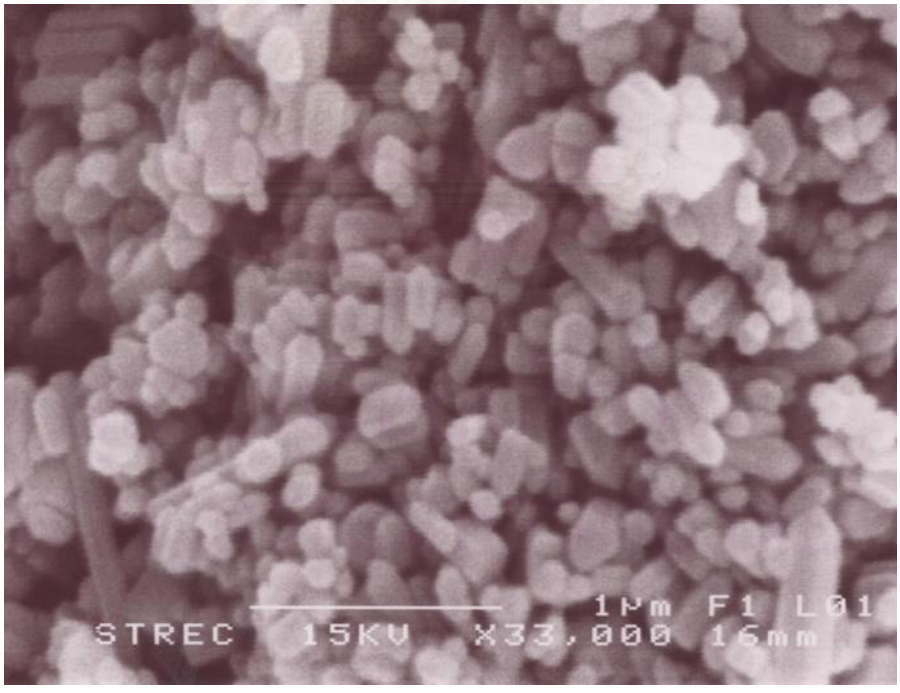

Figure 5.86 SEM image of ZnO nanoparticles as-synthesized in 1-hexanol at 250°C for 2 h by using zinc acetate 15 g.

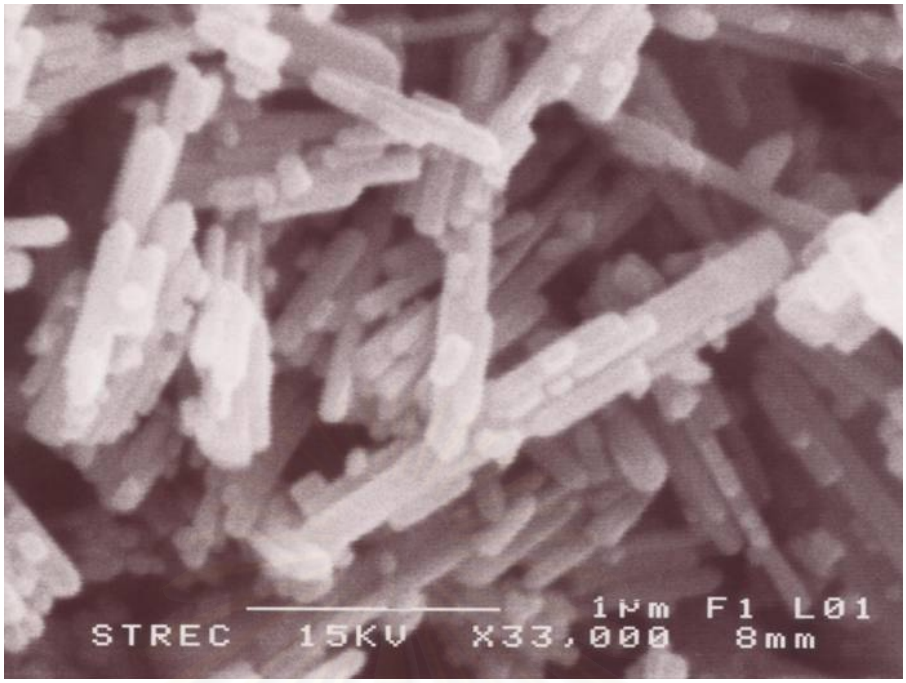

Figure 5.87 SEM image of ZnO nanoparticles as-synthesized in 1-decanol at 250°C for 2 h by using zinc acetate 15 g.

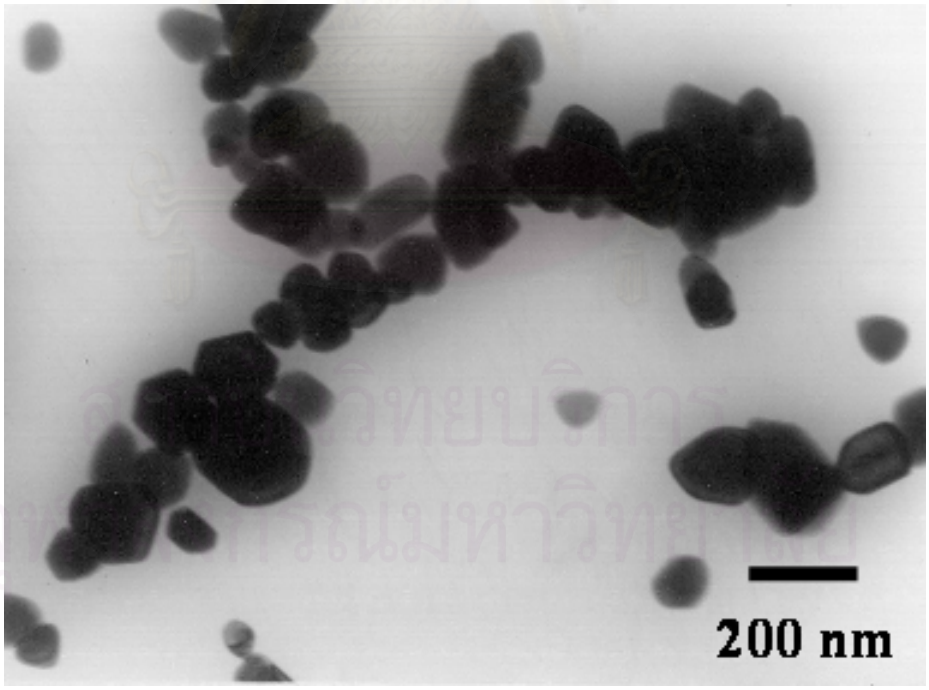

Figure 5.88 TEM image of ZnO nanoparticles as-synthesized in 1-butanol at 250°C for 2 h by using zinc acetate 15 g.

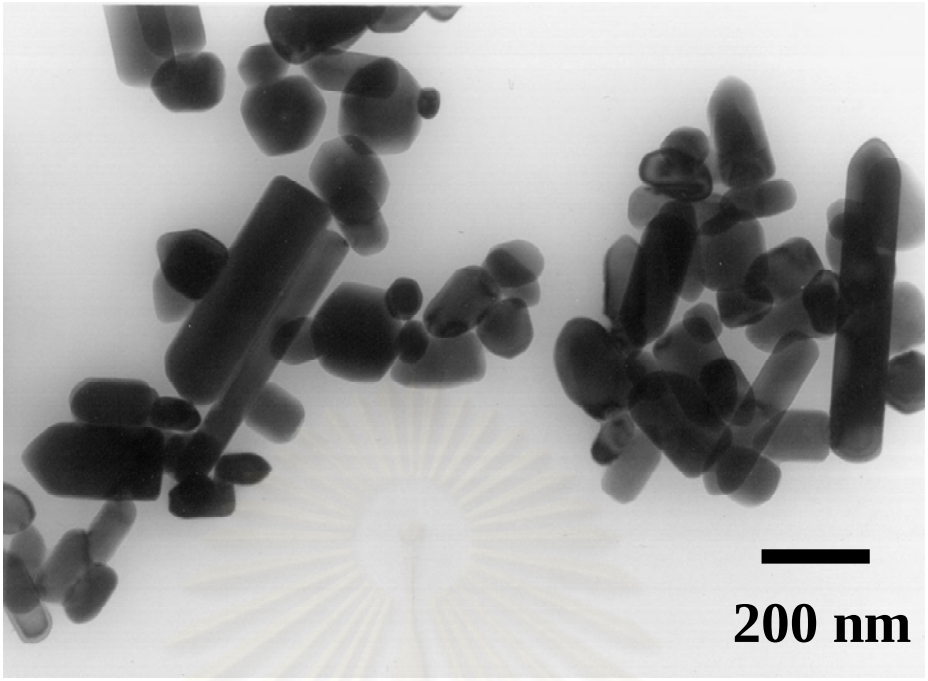

Figure 5.89 TEM image of ZnO nanoparticles as-synthesized in 1-hexanol at 250°C for 2 h by using zinc acetate 15 g.

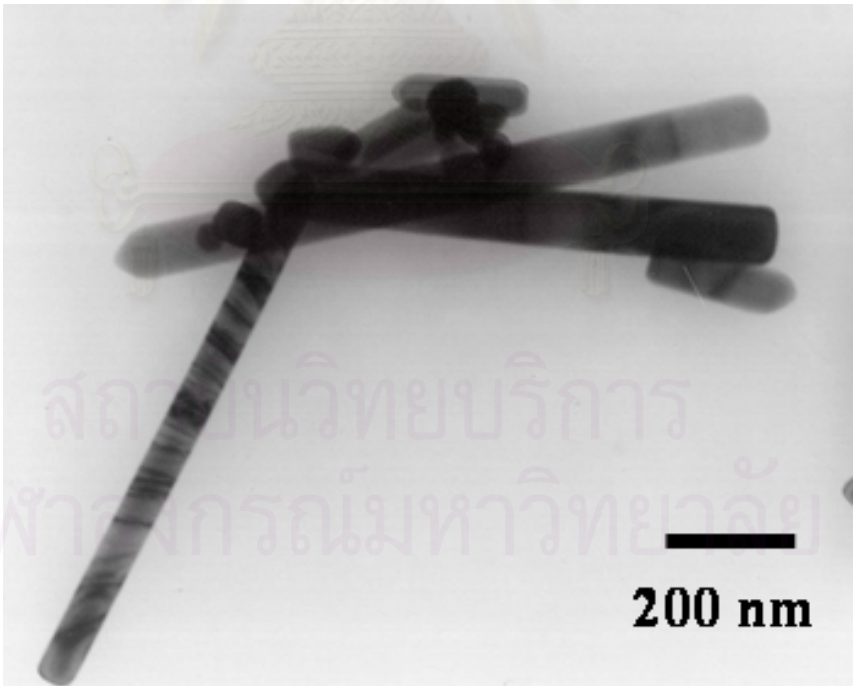

Figure 5.90 TEM image of ZnO nanoparticles as-synthesized in 1-decanol at 250°C for 2 h by using zinc acetate 15 g.

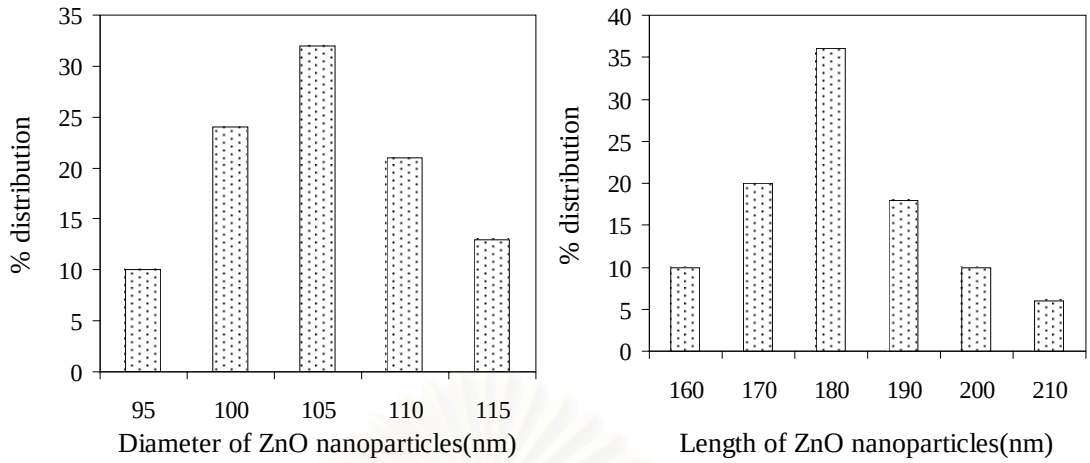

Figure 5.91 Histograms of the diameter and length size distributions obtained from TEM images for ZnO prepared in 1-butanol at 250 °C for 2h by using zinc acetate 15 g.

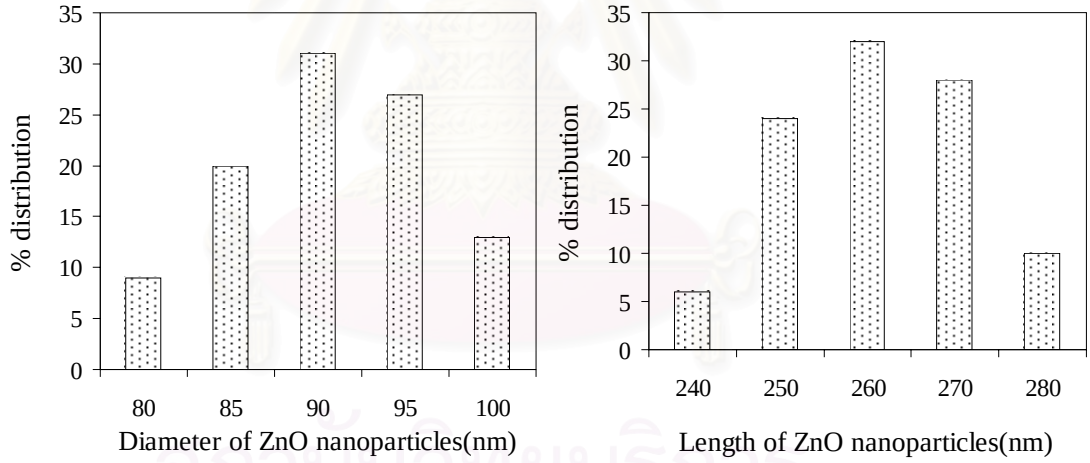

Figure 5.92 Histograms of the diameter and length size distributions obtained from TEM images for ZnO prepared in 1-hexanol at 250 °C for 2h by using zinc acetate 15 g.

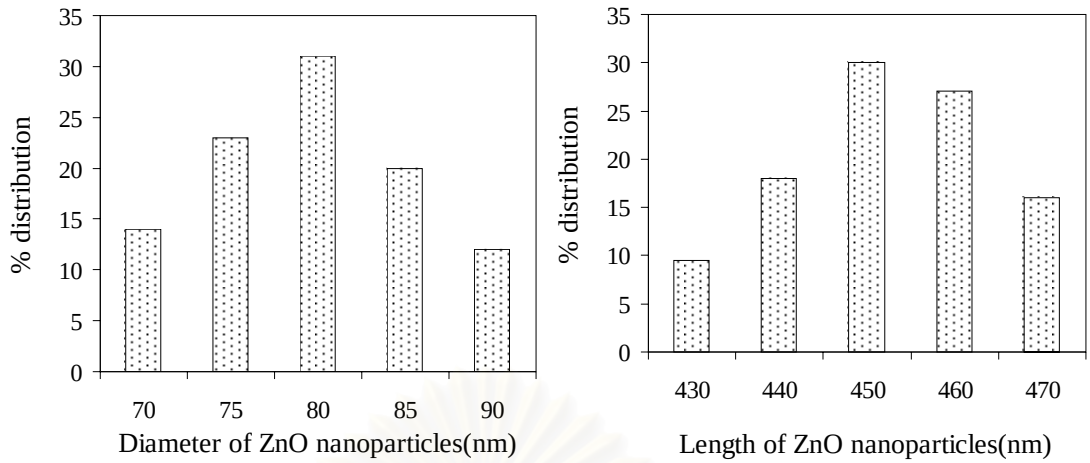

Figure 5.93 Histograms of the diameter and length size distributions obtained from TEM images for ZnO prepared in 1-decanol at 250 °C for 2h by using zinc acetate 15 g.

5.1.3 ZnO nanoparticles prepared in inert solvent

The as-synthesized nanocrystalline ZnO products synthesized by solvothermal reaction in toluene (T-ZnO). The XRD patterns of ZnO powders were prepared in toluene are shown in Figure 5.94. In Figure 5.94 (b) the crystallization of ZnO by the reaction in toluene was completed at 300°C, whereas ZnO as-synthesized was not complete at 280°C as shown in Figure 5.94 (a). In Figure 5.94 (a), it can be seen some peaks of zinc acetate are similar to Figure 5.115(a). In Figure 5.94 (b), the most of ZnO product peaks can be indexed to the hexagonal wurtzite structure. No peak from any else phase of ZnO and impurities were observed. The strong intensity of ZnO diffraction peaks indicates that resulting product have high purity of ZnO wurtzite phase (normalized to (101) reflection about 36.6 of 2θ position in Figure 5.94 (b) which is usually the most intense feature in the ZnO zincite diffraction pattern). This result suggested that ZnO was successfully synthesized by solvothermal reaction at 300°C in toluene.

The ZnO products as-synthesized in toluene were characterized by SEM for analyzing morphology of the products as shown in Figure 5.49. Nanorods of ZnO were observed by the reaction in toluene. As can be seen in the figure, the samples consist of large quantities of strength and smooth solid hexagonal rods. Figure 5.95 shows images at the end of ZnO nanorods. An extreamly surprising feature is that many ZnO nanorods have well defined hexagonal shapes.

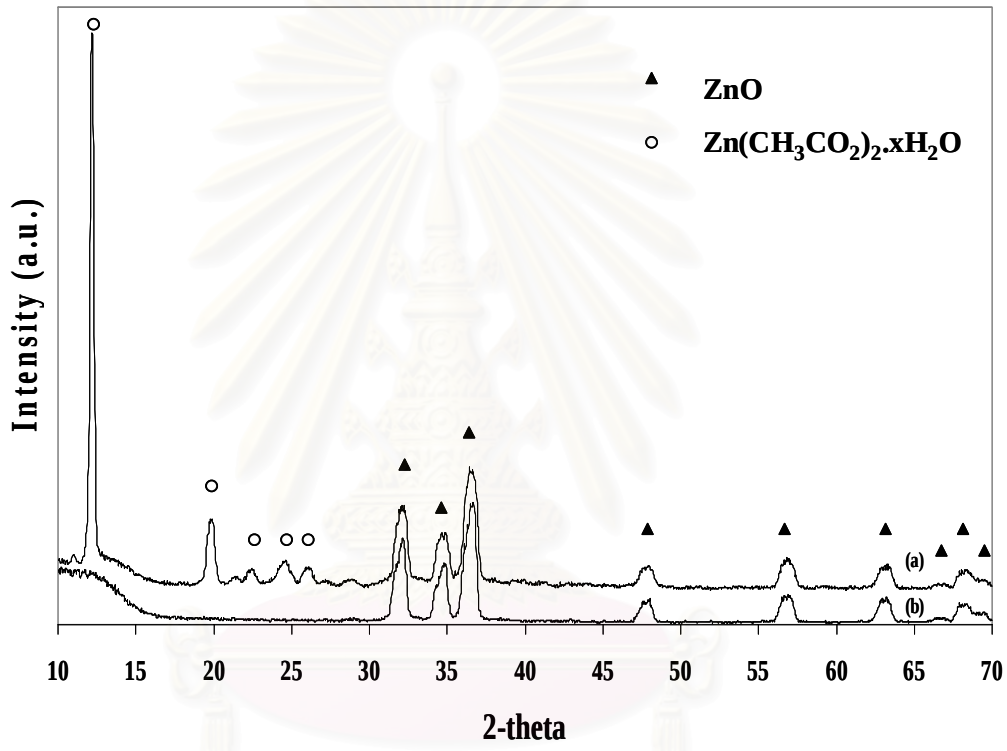

Figure 5.94 XRD patterns of ZnO nanoparticles that synthesized in toluene at (a) 280°C and (b) 300°C for 2 h by using zinc acetate 15g.

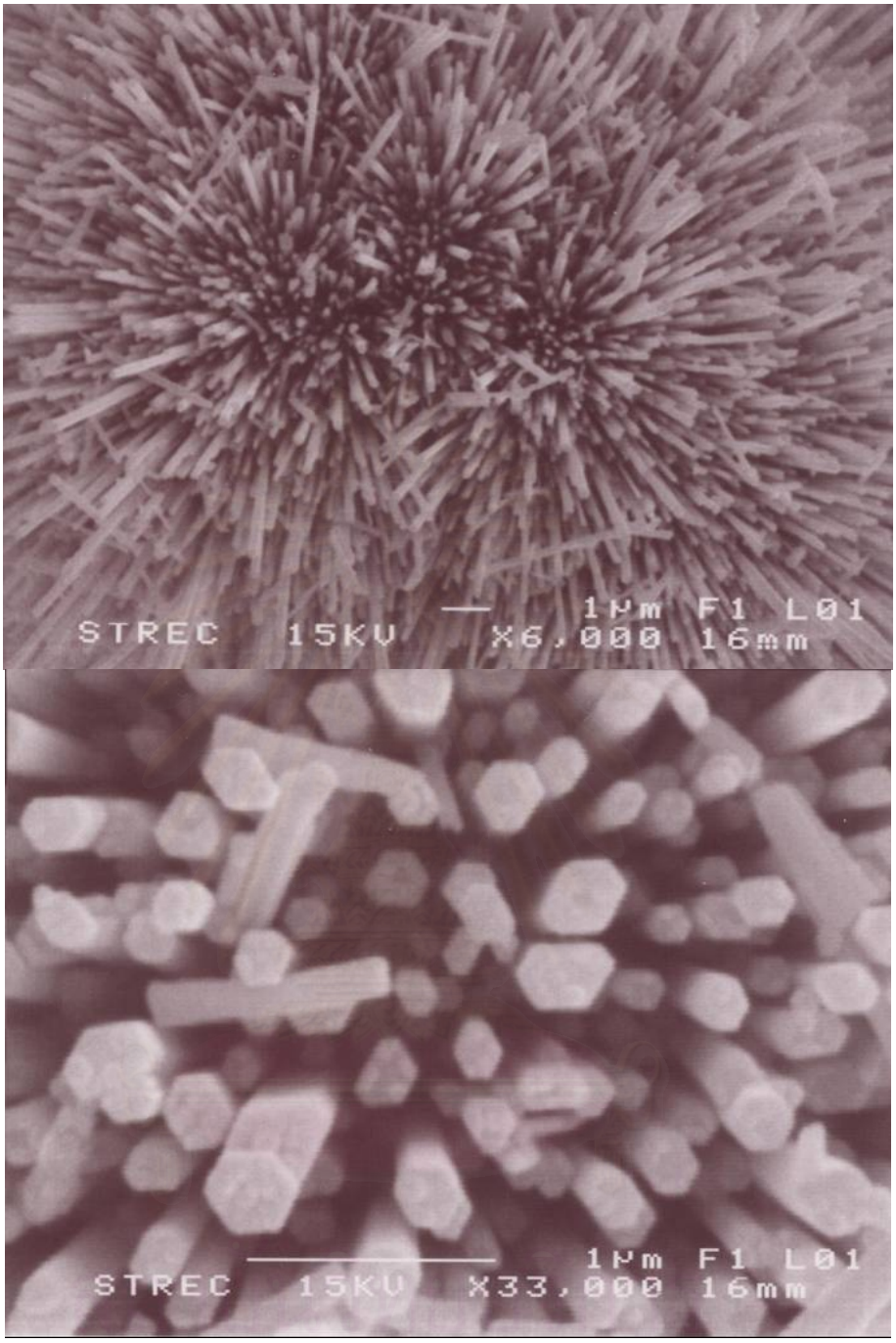

Figure 5.95 SEM image of the end of ZnO nanoparticles as-synthesized in toluene at 300°C for 2 h by using zinc acetate 15 g.

The primary particles are shown as TEM images in Figure 5.60. It indicates that the nanorods is of solid nature of its inside. The morphology of thus-obtained ZnO seemed to be nanorods with relatively straight and their surfaces were smooth. It is notable from the appearance of the individual crystals in Figure 5.60 as well as the other in Figure 5.95 that one end of the nanorod is well-faceted, whereas the other appears to be shape rodlike. The selected-area electron diffraction pattern (SAED) at Figure 5.106 reveals that our products exhibit a single-crystal structure. The diameter distributions and length distribution based on these images are depicted in the histograms as Figure 5.71. The average diameter sizes of ZnO showed the narrowly distribution, found as was deduced from the histogram. It can be seen that most of the rod have a nanosize diameter.

The as-synthesized nanocrystalline ZnO products synthesized by solvothermal reaction in benzene (BZ-ZnO) and xylene (X-ZnO). The XRD patterns of ZnO powders were prepared in benzene and xylene are shown in Figure 5.96. In figure, most of ZnO product peaks can be indexed to the hexagonal wurtzite structure. No peak from any else phase of ZnO and impurities were observed. The strong intensity of ZnO diffraction peaks indicates that resulting product have high purity of ZnO wurtzite phase. This result suggested that ZnO was successfully synthesized by solvothermal reaction at 300°C in benzene and xylene.

The ZnO products as-synthesized in benzene and xylene were characterized by SEM for analyzing morphology of the products as shown in Figure 5.97 and 5.98, respectively. Nanorods of ZnO were observed by the reaction in benzene and xylene. As can be seen the figure, the samples consist of large quantities of strength and smooth solid hexagonal rods. The primary particles are shown as TEM images in Figure 5.99 and 5.100 for as-synthesized in benzene and xylene, respectively. The morphology of thus-obtained ZnO seemed to be nanorods with relatively straight and their surfaces were smooth. The diameter distributions and length distribution of as-synthsized in benzene and xylene based on TEM images are depicted in the histograms as Figure 5.101 and 5.102, respectively. The average diameter sizes of ZnO showed the narrowly distribution, found as was deduced from the histogram. In xylene reaction, it can be seen that most of the rod have a microsize length. The

physical properties of as-synthesized ZnO nanocrystals in toluene, benzene and xylene are summarized in Table 5.3.

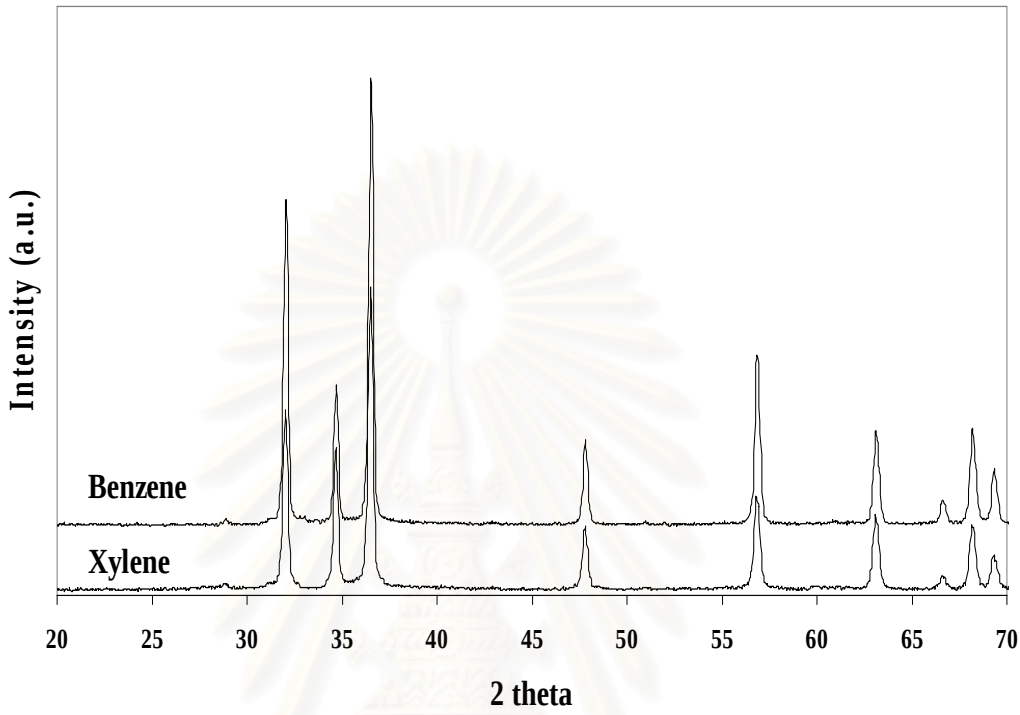

Figure 5.96 XRD patterns of ZnO nanoparticles that synthesized in benzene and xylene at 300°C for 2 h by using zinc acetate 15g.

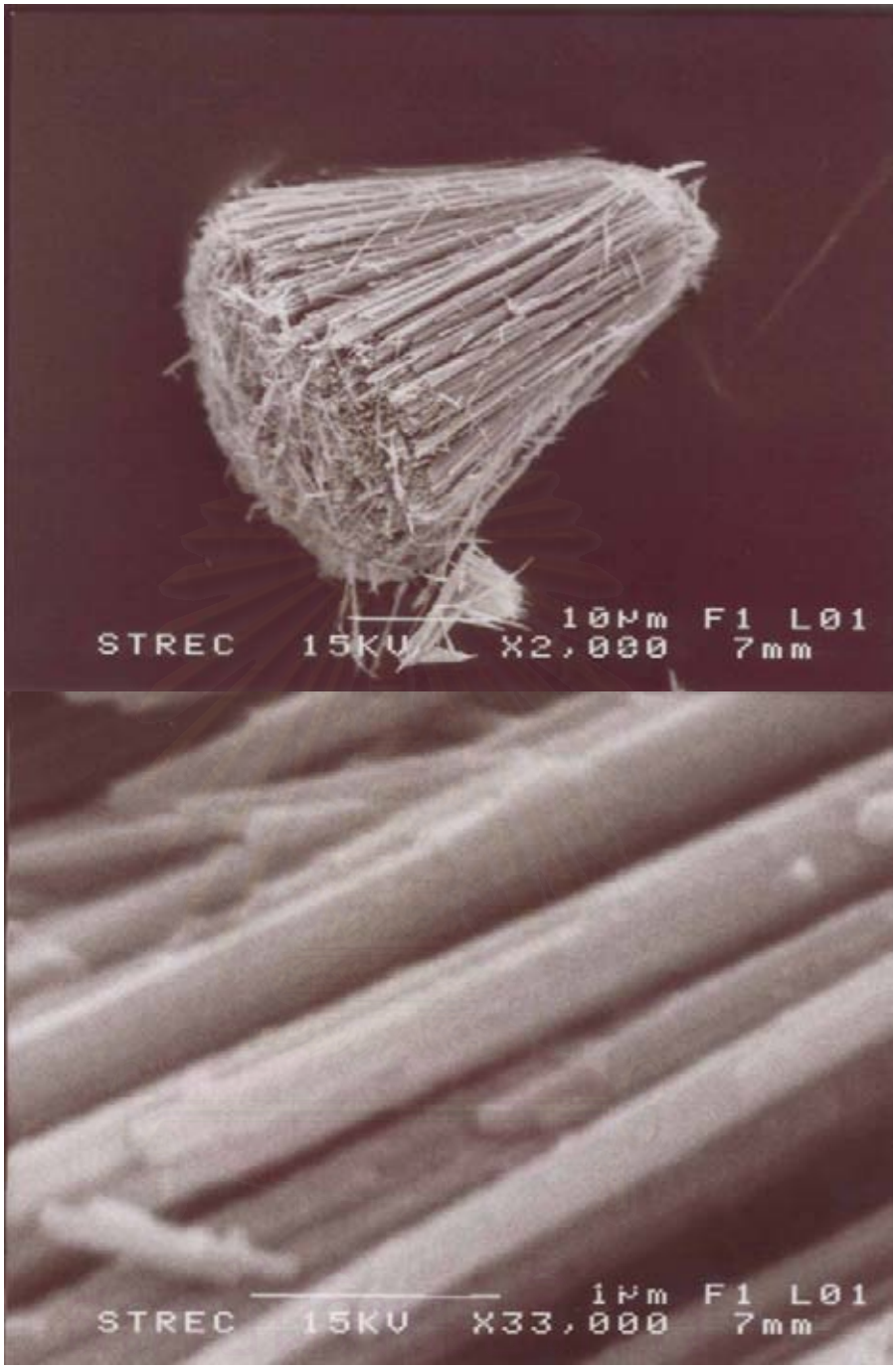

Figure 5.97 SEM image of ZnO nanoparticles as-synthesized in benzene at 300°C for 2 h by using zinc acetate 15 g.

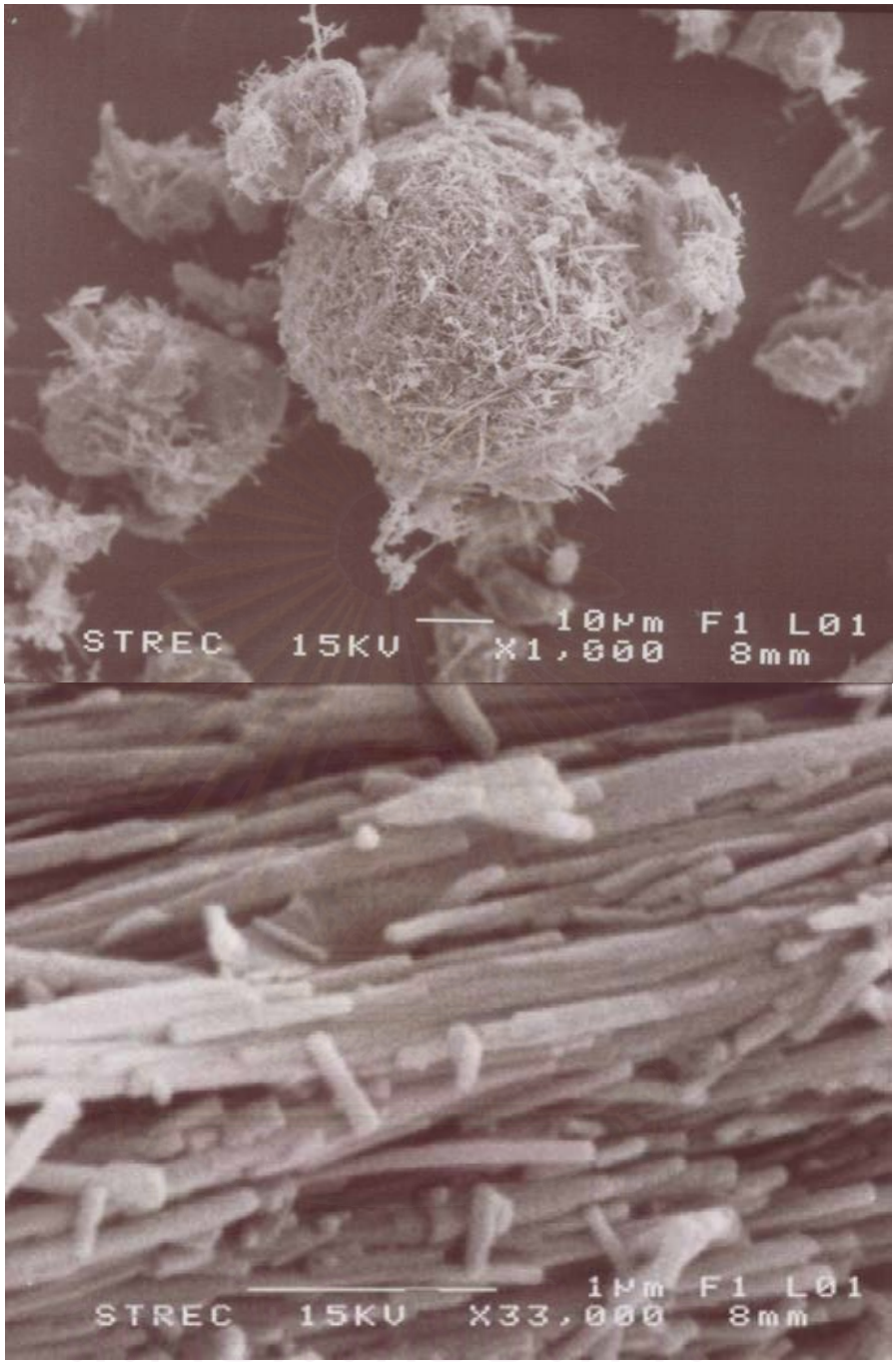

Figure 5.98 SEM image of ZnO nanoparticles as-synthesized in xylene at 300°C for 2 h by using zinc acetate 15 g.

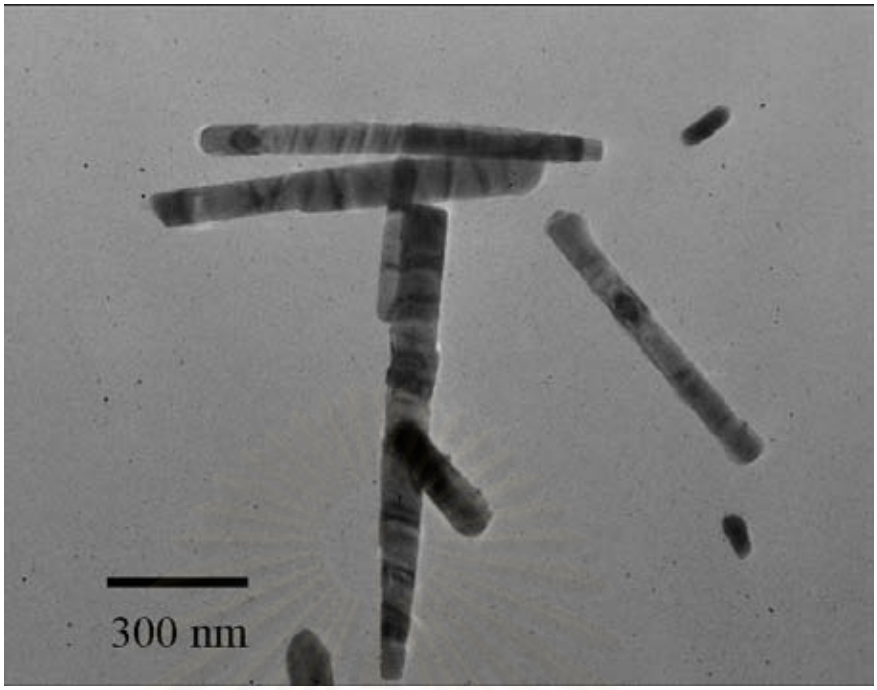

Figure 5.99 TEM image of ZnO nanoparticles as-synthesized in benzene at 300°C for 2 h by using zinc acetate 15 g.

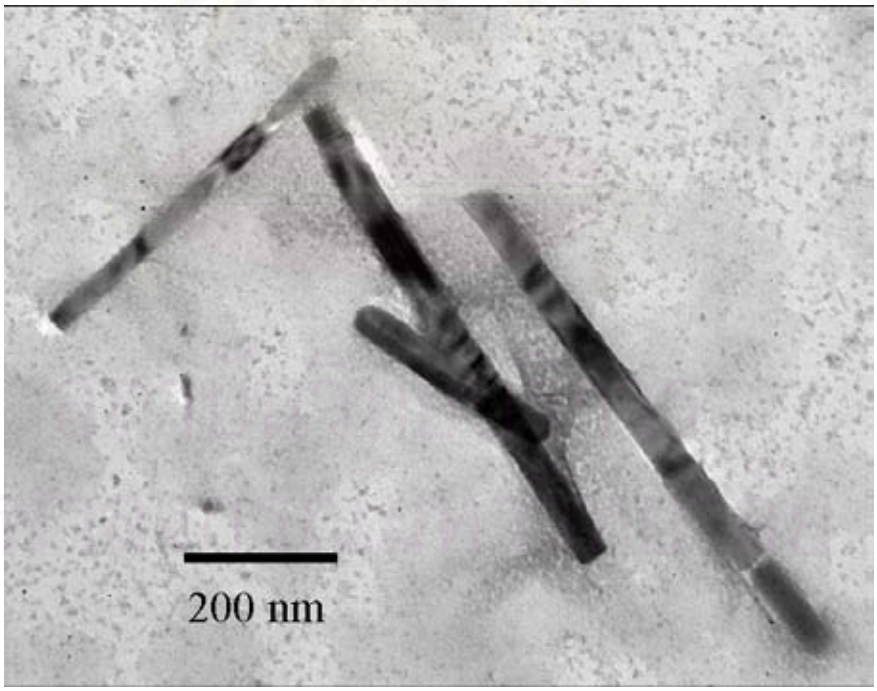

Figure 5.100 TEM image of ZnO nanoparticles as-synthesized in xylene at 300°C for 2 h by using zinc acetate 15 g.

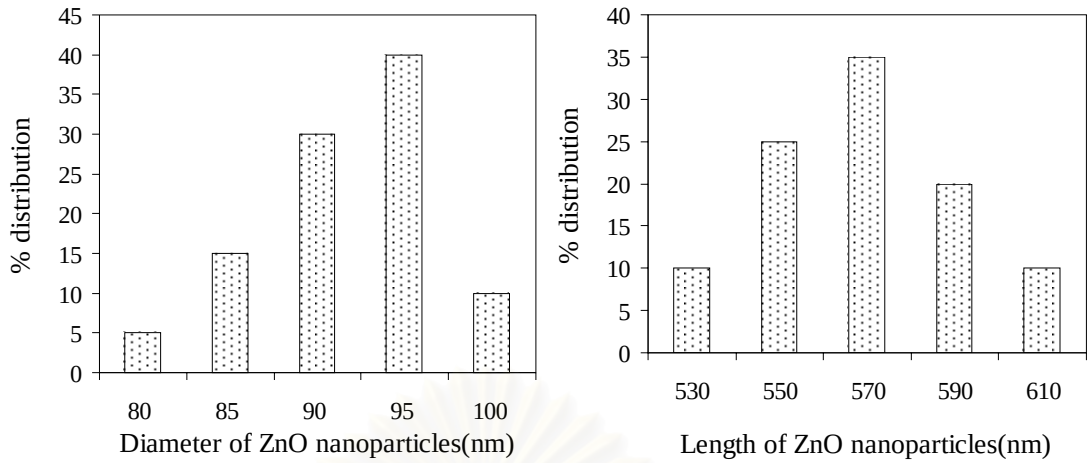

Figure 5.101 Histograms of the diameter and length size distributions obtained from TEM images for ZnO prepared in benzene at 300 °C for 2h by using zinc acetate 15 g.

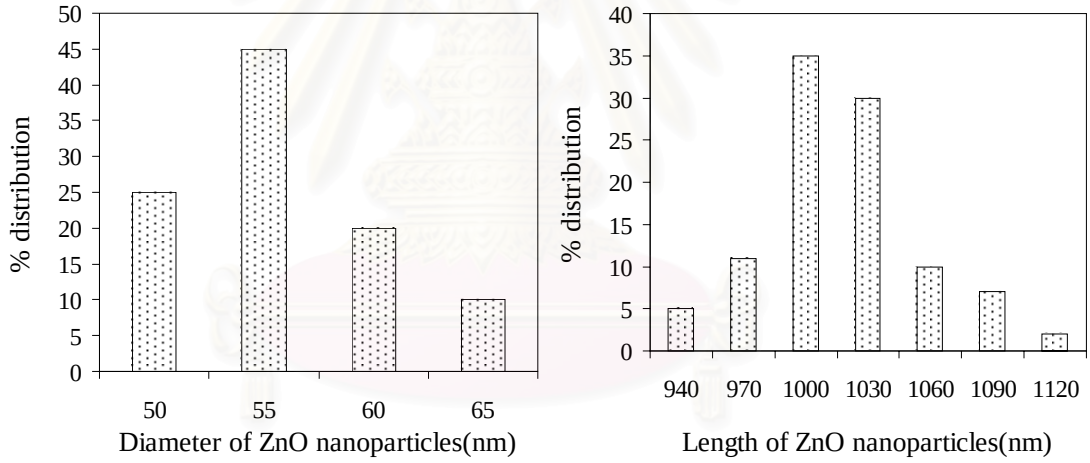

Figure 5.102 Histograms of the diameter and length size distributions obtained from TEM images for ZnO prepared in xylene at 300 °C for 2h by using zinc acetate 15 g.

Table 5.3 The physical properties of ZnO were prepared in various organic solvents.

Sample	Average diameter (nm)	Average length (nm)	Aspect ratio	BET surface area (m^2/g)
PG-ZnO	45	84	1.87	11.69
BG-ZnO	58	115	1.98	9.87
PeG-ZnO	63	124	2.03	8.62
HG-ZnO	67	139	2.07	8.03
B-ZnO	107	184	1.72	10.05
H-ZnO	91	264	2.90	9.33
O-ZnO	84	343	4.08	8.87
D-ZnO	81	455	5.62	7.09
BZ-ZnO	92	558	6.06	6.93
T-ZnO	98	920	9.39	6.89
X-ZnO	60	1034	17.2	4.64

The XRD patterns of ZnO nanoparticles in Figure 5.74, 5.84, 5.94 and 5.96 are similar, which indicates that phase-pure hexagonal structure ZnO has been successfully synthesized in various solvents via solvothermal method.

In case of reaction in glycol, as can be seen from Table 5.3 the average diameter sizes increased from 45 nm to 67 nm and average length increased from 84 nm 139 nm, corresponding to various organic solvent of 1,3 propanediol, 1,4 butanediol, 1,5 pentanediol to 1,6 hexanediol. The aspect ratios of particles as-synthesized in there solvents were increases with an increase of the boiling point of the solvents as shown in Figure 5.103. As can be seen in Figure 5.103, the aspect ratios of as-synthesized ZnO in glycol were slightly increased because the solvent of glycol were slightly different. Smooth solid hexagonal rods were observed with 1,6 hexanediol, the length of the rods increased when chain of glycol were increased.

In case of reaction in alcohol, as can be seen from Figure 5.88 to 5.90 and 5.21 the average diameter sizes of as-synthesized ZnO nanoparticles changed from 107 to 81 nm and the average length increased from 184 to 455 nm, corresponding to various solvents of 1-butanol, 1-hexanol, 1-octanol to 1-decanol, respectively which show in Table 5.3. The growth rate along the *c*-axis in 1-decanol is higher than that in 1-butanol. The aspect ratios of particles as-synthesized in their solvent were increases with the boiling point of alcohol increased are shown in Figure 5.103. It suggests that solvent using in the reaction affected on the growing rate ratio between planes in ZnO crystal. Kubota (2001) were reported the growth rate of a face will be controlled by a combination of internal and external such as supersaturation, temperature and solvent. This can be verified with detailed theoretical simulations of interface-solvent interactions using known parameter, *e.g.*, solvent properties that are dependence on the chain length of alcohols. The (001) faces have higher-symmetry (C6v) than the other faces, growing along *c*-axis, or (001) direction, is the typical crystal habit and growth form of ZnO wurtzite under liquid phase conditions. Bin Cheng et al (2004) had reported the growth rate of a face will be controlled by solvent properties such as chain length of alcohol, which affected on interface-solvent interactions. Hence, it is possible that morphologies of polar inorganic nanocrystals can be controlled by the interface-solvent interactions, which in turn, may be specified by choosing a suitable solvent. The properties of solvent are shown in Table 5.4. It can be clearly seen in TEM image that morphology of particles synthesized in these alcohols are significantly different. Nearly spherical particles were obtained when 1-butanol was used as the reaction medium, while smooth solid hexagonal rods were observed with 1-decanol. It can be seen from Table 5.4 that ZnO nanorods synthesized in alcohol with long carbon chain tended to have smaller diameter and longer in length than those synthesized in short chain alcohol. The aspect ratio of the obtained nanorods increased corresponding to the increasing in length of carbon chain in the reaction medium. Similar to the aspect ratio of ZnO nanorods were increased corresponding to the increasing the boiling point of solvent in the reaction medium.

In case of reaction in toluene, the average diameter size is 98 nm and average length is 920 nm. It indicates that primary particles ZnO nanorods as-synthesized in toluene which shows in Figure 5.60 are very long. The aspect ratio of ZnO nanorods prepared in toluene, benzene and o-xylene were higher than products obtained by the

reaction in alcohol and glycol. The ZnO nanoparticles as-synthesized in 1-octanol, 1,4 butanediol and toluene observed by Selected area electron diffraction pattern (SEAD) are shown in Figure 5.104, 5.105 and 5.106, respectively. It indicated that each primary particle is single-crystalline and confirm a high degree of crystallinity over small regions of the sample.

According to the above results, it is concluded that the morphology of as-prepared ZnO powders markedly depend on the solvents. The aspect ratios of as-synthesized ZnO nanorods were increased when the boiling point of solvent increased. The interesting linear relationship between boiling points and aspect ratios was observed in Figure 5.103. This plot can be used to select the appropriate solvents for preparation of zinc oxide nanorod with desired aspect ratio. However, the behavior shown in Figure 5.103 should prove useful to laboratory as well as industry produces. The correlation allows and estimation of the aspect ratio of ZnO nanorod and types of using alcohols.

Table 5.4 The properties of solvent were prepared ZnO nanoparticles.

Solvent	Formula	Molecular weight	Melting point (°C)	Boiling point (°C)	Dielectric constant
1,3 propanediol	$HO(CH_2)_3OH$	76.10	-27	214	35.10
1,4 butanediol	$HO(CH_2)_4OH$	90.12	16	230	31.90
1,5 pentanediol	$HO(CH_2)_5OH$	104.15	-18	242	26.20
1,6 hexanediol	$HO(CH_2)_6OH$	118.18	42	252	20.30
1-butanol	$CH_3(CH_2)_3OH$	72.12	-90	117	17.24
1-hexanol	$CH_3(CH_2)_5OH$	102.17	-52	156	13.03
1-octanol	$CH_3(CH_2)_7OH$	130.22	-15	196	10.30
1-decanol	$CH_3(CH_2)_9OH$	158.28	7	231	8.10
benzene	C_6H_6	78.11	5.5	80	2.28
toluene	$C_6H_5CH_3$	92.13	-95	110	2.38
o-xylene	$C_6H_4(CH_3)_2$	106.17	-25	144	2.56

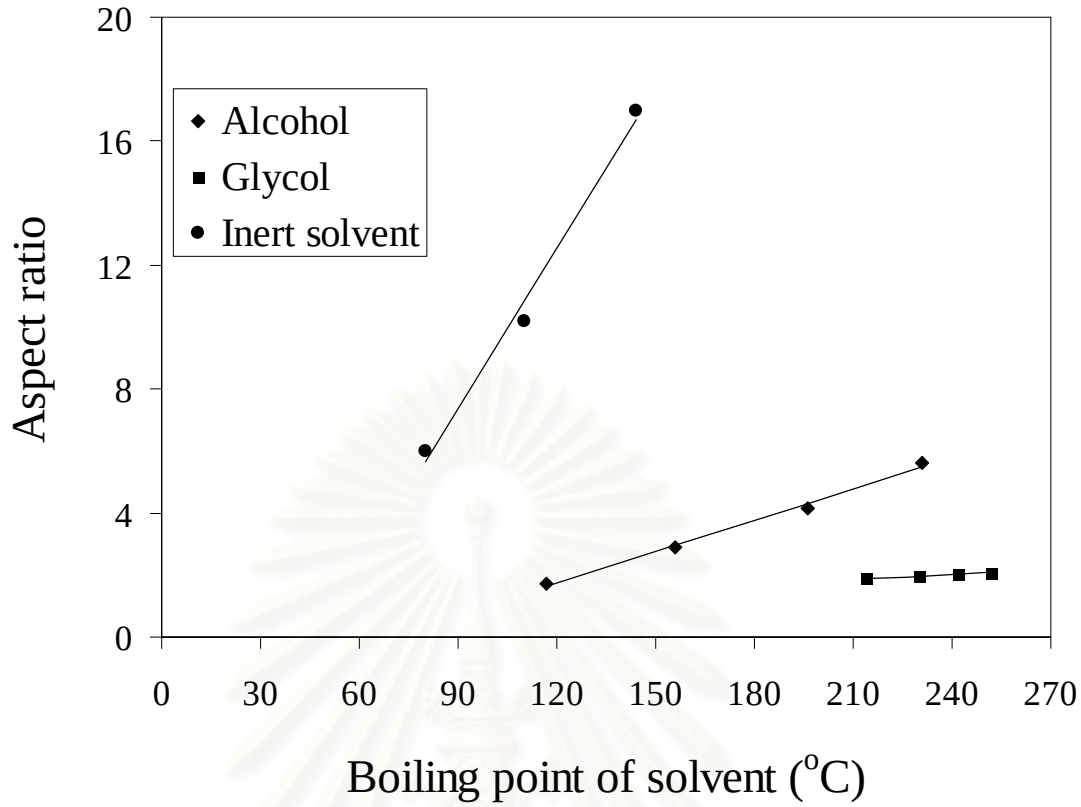

Figure 5.103 The correlation boiling points of solvent and aspect ratio.

Figure 5.104 SEAD pattern of ZnO nanoparticles as-synthesized in 1,4 butanediol

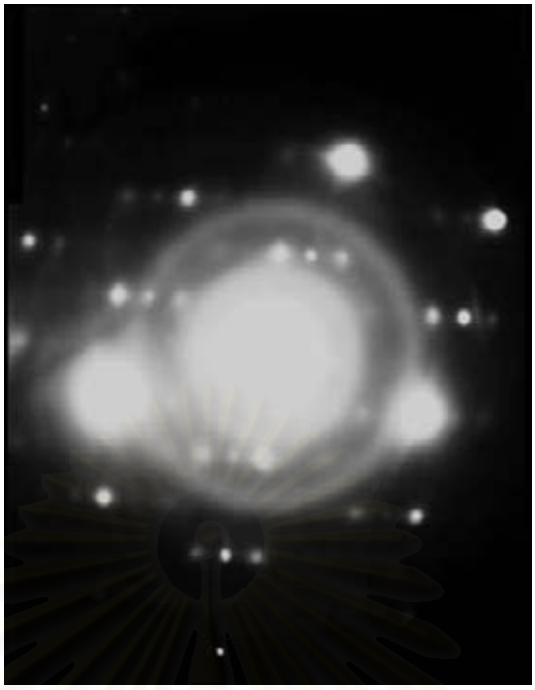

Figure 5.105 SEAD pattern of ZnO nanoparticles as-synthesized in 1-octanol

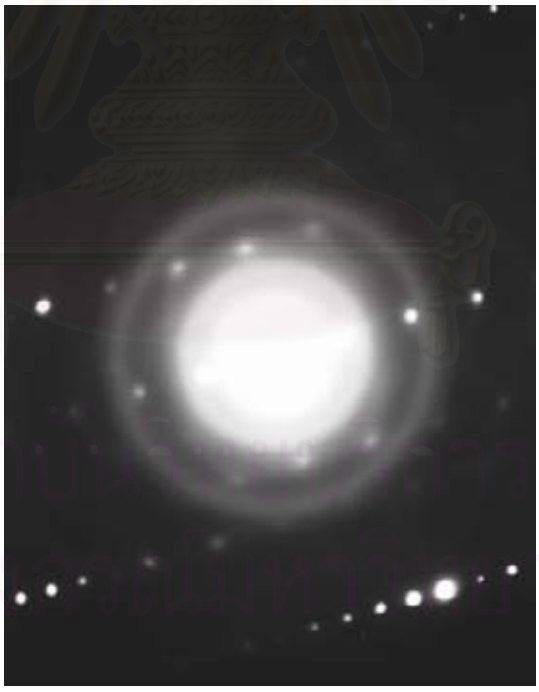

Figure 5.106 SEAD pattern of ZnO nanoparticles as-synthesized in toluene

5.4 The nucleation growth and characteristic of ZnO nanoparticles synthesized by solvothermal method

ZnO nanoparticles were successfully synthesized by the solvothermal reaction of zinc acetate in organic solvents. In this part which aim study nucleation growth process and characteristic ZnO nanoparticles. Figure 5.107 shows the precursor as-synthesized ZnO nanorods. Zinc acetate melt at 210-260°C as indicated by the endothermic peak in the DTA curve as shows in Figure 5.108. The melts zinc acetate decomposes into ZnO and organic compounds by an endothermic reaction and the decomposed organic compounds are oxidized subsequently an exothermic reaction. The decomposition process is complete about 350°C, and the total weight loss is about 82%. From DTA curves, the decomposition of zinc acetate is complete at temperature about 350°C, whereas reaction temperature of ZnO as-synthesized by solvothermal method are complete at 200°C. The white residues of TG/DTA for the precursors were confirmed to be the pure wurtzite ZnO phase by XRD analysis, as can be seen in Figure 5.109. This result can be concluded that by solvothermal method has been synthesized ZnO nanorods at low temperature. ZnO exhibited a wide direct band gap with a large excitation binding energy, which suitable for effective UV emission. Figure 5.110 is the UV-vis absorption spectra of ZnO nanorods. It shows a strong absorption in the range of 350-380 nm. A pronounced excitonic structure is seen in the absorption spectra, as expected for a highly crystalline material. This Figure suggests that solvent using in the reaction medium not affected on the UV absorption in ZnO nanoparticles.

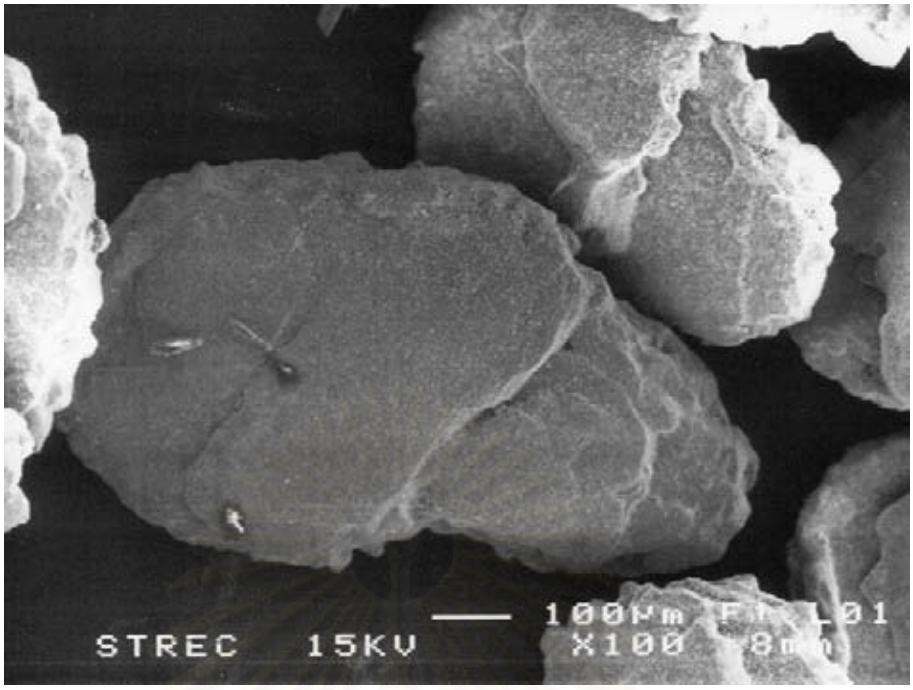

Figure 5.107 SEM images of zinc acetate

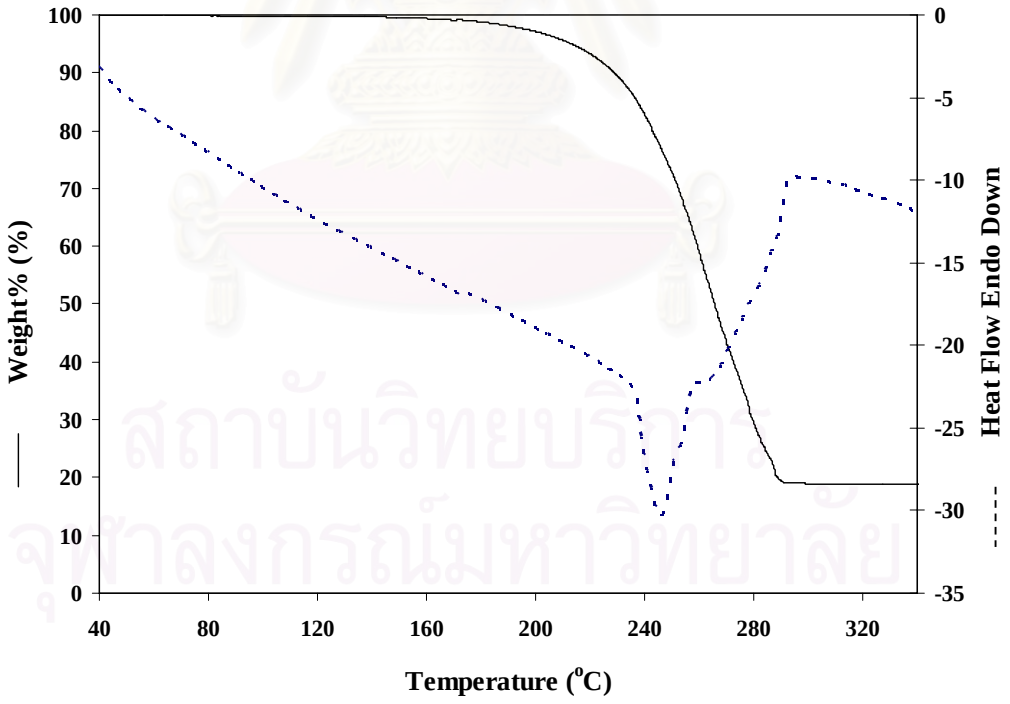

Figure 5.108 TG and DTA curves of zinc acetate heated at 10°C/min

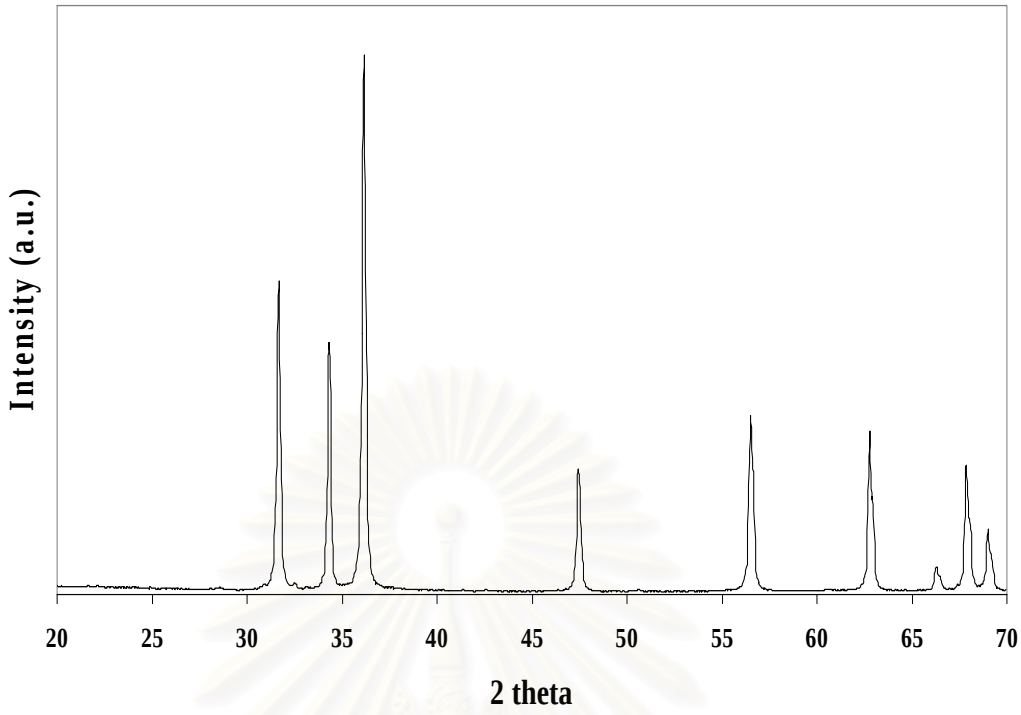

Figure 5.109 XRD pattern of ZnO powder residue from TG/DTA

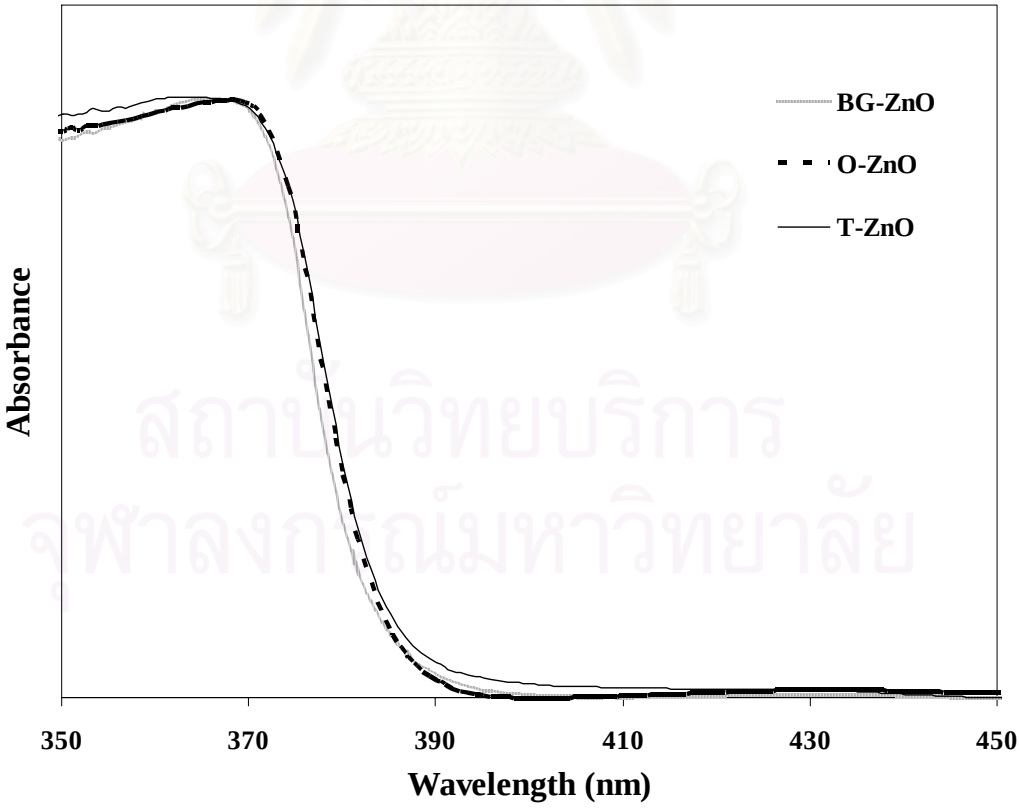

Figure 5.110 UV-vis absorption spectra of ZnO nanorods.

Figure 5.111 shows SEM images of thus-obtained sample at 150°C for 2h. Products prepared at 150^{o}C composed of two types of particles. The particles with irregular shape and smooth surface, which assigned to zinc acetate, and rod shape particles of ZnO were observed together. This finding may imply that the crystal growth direction is from the surface of zinc acetate end to ZnO hexagonal wurtzite. The elemental mapping in Figure 5.112 showed that carbon atoms were distributed perfectly on smooth surface particle. While the carbon contents decreased at the boundary on the particle and became zero. This indicate the formation of the rod shape ZnO particles crystallized from the irregular shape particles of zinc acetate seed, as seen in Figure 5.111. The chemical stoichiometry of ZnO nanorods as-synthesized was investigate with Energy dispersive spectrometry (EDS) measurement shows in Figure 5.113 that the nanoparticles were composed of mainly Zn, O and C element, it indicated that ZnO as-synthesized at 150°C for 2h. in 1-octanol was not completed. And it can be confirm in the element mapping in Figure 5.112. The chemical stoichiometry shows in Figure 5.114, which indeed gave an atomic ratio of Zn:O ≈ 1:1. The EDS spectrum was taken from the nanorods in Figure 5.111 in the part of rods shape, in which Zn and O were marked. The EDS analysis has further confirmed that the composition of nanorods was ZnO.

To understand the reaction mechanism, the reaction temperature in 1-octanol was decreased to 200^{o}C for 2 h. Figure 5.115 shows the XRD pattern of thus-obtained products fabricated in 1-octanol at 150°C for 2h. It was found that the prepared powder at 150^{o}C was a mixture of zinc acetate and zinc oxide. No peaks shift was observed. IR spectra of particles are shown in Figure 5.116. The results confirmed the existence of zinc acetate without the present of alcohol functional groups. The spectrum in Figure 5.116(a) is shown IR spectrum of zinc acetate which the wavenumber of bands around 700 to 1800 cm^{-1} are observed typically for acetate group complexed with zinc and corresponding to C=O stretching and C-O stretching, respectively. However, Figure 5.116(b) indicates the existence of O-H vibrations at wavenumber about 3500 cm^{-1} and various acetate vibration and ZnO. It can be seen ZnO as-synthesized at 150°C for 2h in 1-octanol are change from zinc acetate to ZnO only. The spectrum in Figure 5.116(c) has a large absorption band. A large band is

observed typical for zinc oxide. This result indicates that the zinc acetate did not form the new molecular structure with alcohols.

To investigate the reaction mechanism, the recovered solvent was analyzed by gas chromatography are shown in Appendix C. Butylacetate, hexylacetate, octylacetate and decylacetate were obtained as the other products with changing the alcohol from 1-butanol, 1-hexanol, 1-octanol to 1-decanol, respectively. Thus the overall reaction should be:

$$Zn(CH_3COO)_2 + 2R\text{-}OH \longrightarrow ZnO + 2CH_3\text{-}\overset{\overset{O}{\|}}{C}\text{-}O\text{-}R + H_2O$$

We speculated that zinc acetate was attached by alcohol. Then, the esterifaction reaction was preceded and yielded ZnO, ester and water.

From GC/MS result in Appendix C, the recovered toluene was analyzed by gas chromatography. It can be found acetic acid and water in recovered toluene which suggested that the reaction between zinc acetate and toluene has been thermal decomposition of zinc acetate.

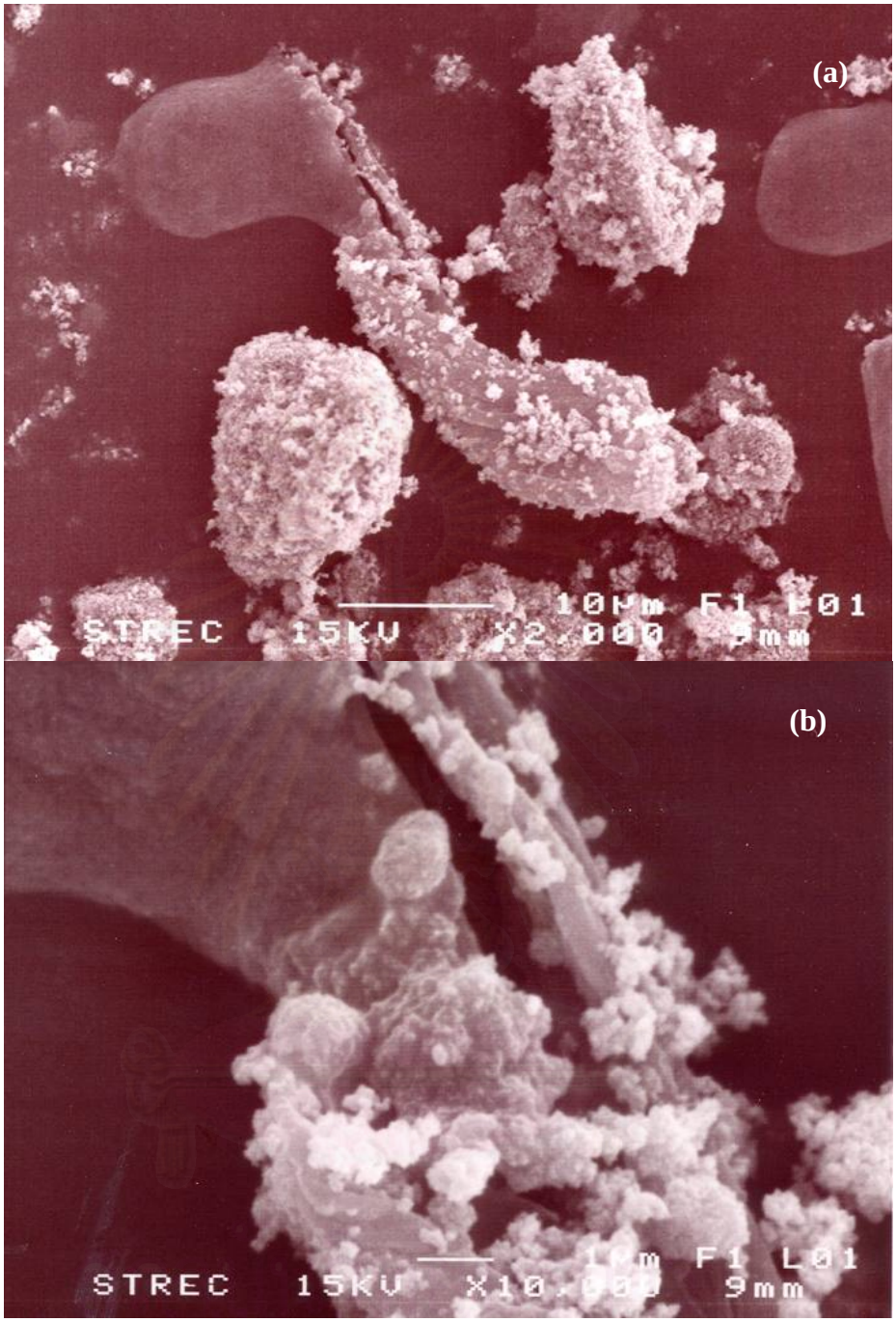

Figure 5.111 SEM images of ZnO nanoparticles as-synthesized at 150°C for 2 h. by using zinc acetate 15 g. in 1-octanol

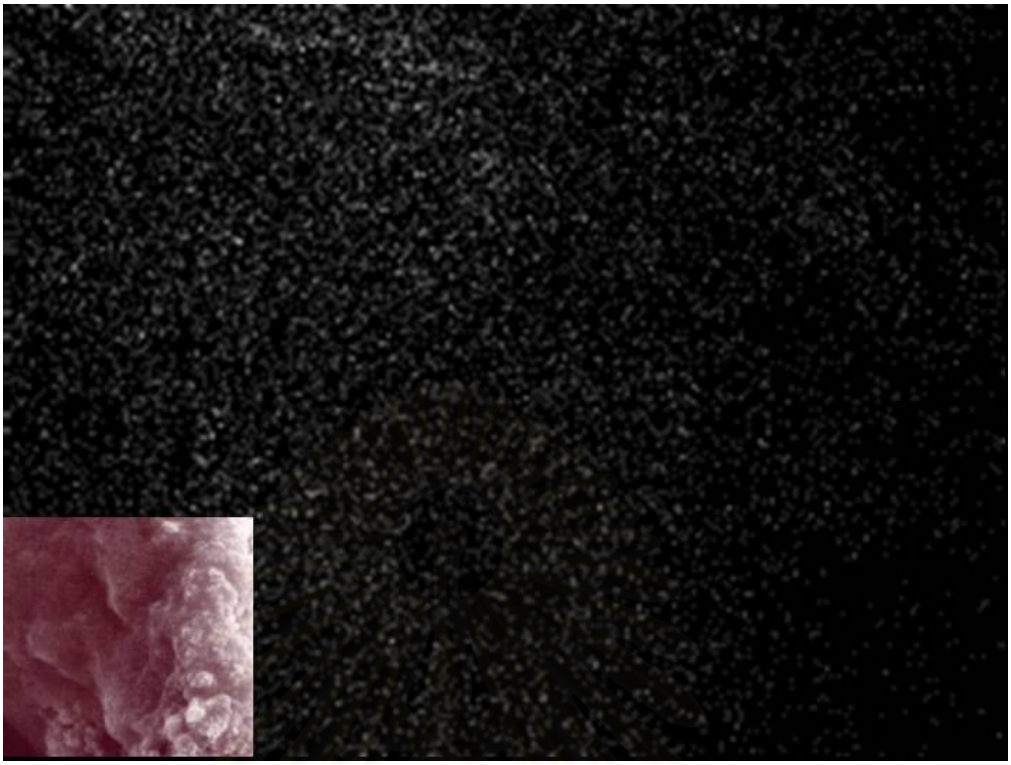

Figure 5.112 The elemental mapping of ZnO nanoparticles as-synthesized at 150°C for 2h. in 1-octanol by using zinc acetate 15g.

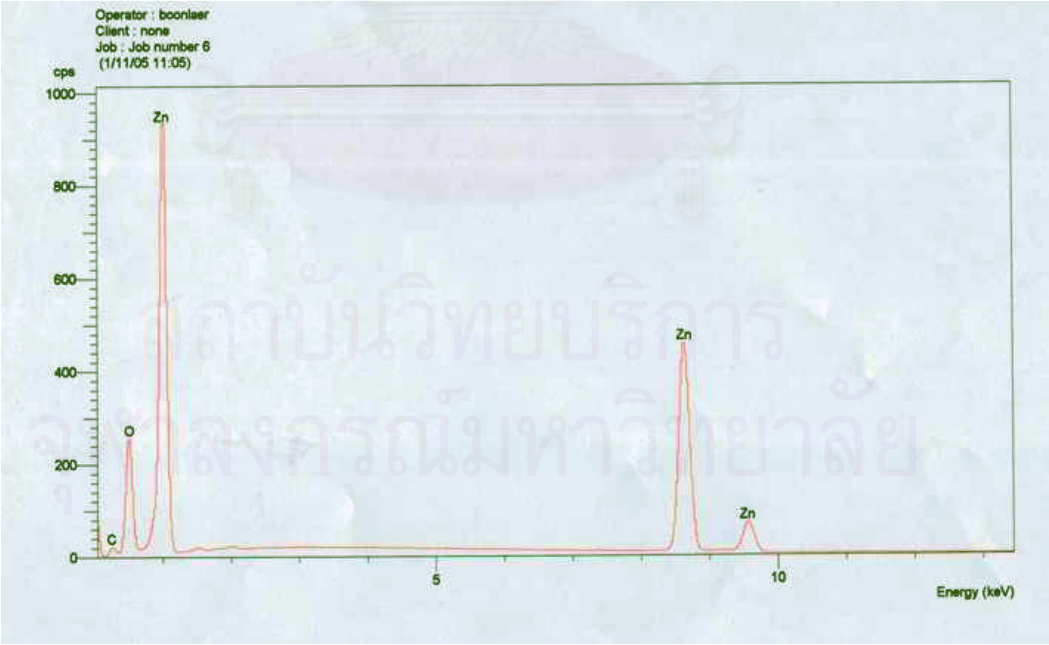

Figure 5.113 EDS of ZnO as-synthesized at 150°C for 2h. in 1-octanol by using zinc acetate 15 g.

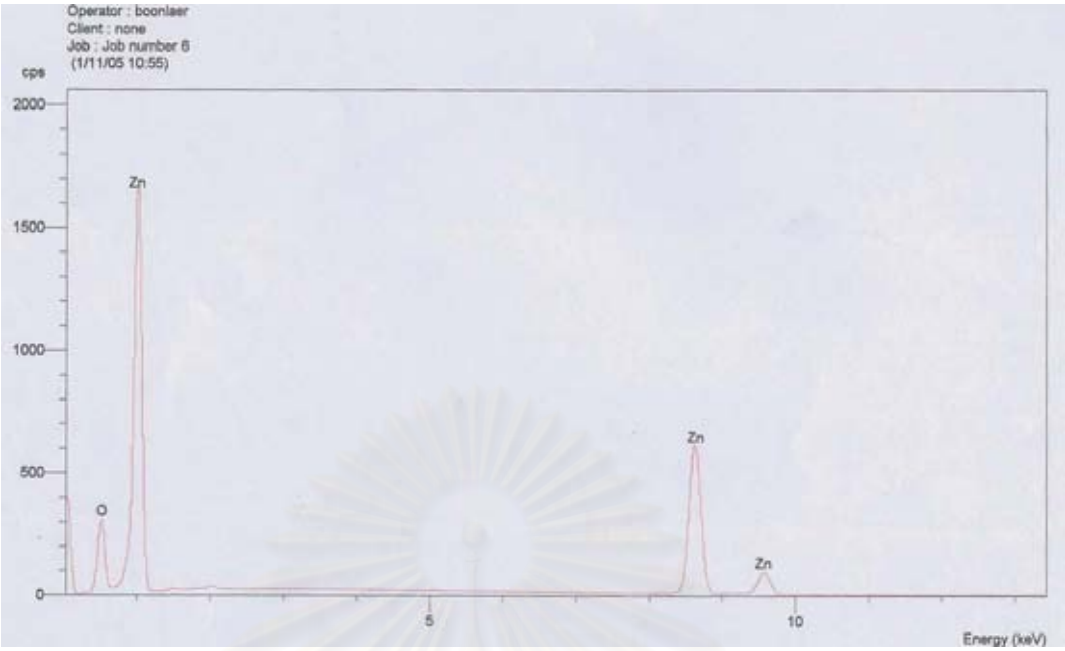

Figure 5.114 EDS of ZnO as-synthesized at 200°C for 2h. in 1-octanol by using zinc acetate 15 g.

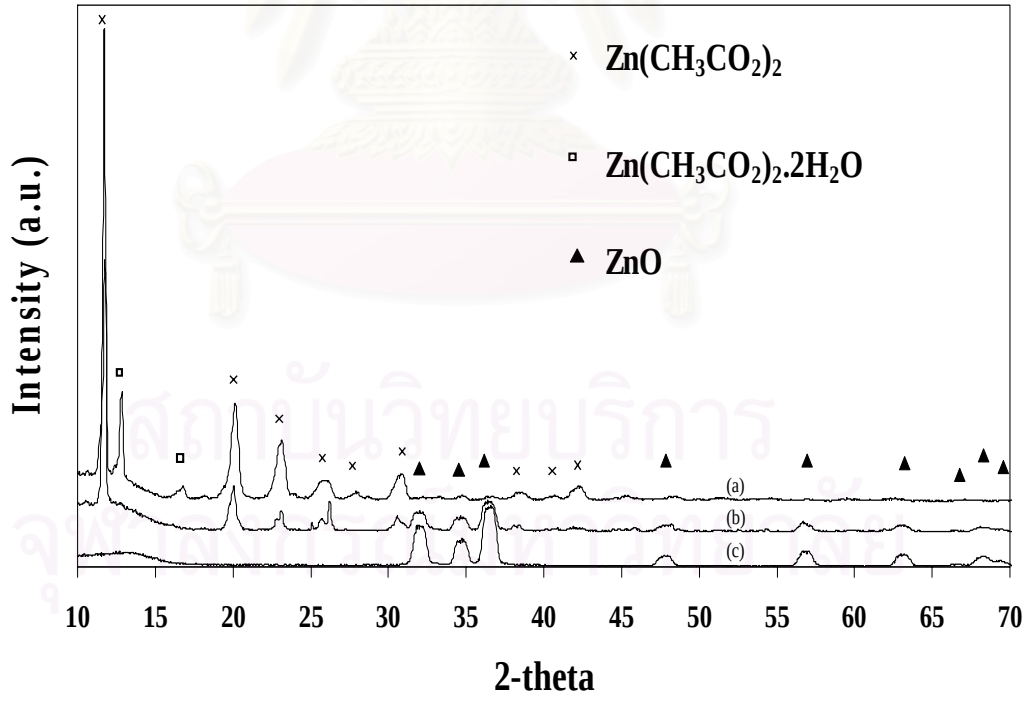

Figure 5.115 XRD patterns of (a) Zinc acetate and ZnO nanoparticles that synthesized 1-octanol at (b) 150 °C and (c) 200°C for 2 h.

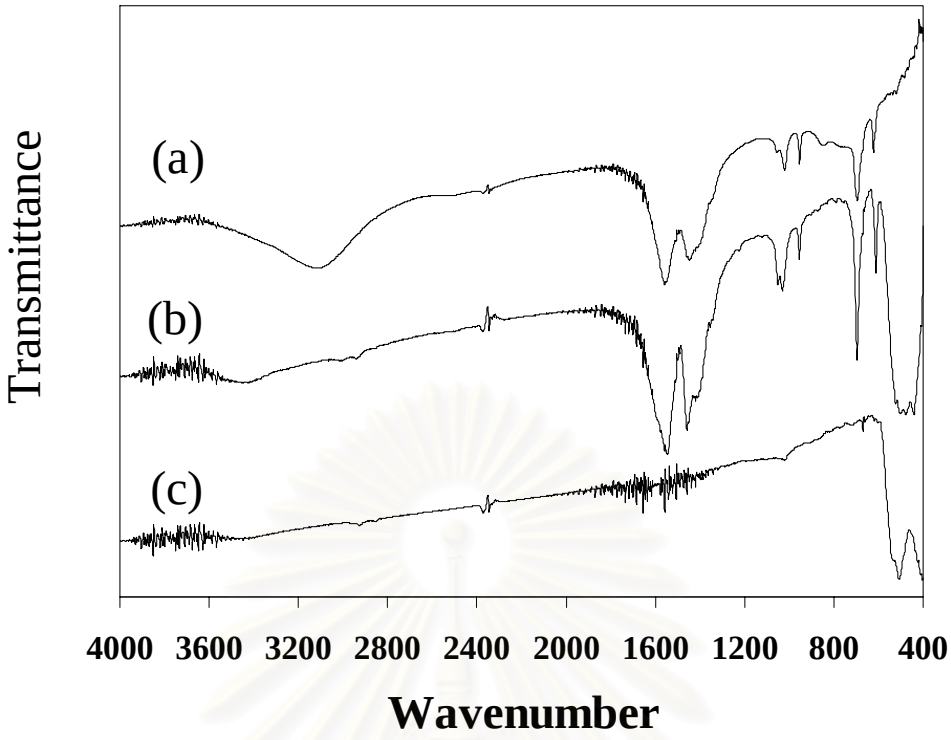

Figure 5.116 IR spectra of (a) zinc acetate, (b) as-synthesized ZnO synthesized in 1-octanol at (b) 150°C and (c) 200 °C for 2 h.

From all TEM and SEM figure are shown ZnO nanorods, It has been observed that the maximum growth velocity is fixed in the {0001}.These results are very similar to the observations reports in many papers. Furthermore, each nanorod as-synthesized by various the amount of precursor and the reaction temperature has a uniform aspect ratio in each solvent, indicating the growth anisotropy in the +*c*-axis is strictly maintained throughout the process. In particularly, no branching is observed, which implies that the ZnO nanorods were growth from spontaneous nucleation with high crystal perfection. It can be seen in Figure 5.117 to 125, which shows the water of crystallization is removed and the weight loss of ZnO nanorods as-synthesized in various organic solvents are very low and it not have carbon in ZnO nanoparticles. Indeed crystal boundaries of the rods are well defined.

In this chapter, it can be conclude that perfect single crystal can be obtained by solvothermal method. This synthesis route is easily controllable, well-repeatable, mild and feasible to apply to the fabrication of nanorods of other materials. ZnO nanorods can be controlled aspect ratios by using different solvents. These high-qualities,

single-crystalline ZnO nanorods represent good candidates for further studies of low-dimensional physics as well as for applications in various fields of nanoscale science and technology.

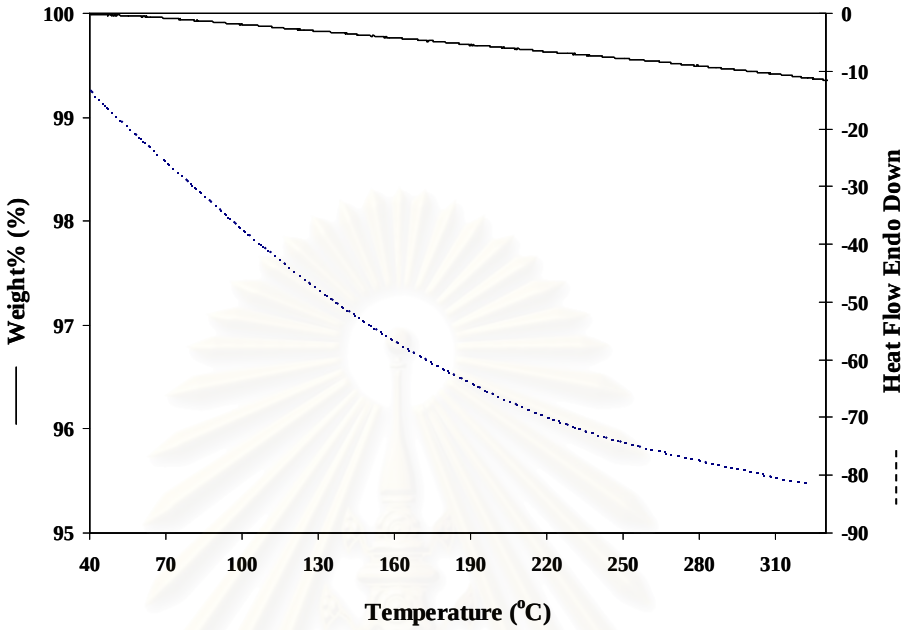

Figure 5.117 TG and DTA curves of ZnO as-synthesized in 1,3 propanediol at 250°C for 2 h by using zinc acetate 15g.

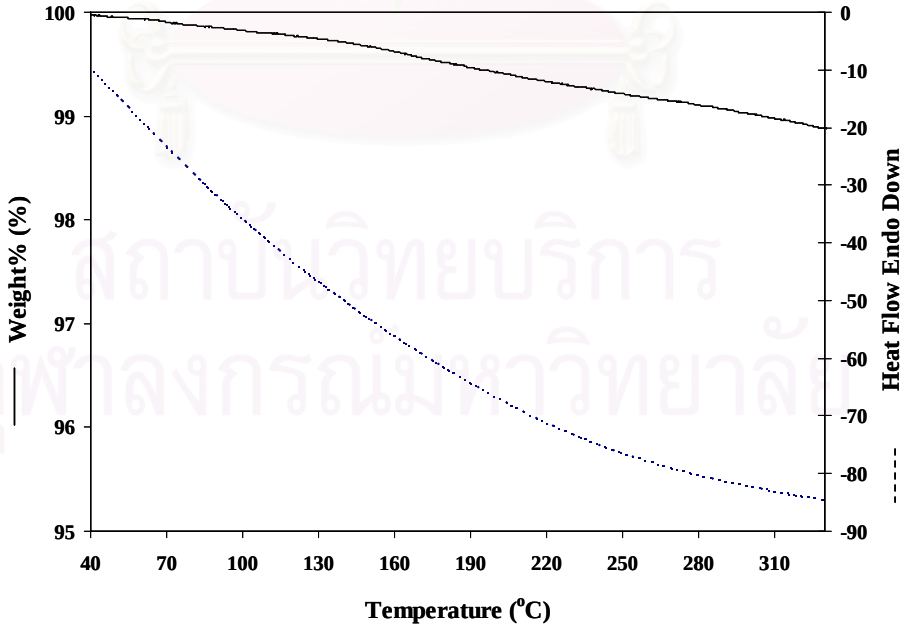

Figure 5.118 TG and DTA curves of ZnO as-synthesized in 1,4 butanediol at 250°C for 2 h by using zinc acetate 15g.

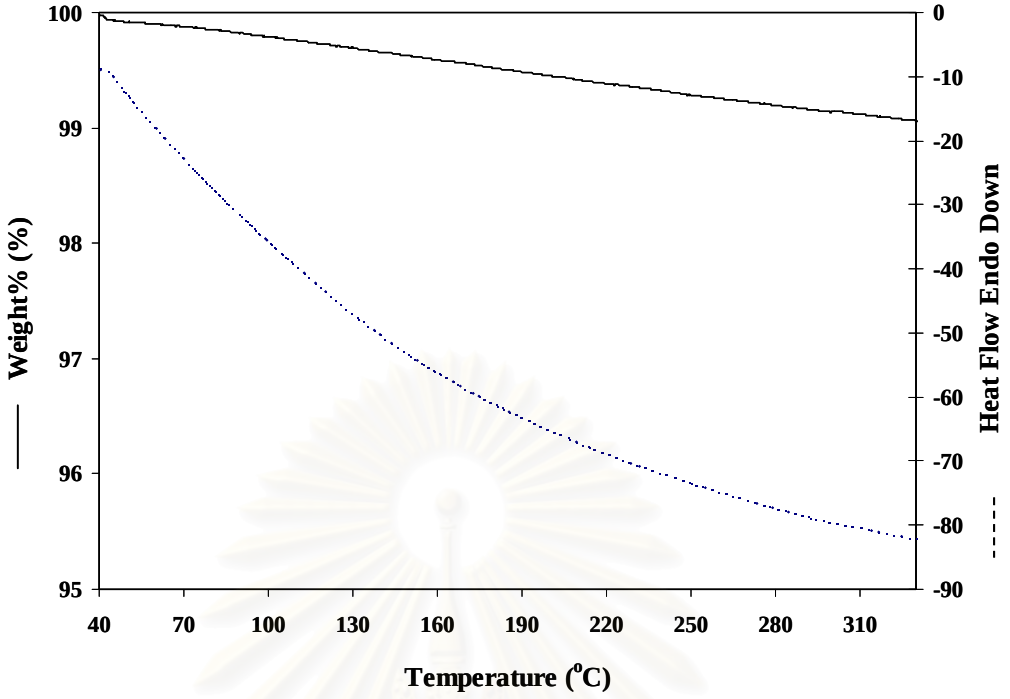

Figure 5.119 TG and DTA curves of ZnO as-synthesized in 1,5 pentanediol at 250°C for 2 h by using zinc acetate 15g.

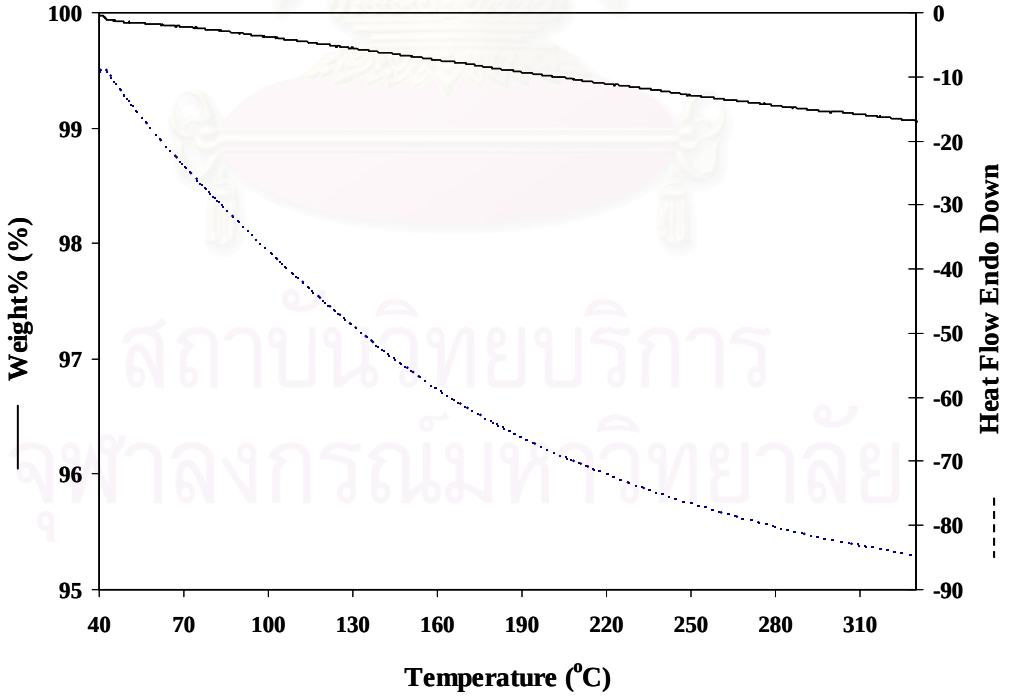

Figure 5.120 TG and DTA curves of ZnO as-synthesized in 1,6 hexanediol at 250°C for 2 h by using zinc acetate 15g.

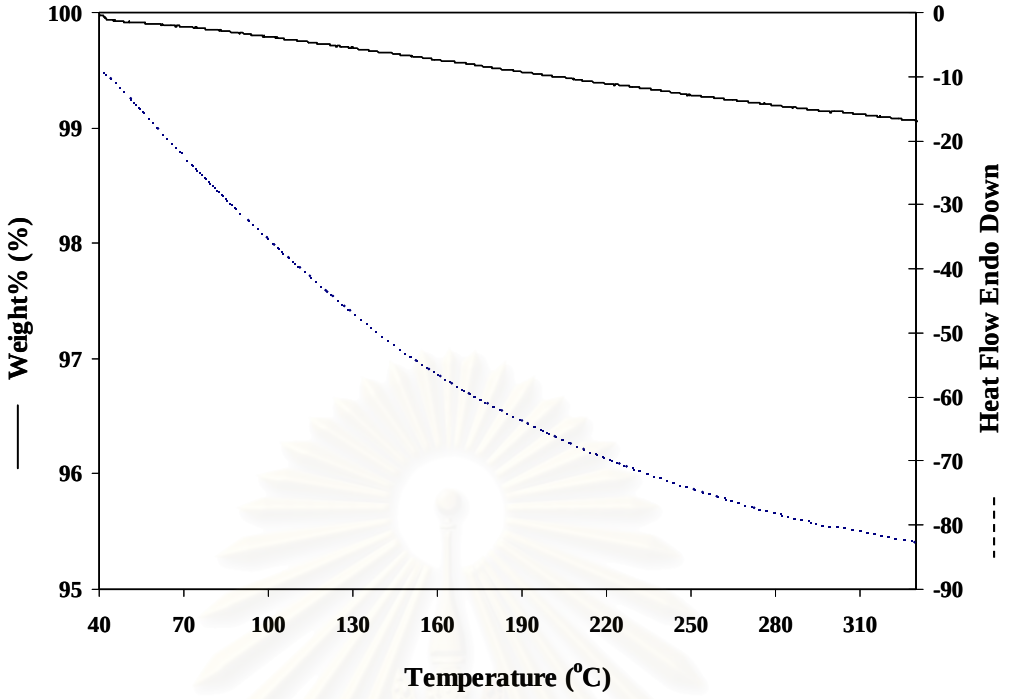

Figure 5.121 TG and DTA curves of ZnO as-synthesized in 1-butanol at 250°C for 2 h by using zinc acetate 15g.

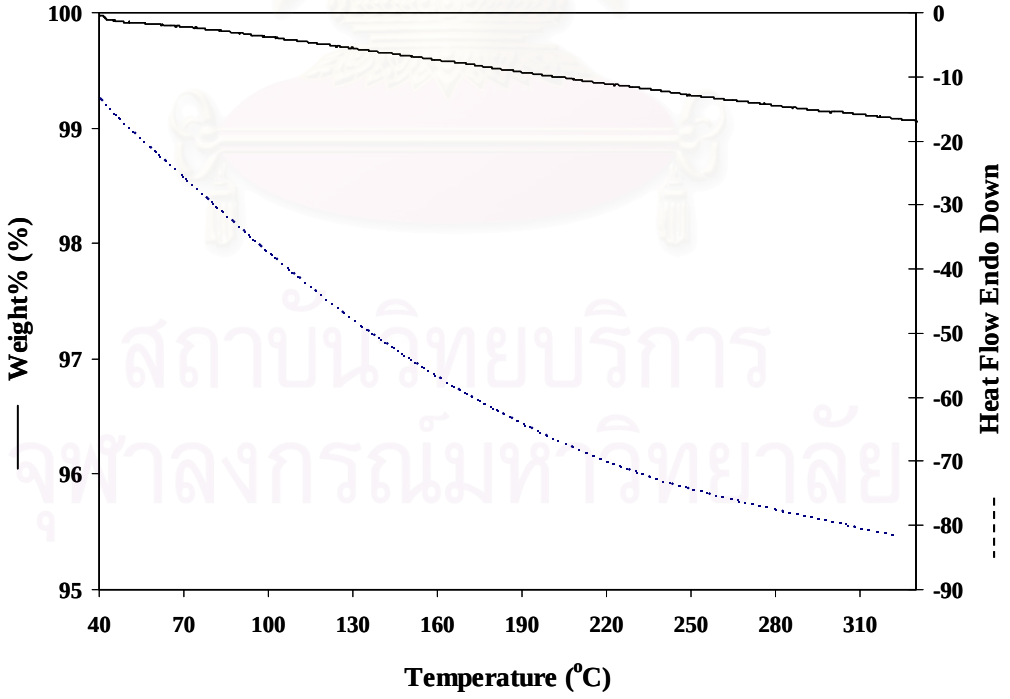

Figure 5.122 TG and DTA curves of ZnO as-synthesized in 1-hexanol at 250°C for 2 h by using zinc acetate 15g.

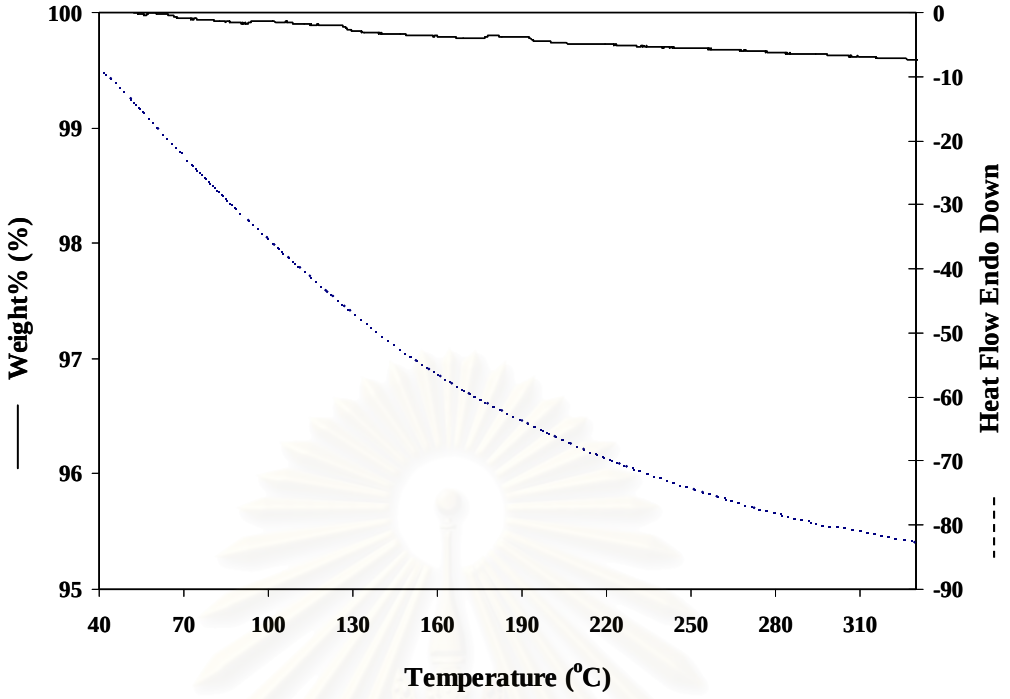

Figure 5.123 TG and DTA curves of ZnO as-synthesized in 1-octanol at 250°C for 2 h by using zinc acetate 15g.

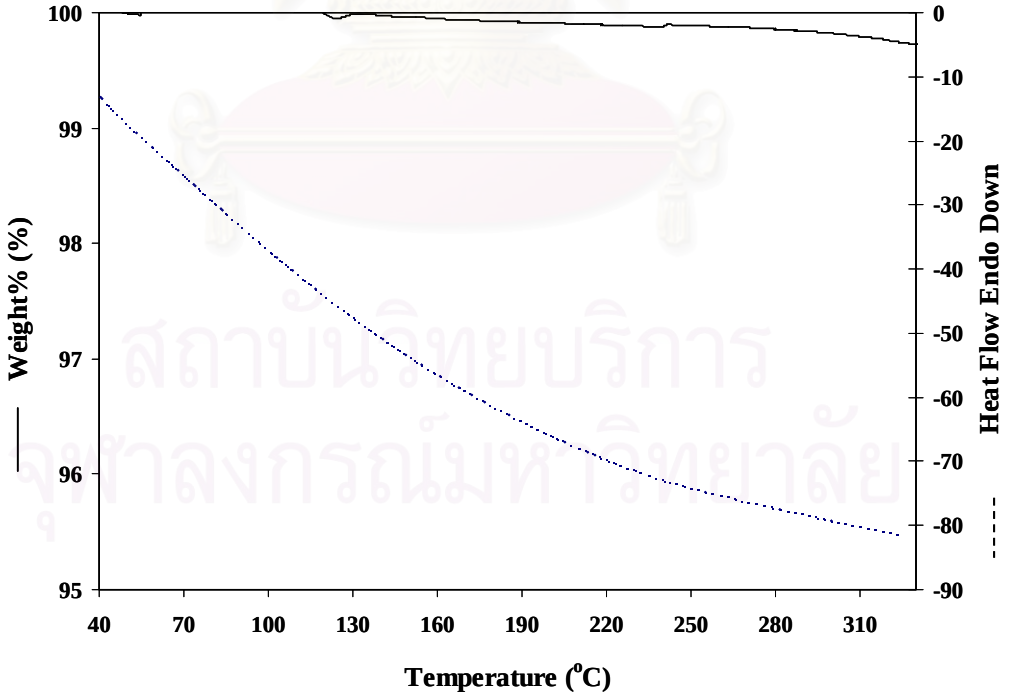

Figure 5.124 TG and DTA curves of ZnO as-synthesized in 1-decanol at 250°C for 2 h by using zinc acetate 15g.

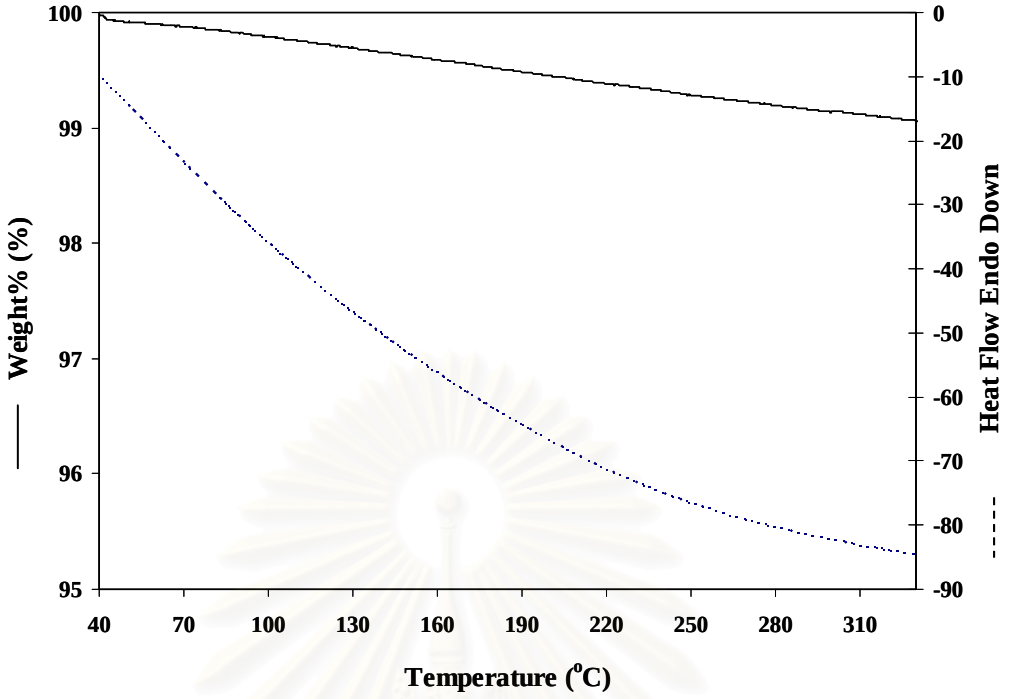

Figure 5.125 TG and DTA curves of ZnO as-synthesized in toluene at 250°C for 2 h by using zinc acetate 15g.

CHAPTER VI

CONCLUSIONS AND RECOMMENDATION

6.1 Conclusions

In this thesis, the crystal shape and properties of ZnO is investigated by using XRD, SEM, TEM, UV/vis, IR, GC/MS and TG/DTA technique. The conclusions of these results are summarized as follow:

1. ZnO nanorods with a narrow particle size distribution were successfully fabricated via one-step solvothermal reaction of zinc acetate in various organic solvent.

2. The average diameter and length of nanorod increased with reaction temperature and amount of starting material, while the aspect ratios were constant. It suggests that the reaction temperature and amount of starting material was not affected on the grow rate ratio between plane in ZnO crystal.

3. The aspect ratio of ZnO nanorods as-synthesized via solvothermal method depended on organic solvent.

4. The linear relationship between boiling points of organic solvent and aspect ratios was observed. This result can be used to select the appropriate solvents for preparation of zinc oxide nanorods with desired aspect ratio.

5. The mechanism of the reaction in alcohol had seemed to be the esterification of zinc acetate and alcohol on starting at the surface of zinc acetate seeds and ZnO nanorods, as-synthesized in toluene, was obtained directly by thermal decomposition of zinc acetate.

6. The solvent using in the reaction medium had neligible effect on the UV absorption in ZnO nanoparticles.

6.2 Recommendation

From the previous conclusion, the following recommendation for further studies can be as the following:

1. The linear relationship between boiling points of organic solvent such as n-hexane, n-octane and n-decane and aspect ratios was studied. To investigate a range of boiling influenced on aspect ratios, other various solvents should be introduced to this method.

2. The solvent was affected on the aspect ratio, therefore the relationship between glycol, alcohol and toluene should be done.

REFERENCES

Ahmed, S. R. Nano-Structure Materials. University of Maryland [Online]. 1999. Available from: http://www.glue.umd.edu/~srahmed/nanocomposite.html [2002, October 28].

Ajayan, P.M., Schadler, L.S. and Braun, P.V., Nanocomposite science andtechnology, Weinheim, WILEY-VCH Verleg Gmbh&Co., 2003.

Bae, D.S., Han, K.S., Cho, S.B., and Choi, S.H. Synthesis of ultrafine Fe_3O_4 powder by glycothermal process. Mater. Lett. 37(1998): 255-258.

Cheng, B. and Samulski, E.T. Hydrothermal synthesis of one-dimensional ZnO nanostructures with different aspect ratios. Chem. Comm. 1(2004): 986-987.

Chittofrati, A., and Matijevic, E. Uniform particles of zinc oxide of different morphologies. Coll. Surf. 48(1990): 65–78.

Demazeau, G., Millet, J.M., Cros, C. and Largeteau, A. Solvothermal synthesis of microcrystallites of transition metal oxides. J. Alloys and Compounds. 262-263(1997): 271-274.

Gardner, T.J. and Messing, G.L. Magnesium salt decomposition and morphological development during evaporative decomposition of solutions. Thermochim. Acta. 78(1984): 17-27.

Ghosh, M. and Rao, C.N.R. Solvothermal synthesis of CdO and CuO nanocrystals. Chem. Phys. Lett. 393(2004): 493-497.

Greta, r., Krumeich, F. and Nesper., R. Oxidic nanotubes and nanorods-anisotropic modules for a future nanotechnology. Angew. Chem. Int. Ed. 41(2002): 2446-2461.

Guo, L., Ji, Y.L. and Xu, H. Regularly shaped, single-crystalline ZnO nanorods with wurtzite structure. J. Am. Chem. Soc. Comm. 124(2002): 4864-14865.

HaiYan, X. and Hao, W. Hydrothermal synthesis of zinc oxide powders with controllable morphology. Ceram. Int. 30(2004): 93-97.

Hu, J.Q., Ma, X.L., Xie, z.Y., Wong, N.B., Lee, C.S. and Lee, S.T. Characterization of zinc oxide crystal whiskers grown by thermal evaporation. Chem. Phys. Lett. 344(2001): 97-100.

Hussien, G.A.M. Characterization of the thermal genesis course of zinc oxide from zinc acetoacetonate dehydrate. Thermochimica Acta. 186(1991): 187-197.

Inoue, M., Kondo, Y., and Inui T. An ethylene glycol derivative of boehmite. Inorg. Chem. 27(1988): 215-221.

Inoue, M.; Kominami, H., and Inui, T. Thermal Transformation of χ-Alumina Formed by Thermal Decomposition of Aluminum Alkoxide in Organic Media. J. Am. Ceram. Soc. 79[9] (1992): 2597 – 2598.

Inoue, M., and Kominami H. Novel synthetic method for the catalytic use of thermally stable zirconia: Thermal decomposition of zirconium alkoxide in organic media. Appl. Catal. A 97(1993): L25-L30.

Inoue, M., Kominami, H. and Inui, T. Novel synthesis method for thermally stable monoclinic zirconia: hydrolysis of Zirconium alkoxides at high temperatures with a limited amount of water dissolved in inert organic solvent from the gas phase. App. Catal. A. 121(1995): L1-L5.

Iwamoto, S., Saito, K., Inoue, M. and Kagawa, K. Preparation of the xerogels of nanocrystalline Titanias by the removal of the glycol at the reaction temperature after the Glycothermal method and their enhanced photocatalytic activities. Nano Letter. 1(2001): 417-21.

Kamalasanan, M.N. and Chandra, S. Sol-gel synthesis of ZnO thin films. Thin Solid Films. 288(1996): 112-115.

Kim, K.S. and Kim, H.W. Synthesis of ZnO nanorods on bare Si substrate using metal organic chemical vapor deposition. Physica B. 328(2003): 368-371.

King, Y.J. and Xi, Z.H. Nanotubular structures of zinc oxide. Solid State Comm. 129(2004): 671-675.

Koch, C.C. Processing, Particles and Applications, New York, William Andrew publishing, 2002.

Kongwudthiti, S., Praserthdam, P., Silveston, P. and Inoue, M. Influence of synthesis conditions on the preparation of zirconia powder by the glycothermal method. Ceram. Int. 29(2003): 807-814.

Kubota N., Effect of impurities on the growth kinetics of crystals. Cryst. Res. Tech. 36 (2001): 749-769.

Li, J.Y., Chen, X.L., Li, H., He, M., and Qiao, Z.Y. Fabrication of zinc oxide nanorods. J. Crys. Growth. 233(2001): 5-7.

Li,Q., Kumar,V., Li,Y., Zhang,H., Marks, T.J., and Chang R.P.H. Fabrication of ZnO nanorods and nanotubes in aqueous solutions. J. Am. Ceram. Soc. 17[5] (2005): 1001-1006.

Li, W.J., Shi, E.W., Zhong, W.Z. and Yin. Z.W. Growth mechanism and growth habit of oxide crystals. J. Cryst. Growth. 203(1999): 186-196.

Li, y., Lioa, H., Fan, Y., Li, L. and Qian, Y., A solvothermal synthetic route to CdE (E=S, Se) semiconductor nanocrystalline. Mater. Chem. Phys. 58(1999):87-89.

Lieber, C.M. One-dimensional nanostructures: Chemistry, Physicals & Applications. Solid State Commu. 107(1998): 607-616.

Liu, B. and Zeng, H.C. Hydrothermal synthesis of ZnO nanorods in the diameter regime of 50 nm. J. Am. Chem. Soc. 125(2003): 4430-4431.

Liu, Y., Liu, Z., and Wang, G. Synthesis and characterization of ZnO nanorods. J. Cryst. Growth. 252(2003): 213-218.

Lu, C.H. and Yeh C.H. Influence of hydrothermal conditions on the morphology and particle size of zinc oxide powder. Ceram. Int. 26(2002): 351-357.

Lyu, S.C., Zhang, Y., Ruh, H., Lee, H.J., Shim, H.W., Suh, E.K., and Lee, C.J. Low temperature growth and photoluminescence of well-aligned zinc oxide nanowires. Chem. Phys. Lett. 363(2002): 134-138.

McGraw-Hill encyclopedia of science & technology, New York, McGraw-Hill Book, 5 th ed., 1982: 435.

Mekasuwandumrong, O., Kominami, H., Praserthdam, P., Inoue, M. Synthesis of thermally stable x-alumina by thermal decomposition of aluminum isopropoxide in toluene. J. Am. Ceram. Soc. 87(2004): 1543-1549.

Mueller, R., Mädler, L., and Pratsinis, S.E. Nanoparticle synthesis at high production rates by flame spray pyrolysis. Chem. Eng. Sci. 58(2003): 1969-1976.

Music, S. and Dragcevic, D. Influence of chemical synthesis on the crystallization and properties of zinc oxide. Mat. Chem. Phys. 77(2002): 521-530.

Pan, Z.W., Dai, Z.R., and Wang Z.L. Nanobelts of semiconducting oxides. Science. 91(2001): 947-1949.

Pearton, S.J., Norton, D.P., Ip, K., Heo, Y.W. and Steiner, T. Recent progress in processing and properties of ZnO. Progress in Materials Science. 50(2005): 293-340.

Peng, Q., Dong, Y., Deng, Z., Sun, X., and Li,Y. Low-temperature elemental-direct-reaction route to II-VI semiconductor nanocrystalline ZnSe and CdSe. Inorg. Chem.40(2001): 3840-3841.

Praserthdam, P., Inoue, M., Mekasuvandumrong, O., Thanakulrangsan, W., and Phatanasri, S. Effect of organic solvents on the themal stability of porous silica-modified alumina powders prepared via one pot solvothermal synthesis. Inorg. Chem. Commun. 3(2002): 671-676.

Pratsinis, S.E. Flame aerosol synthesis of ceramic powders. Progress in energy and combustion science. 24[3] (1998): 197-219.

Qu, F., Santos, Jr. D.R., Dantas, N.O., Monte, A.F.G., and Morais, P.C. Effects of nanocrystal shape on the physical properties of colloidal ZnO quantum dots. Physica E. 23(2004): 410-415.

Rataboul, F. and Nayral, C. Synthesis and characterization of nanodisperse zinc and zinc oxide nanoparticles from the organometallic precursor [$Zn(C_6H_{11})_2$]. J. Organo Chem. 643-644(2002): 307-312.

Rodriguez, J.E. and caballero, A.C. Controlled precipitation methods: formation mechanism of ZnO nanoparticles. J. Eur. Ceram. Soc. 21(2001): 925-930.

Sakagami N. Hydrothermal growth and characterization of ZnO single crystals of high purity. J. Cryst. Growth. 99(1990): 905–909.

Saravanan, P., Alam, S., and Mathur, G.N. Synthesis of ZnO and ZnS nanocrystals by thermal decomposition of zinc (II) cupferron complex. Mater. Lett. 58(2004): 3528-3531.

Sue, K., Kimura, K., Yamamoto, M. and Arai, K. Rapid hydrothermal synthesis of ZnO nanorods without organics. Mater. Lett. 58(2004): 3350-3352.

Sun, X.M., Chen, X., Deng, Z.X., and Li, Y.D. A CTAB-assisted hydrothermal orientation growth of ZnO nanorods. Mater. Chem. Phys. 78(2002): 99–104.

Verdon, E., Devalette, M., and Demazeau, G. Solvothermal synthesis of cerium dioxide microcrystallites: effect of the solvent. Mater. Lett. 25(1995): 127-131.

Wang, J. and Gao, L. Synthesis and characterization of ZnO nanoparticles assembled in one-dimensional order. Inorg. Chem. Comm. 6(2003): 877-881.

Wei, H., Wu, Y., Lun, N., and Hu, C. Hydrothermal synthesis and characterization of ZnO nanorods. Mater. Sci. Eng. A. 393(2003): 80-82.

West, A. R. Basic solid state chemistry and its application. 1 st ed., Great Britain, John Wiley & Sons, 1997.

Wu, H.Q. and Wei, X.W. Synthesis of zinc oxide nanorods using carbon nanotubes as templates. J. Crys. Growth. 265(2004):184-189.

Xing, Y.J., Xi, Z.H., Zhang, X.D., Song, J.H., Wang, R.M., Xu, J., Xue, Z.Q. and Yu, D.P. Nanotubular structures of zinc oxide. Solid State Comm. 129(2004): 671-675.

Xu, C., Xu, G., Liu, Y., and Wang, G. A simple and novel route for the preparation of ZnO nanorods. Solid state comm. 122(2002): 175-179.

Xu, C., Xu, G., Liu, Y., Zhao, X., and Wang, G. Preparation and characterization of SnO_2 nanorods by thermal decomposition of SnC_2O_4 precursor. Scripta Materialia. 46(2002): 789-794.

Xu, H.Y., Wang, H., Zhang, Y.C., He, W.L., Zhu, M.K., Wang, B. and Yan, H. Hydrothermal synthesis of zinc oxide powders with controllable morphology. Ceram. Int. 30(2004): 93-97.

Yang, Y. and Chen, h. Size control of ZnO nanoparticles via thermal decomposition of zinc acetate coated on organic additives. J. Crys. Growth. 263(2004): 447-453.

Yang, Y., Li, X., Chen, J., Chen, H., and Bao, X. ZnO nanoparticles prepared by thermal decomposition of β-cyclodextrin coated zinc acetate. Chem. Phys. Lett. 373(2003): 22-27.

Yin, M., Gu, Y., Kuskovsky, I.L., Andelman, T., Zhu, Y., Neumark, G.F. and O'Brien, S. Zinc oxide quantum rods. J. Am. Chem. Soc. 126(2004): 6206-6207.

Yoshimura, M. Importance of soft solution processing for advanced inorganic materials, J. Mater. Res. 13(1998): 796–802.

Yu, H., Zhang, Z., Han, M., Hao, X., and Zhu, F. A general low-temperature route for large-scale fabrication of highly oriented ZnO nanorods/nanotue arrays. J. Am. Chem. Soc. 130(2005): 9-10.

Zhang, Y., Dai, Y., Huang, Y., and Zhou, C. Shape controlled synthesis and growth mechanism of one-dimensional zinc oxide nanomaterials. Journal of University of science and technology Beijing. 11(2004): 23-29.

Zhong, W.L. Nanostructures of zinc oxide. Materialtoday. (2004): 26-33.

APPENDICES

APPENDIX A

CALCULATION OF CRYSTALLITE SIZE FROM TEM PHOTOGRAPH

Diameter sizes measured from TEM photograph of the as-synthesized products of the zinc oxides were calculated as follows,

Example A1: The measurement of as-synthesized diameter size of zinc oxide synthesized at 300°C for 2h in 1-octanol by using zinc acetate 15 g.

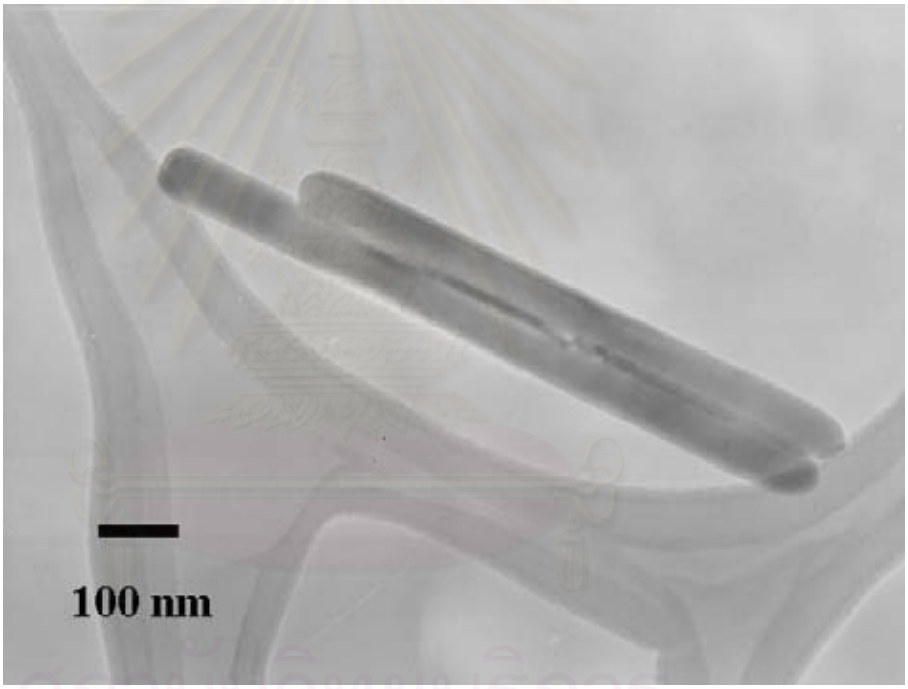

Figure A1 TEM photograph of as-synthesized zinc oxide synthesized at 300°C for 2h in 1-octanol by using zinc acetate 15 g.

At x60000 magnification, the scale is

1 cm = 100 nm

From TEM photograph, it was found that the diameter size of the particles closed to each other and that was 0.9 cm. Therefore, the diameter size observed by TEM is

$$\text{Diameter size} = \frac{100\ nm}{1\ cm} \times 0.9\ cm$$

$$\text{Diameter size} = 90 \text{ nm}$$

The measured Diameter sizes from TEM photograph were 90, 95, 120, 92, 97, 111, 94, 102, 116, 98, 105, 106 and 94 nm. The average crystallite size was

$$\text{Crystallite size} = \frac{90+95+120+92+97+111+94+102+116+98+105+106+94}{12}$$

$$= 110 \text{ nm}$$

APPENDIX B

SAMPLE OF SURFACE AREA CALCULATIONS

Calculation of the specific surface area

From Brunauer-Emmett-Teller (BET) equation

$$\frac{p}{n(1-p)} = \frac{1}{n_m C} + \frac{(C-1)p}{n_m C} \qquad \text{(B-1)}$$

Where p = Relative partial pressure of adsorbed gas , P/Po

Po = Saturated vapor pressure of adsorbed gas in the condensed state at the experimental temperature, atm

P = Equilibrium vapor pressure of adsorbed gas, atm

n = Gas adsorbed at pressure P, ml. At the NTP/g of sample

n = Gas adsorbed at monolayer, ml. At the NTP/g of sample

$C = \text{Exp}[(H_c - H_l)/RT]$

H_c = Heat of condensation of adsorbed gas on all other layers

H_l = Heat of adsorption into the first layer

Assume $C \rightarrow \infty$, then

$$\frac{p}{n(1-p)} = \frac{p}{n_m}$$

$$n_m = n(1-p) \qquad \text{(B-2)}$$

The surface area, S, of the catalyst is given by

$$S = S_b \times n_m \qquad \text{(B-3)}$$

From the gas law

$$\frac{P_b V}{T_b} = \frac{P_t V}{T_t} \qquad \text{(B-4)}$$

Where, P_b = Pressure at 0 ^oC

P_t = Pressure at t ^oC

T_b = Temperature at 0 ^oC = 273.15 K

T_t = Temperature at t ^oC = 273.15 + t K

V = Constant volume

Then, $P_b = (273.15/T_t)\ P_t = 1$ atm

Partial pressure

$$P = \frac{\left[\text{Flow of } (He + N_2) - \text{Flow of } He\right]}{\text{Flow of } (He + N_2)}$$

= 0.3 atm

For nitrogen gas , the saturated vapor pressure equals to

P_o = 1.1 atm

Then, $p = P/P_o = 0.3 / 1.1 = 0.2727$

To measure the volume of nitrogen adsorbed, n

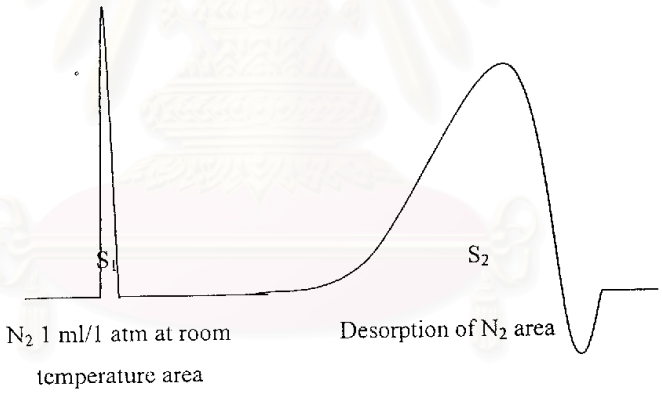

$$n = \frac{S_2}{S_1} \times \frac{1}{W} \times \frac{273.15}{T} \text{ ml. / g of catalyst} \qquad \text{(B-5)}$$

Where, S_1 = N_2 1 ml/ 1 atm at room temperature area

S_2 = Desorption of N_2 area

W = Sample weight, g

T = Room temperature, K

Therefore,

$$n_m = \frac{S_2}{S_1} \times \frac{1}{W} \times \frac{273.15}{T} \times (1 - p)$$

$$n_m = \frac{S_2}{S_1} \times \frac{1}{W} \times \frac{273.15}{T} \times 0.7273 \qquad \text{(B-6)}$$

Whereas, the surface area of nitrogen gas from literature equal to

$S_b = 4.373\ m^2$ / ml of nitrogen gas

Then,

$$S = n_m = \frac{S_2}{S_1} \times \frac{1}{W} \times \frac{273.15}{T} \times 0.7273 \times 4.343$$

$$S = n_m = \frac{S_2}{S_1} \times \frac{1}{W} \times \frac{273.15}{T} \times 3.1582\ m^2 / g \qquad \text{(B-7)}$$

APPENDIX C

PICTURES OF GC/MS SPECTRUM

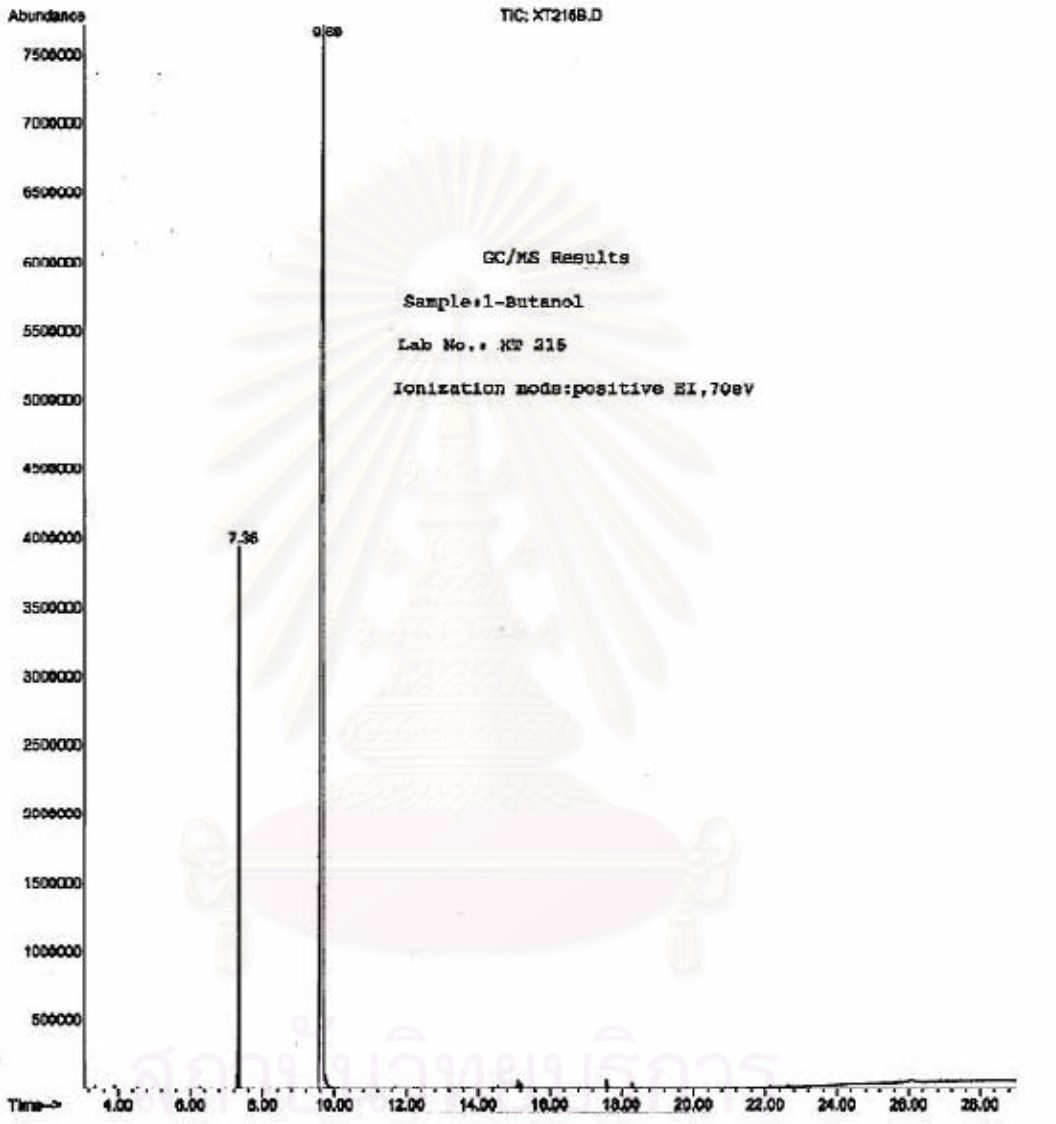

Figure C.1 GC/MS spectrum of solvent as-synthesized ZnO in 1-butanol at 250°C for 2h by using zinc acetate 15 g.

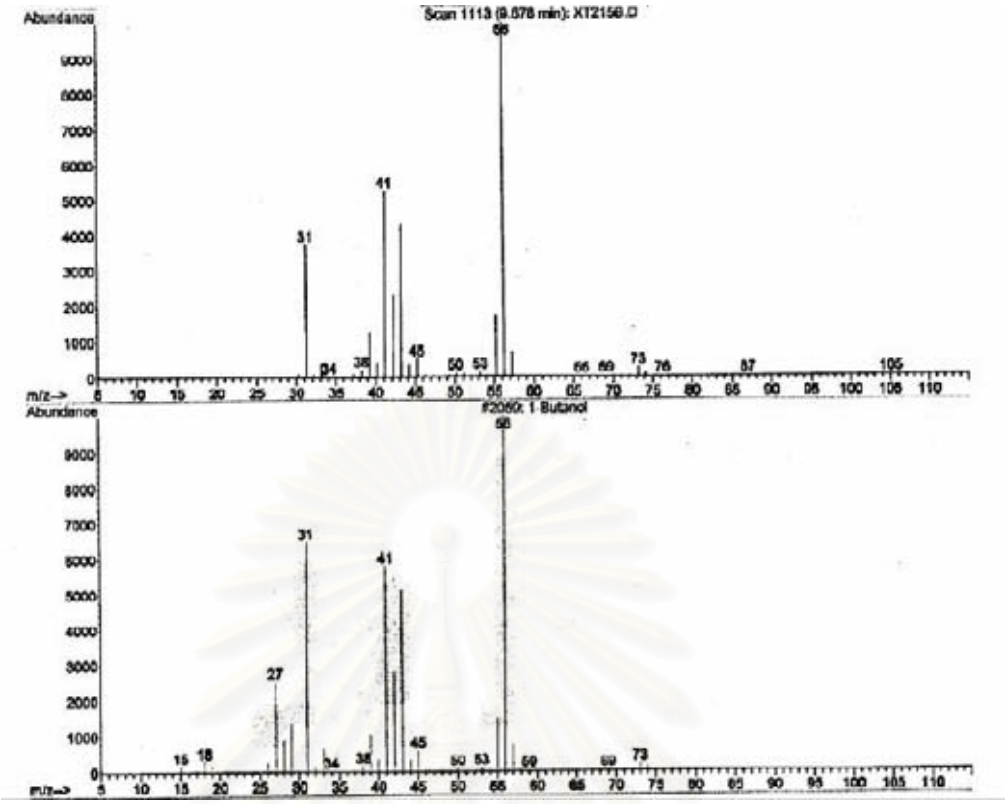

Figure C.2 GC/MS spectrum for 1-butanol in 1-butanol as-synthesized ZnO at 250°C for 2h by using zinc acetate 15 g.

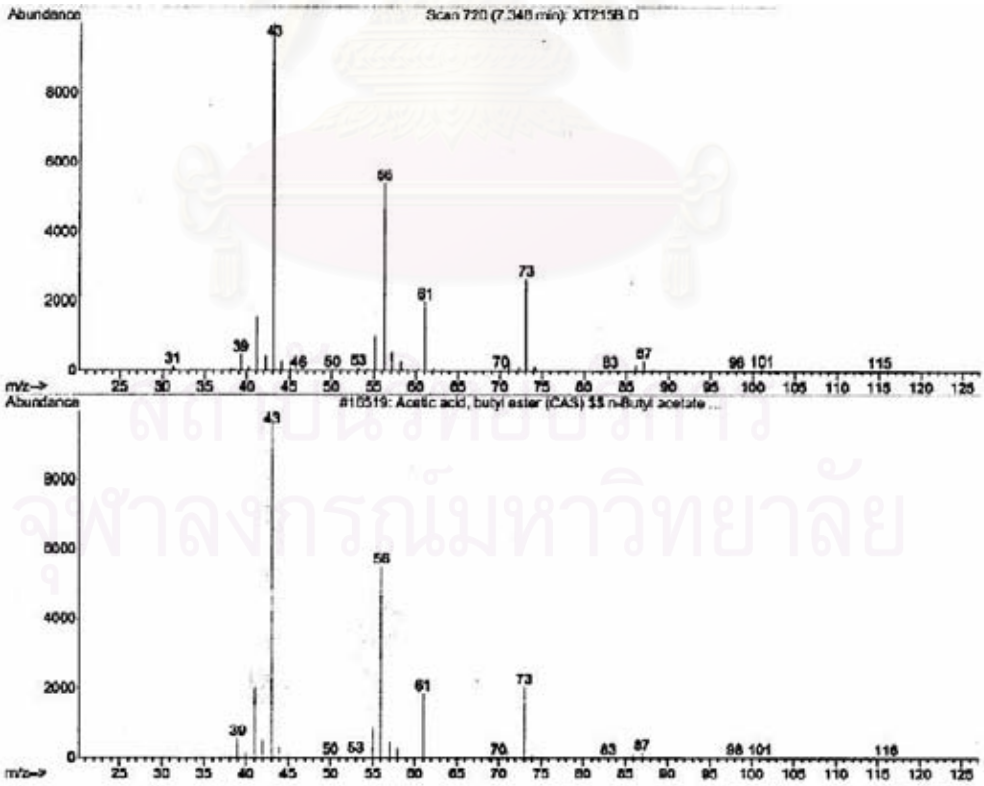

Figure C.3 GC/MS spectrum for butyl acetate in 1-butanol as-synthesized ZnO at 250°C for 2h by using zinc acetate 15 g.

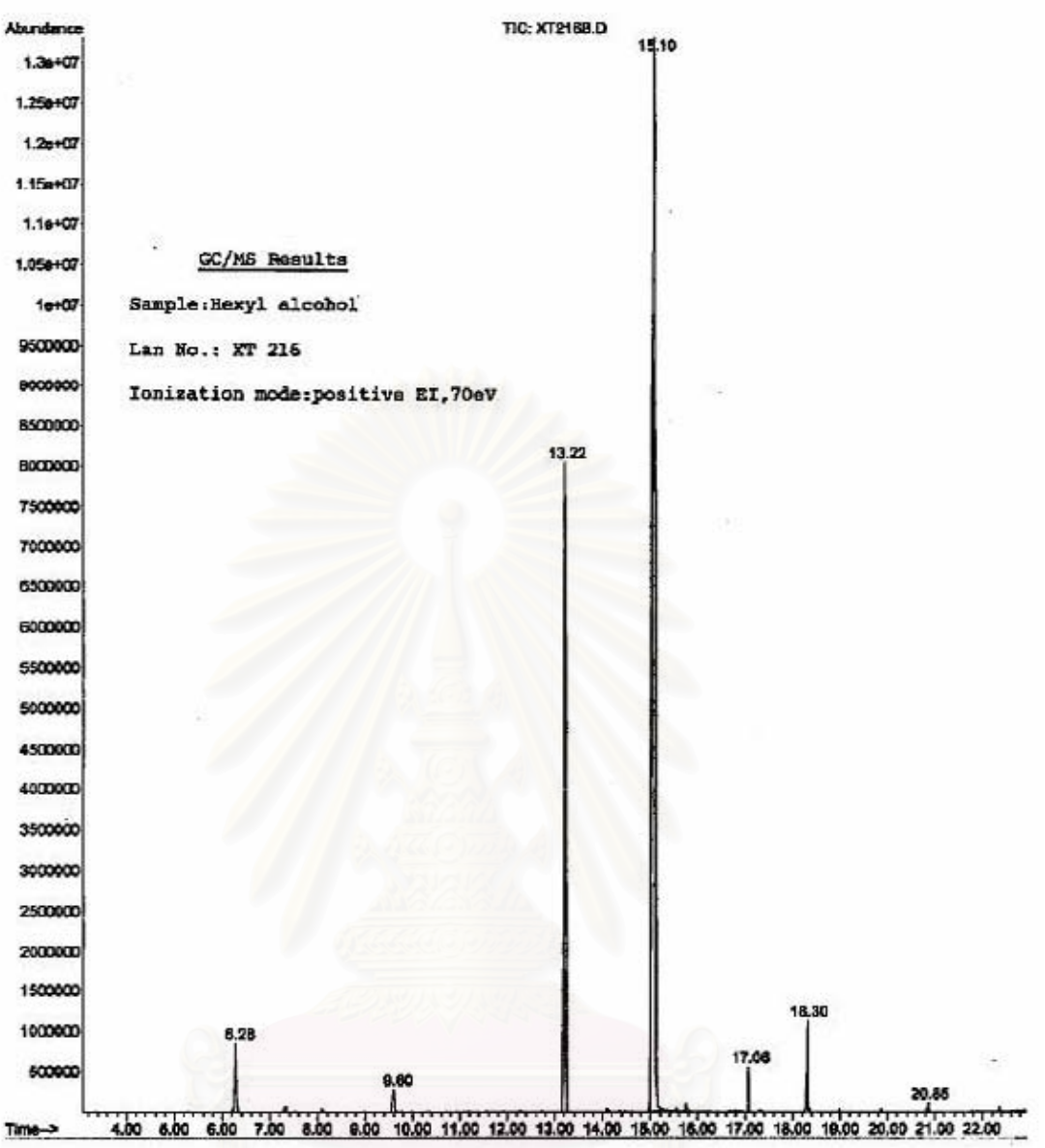

Figure C.4 GC/MS spectrum of solvent as-synthesized ZnO in 1-hexanol at 250°C for 2h by using zinc acetate 15 g.

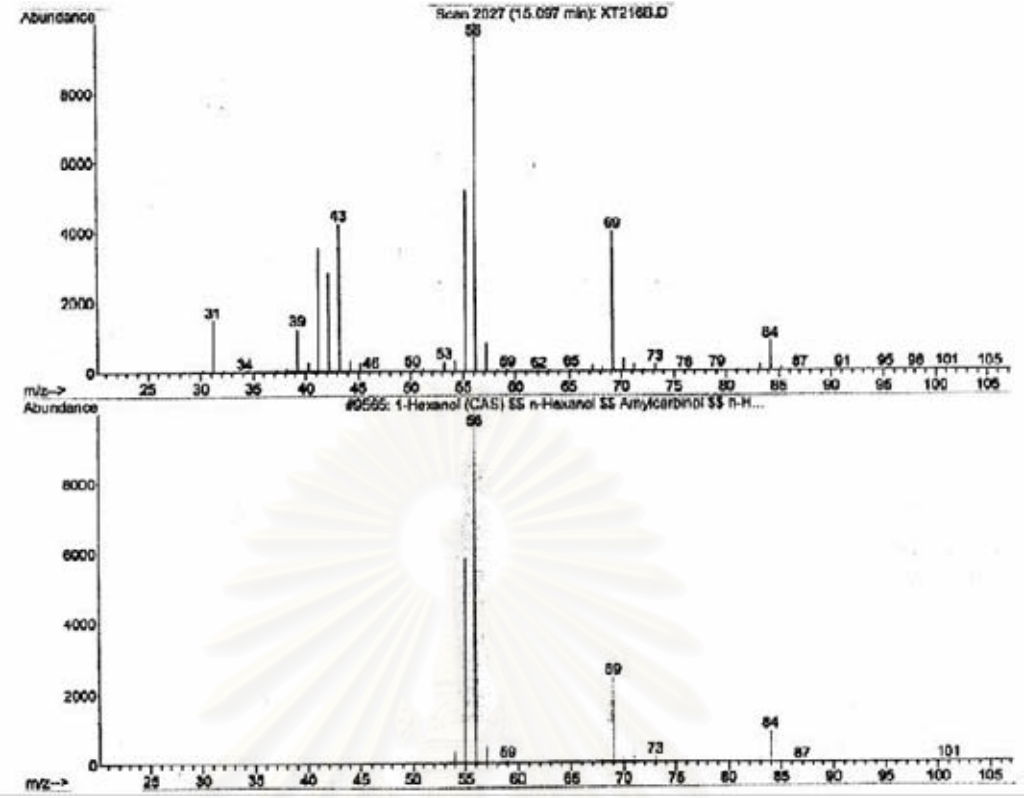

Figure C.5 GC/MS spectrum for 1-hexanol in 1-hexanol as-synthesized ZnO at 250°C for 2h by using zinc acetate 15 g.

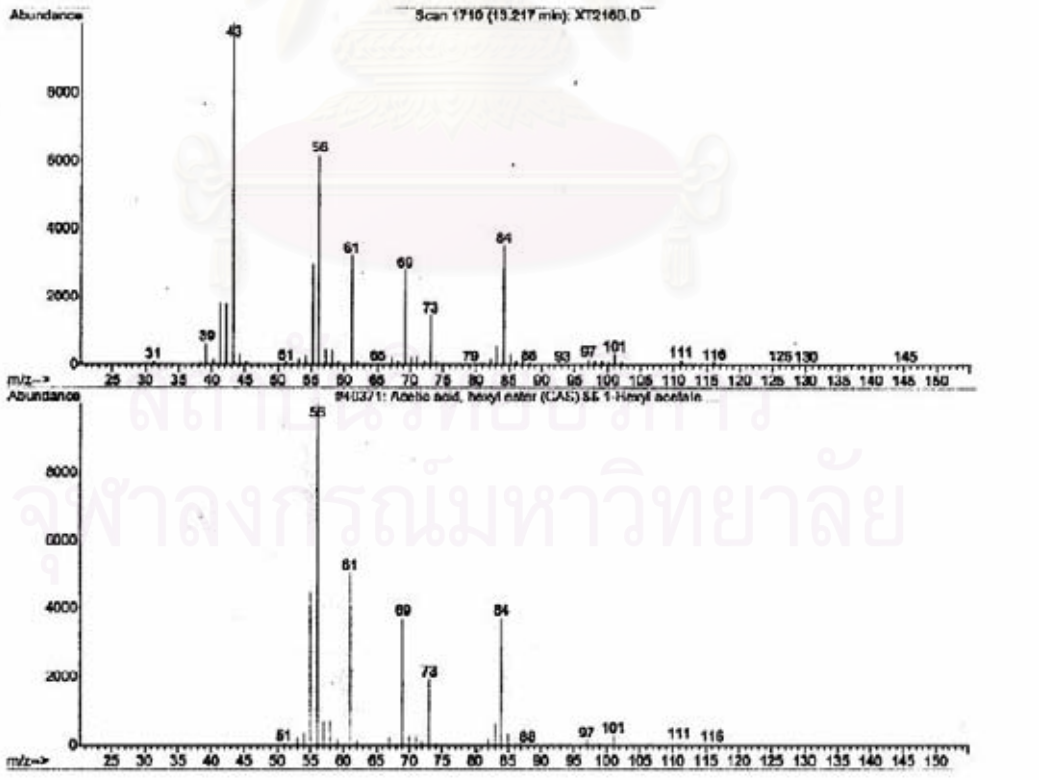

Figure C.6 GC/MS spectrum for hexyl acetate in 1-hexanol as-synthesized ZnO at 250°C for 2h by using zinc acetate 15 g.

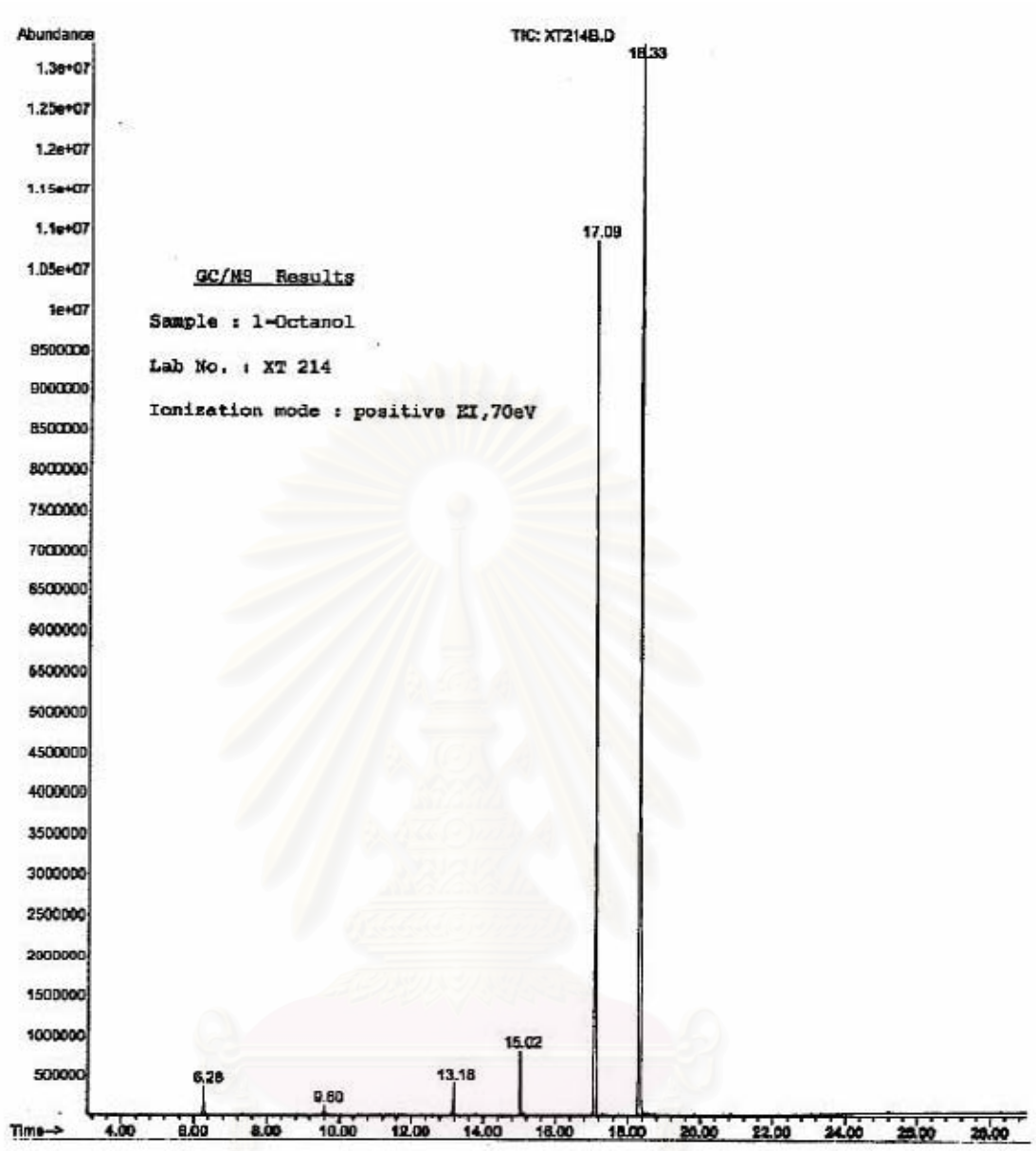

Figure C.7 GC/MS spectrum of solvent as-synthesized ZnO in 1-octanol at 250°C for 2h by using zinc acetate 15 g.

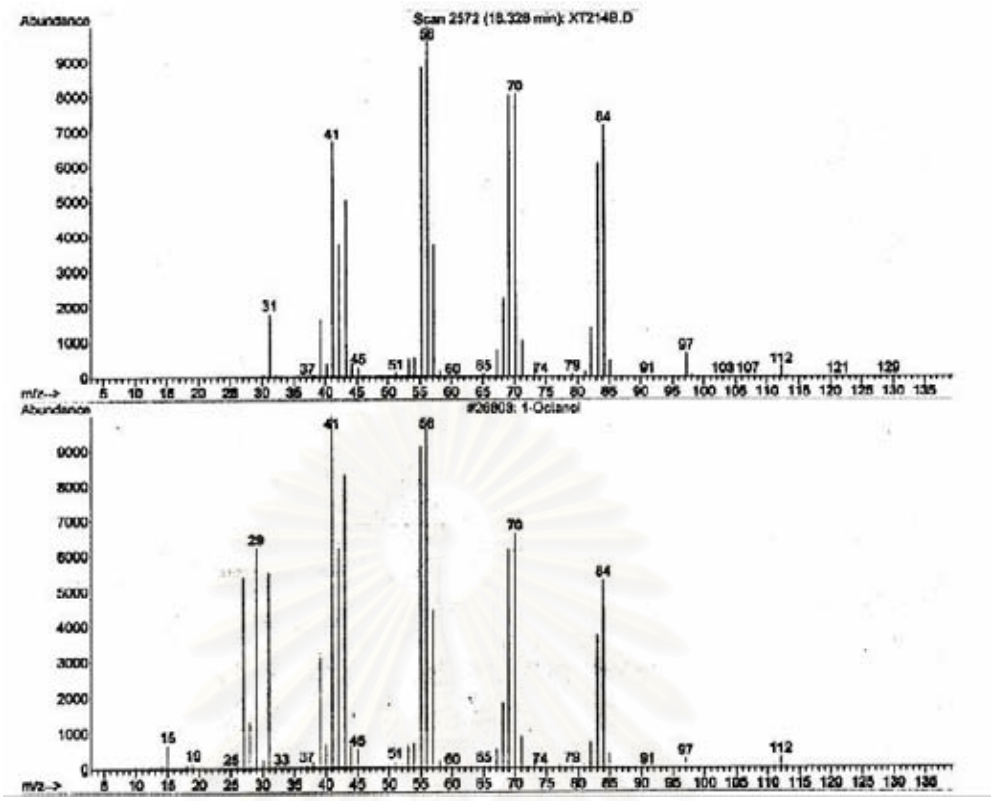

Figure C.8 GC/MS spectrum for 1-octanol in 1-octanol as-synthesized ZnO at 250°C for 2h by using zinc acetate 15 g.

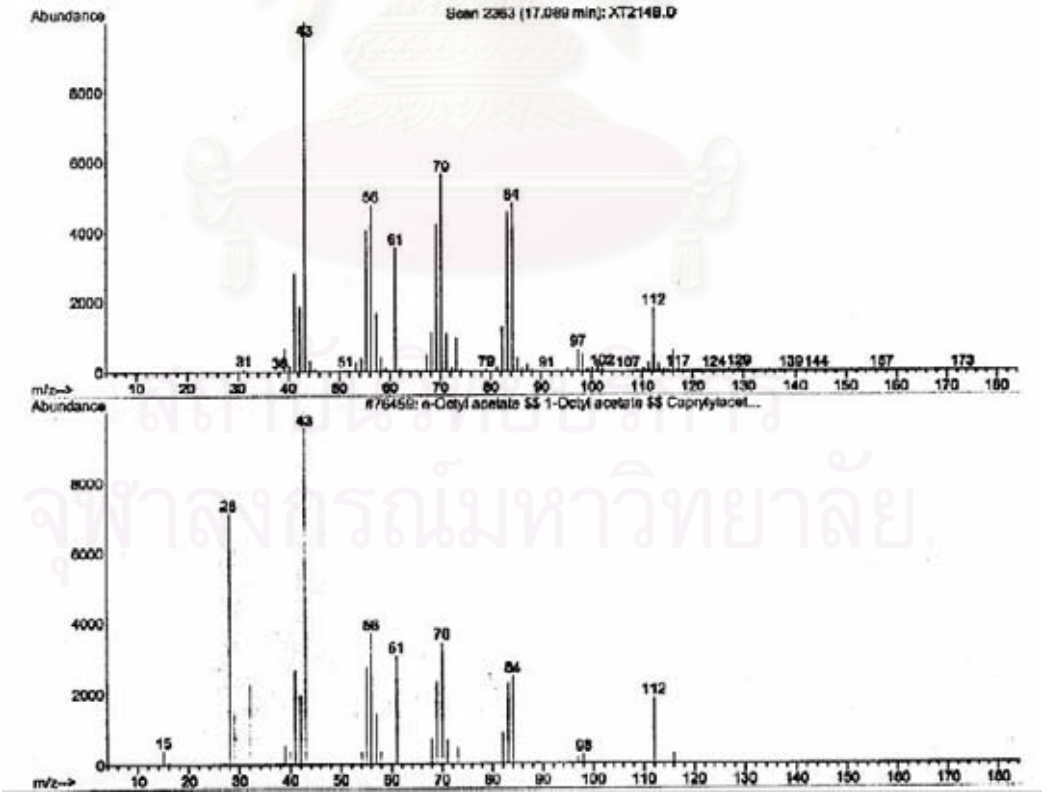

Figure C.9 GC/MS spectrum for octyl acetate in 1-octanol as-synthesized ZnO at 250°C for 2h by using zinc acetate 15 g.

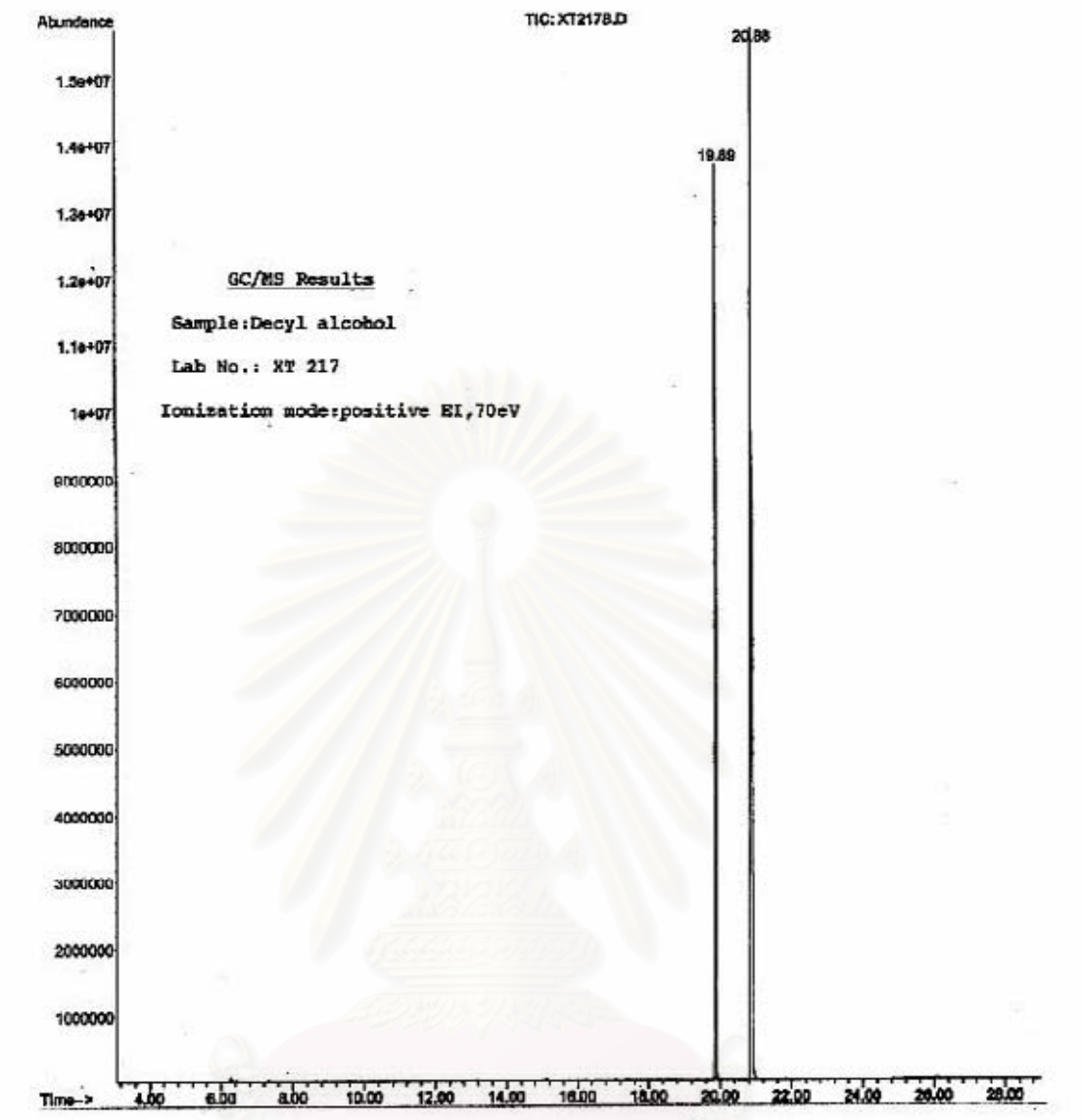

Figure C.10 GC/MS spectrum of solvent as-synthesized ZnO in 1-decanol at 250°C for 2h by using zinc acetate 15 g.

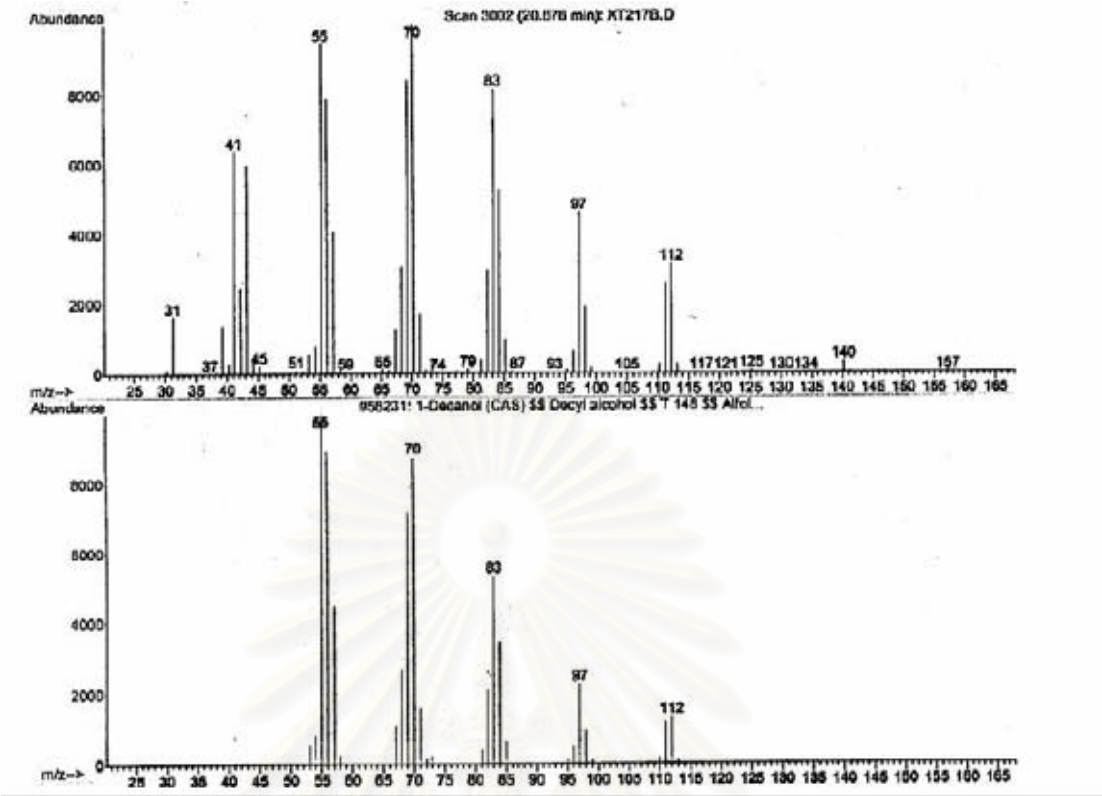

Figure C.11 GC/MS spectrum for 1-decanol in 1-decanol as-synthesized ZnO at 250°C for 2h by using zinc acetate 15 g.

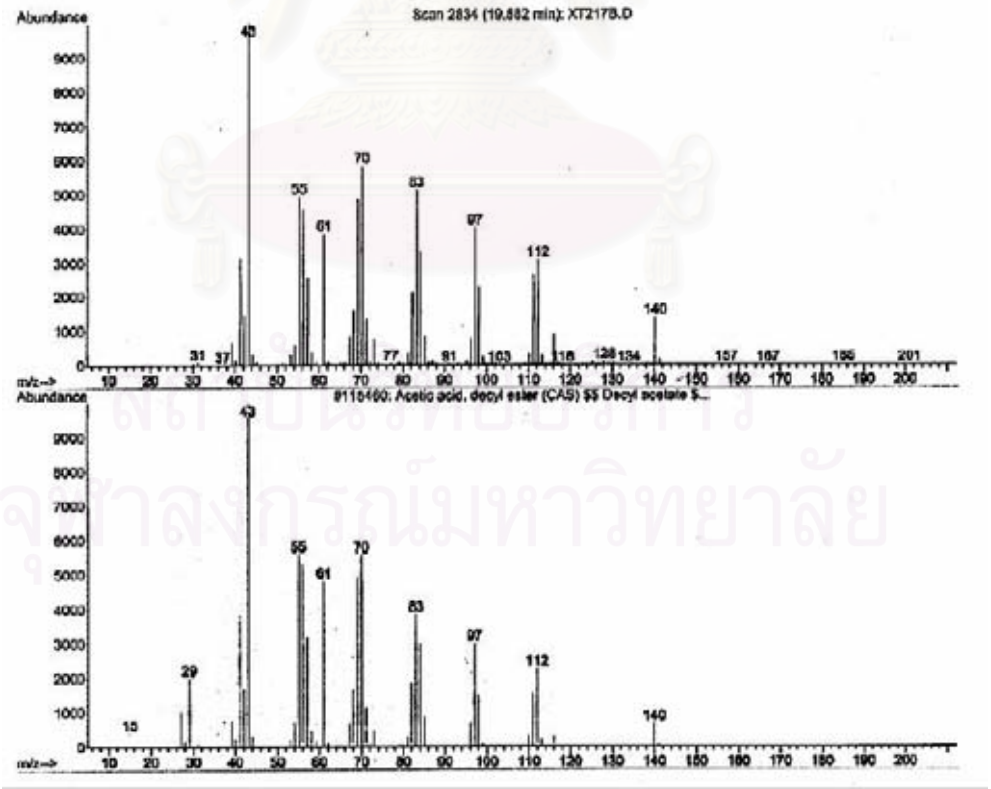

Figure C.12 GC/MS spectrum for decyl acetate in 1-decanol as-synthesized ZnO at 250°C for 2h by using zinc acetate 15 g.

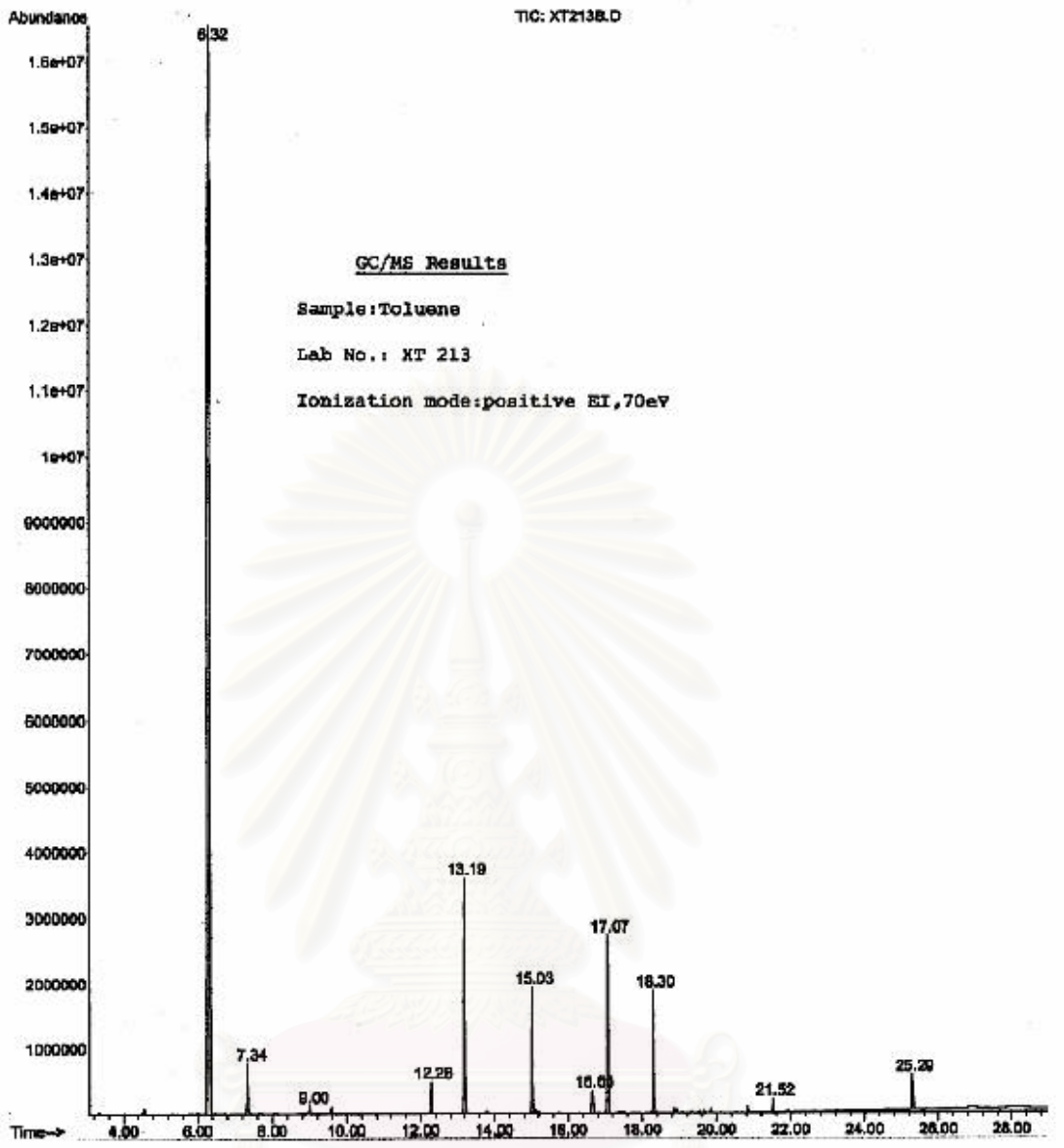

Figure C.13 GC/MS spectrum of solvent as-synthesized ZnO in toluene at 250°C for 2h by using zinc acetate 15 g.

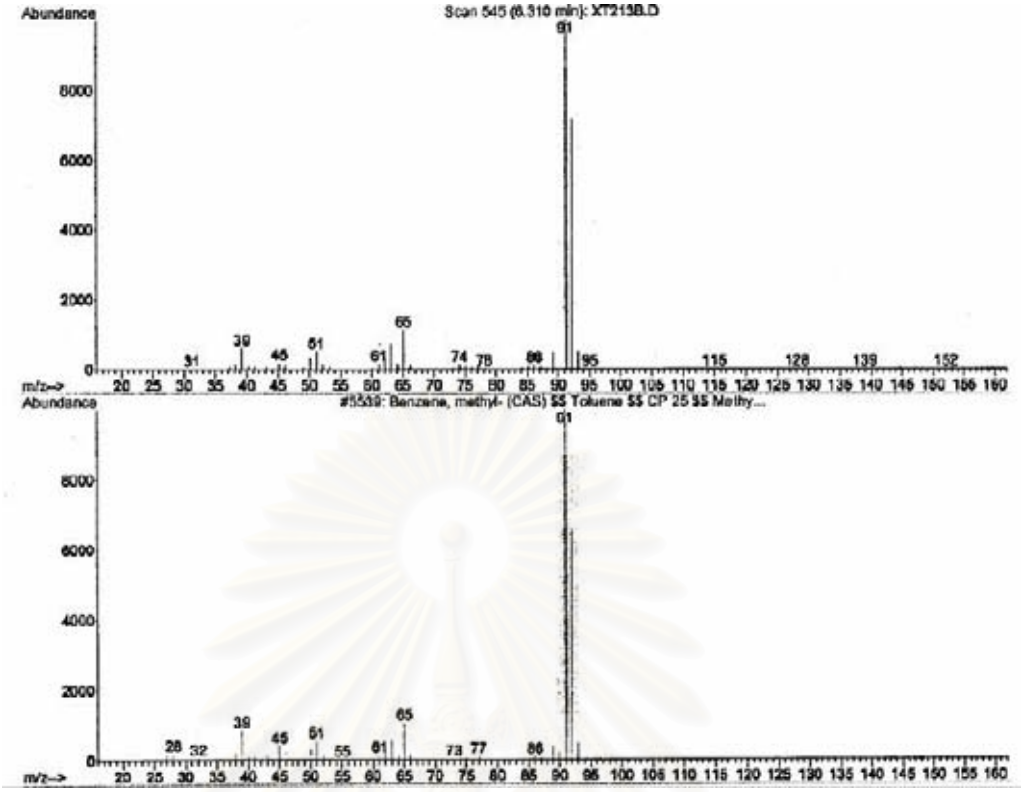

Figure C.14 GC/MS spectrum for toluene in toluene as-synthesized ZnO at 250°C for 2h by using zinc acetate 15 g.

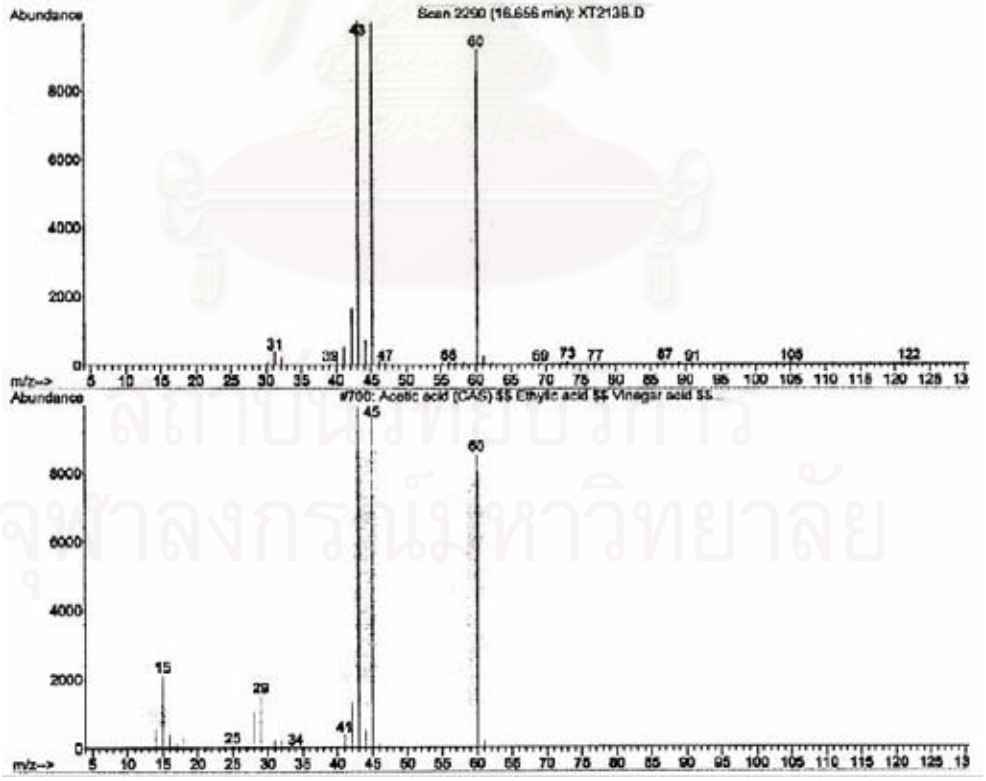

Figure C.15 GC/MS spectrum for acetic acid in toluene as-synthesized ZnO at 250°C for 2h by using zinc acetate 15 g.

APPENDIX D

LIST OF PUBLICATION

1. Tonto, P., Praserthdam, P., Mekasuvandumrong, O., and Patanasri, S. Effect of organic solvents on crystal shape of zinc oxide synthesized via thermal decomposition method. Regional Symposium on Chemical Engineering, 2004 (Conference)

2. Tonto, P., Mekasuvandumrong, O., Patanasri, S., Pavarajarn. V., and Praserthdam, P., Aspect Ratios Controlling of ZnO Nanorod Synthesized via Solvothermal Reaction of Zinc Acetate in Various Alcohols. Journal of Crystal Growth. (Submitted)

3. Tonto, P., Mekasuvandumrong, O., Patanasri, S., Pavarajarn. V., and Praserthdam, P., Synthesis of ZnO Nanorod by Thermal Decomposition of Zinc Acetate in Organic Solvents. (To be submit)

VITA

Miss Parawee Tonto was born on July, 1980 in Khonkhan, Thailand. She received the Bachelor Degree from Faculty of Engineering, Burapha University in 2003. She continued her Master's Study at Chulalongkorn University in June, 2003.